



**MEASUREMENT OF CORTICAL, NERVE,
AND MUSCLE EXCITABILITY IN EARLY
PHASE CLINICAL DRUG DEVELOPMENT**

TITIA QUIRINE RUIJS

MEASUREMENT OF CORTICAL, NERVE, AND MUSCLE EXCITABILITY
IN EARLY PHASE CLINICAL DRUG DEVELOPMENT



MEASUREMENT
OF CORTICAL, NERVE,
AND MUSCLE EXCITABILITY
IN EARLY PHASE CLINICAL
DRUG DEVELOPMENT

Proefschrift

ter verkrijging van
de graad van doctor aan de Universiteit Leiden,
op gezag van rector magnificus prof.dr.ir. H. Bijl,
volgens besluit van het college voor promoties
te verdedigen op donderdag 18 april 2024
klokke 15:00 uur

door
Titia Quirine Ruijs
geboren te 's-Gravenhage
in 1990

DESIGN

Caroline de Lint, Den Haag (caro@delint.nl)
Photos by Tuari Studio (www.tuaristudio.com)

The publication of this thesis was financially supported by the
foundation Centre for Human Drug Research (CHDR), Leiden,
the Netherlands

PROMOTOR

Prof. Dr. G.J. Groeneveld

COPROMOTOR

Dr. J.A.A.C. Heuberger

LEDEN PROMOTIECOMMISSIE

Prof. Dr. J.M.A. van Gerven

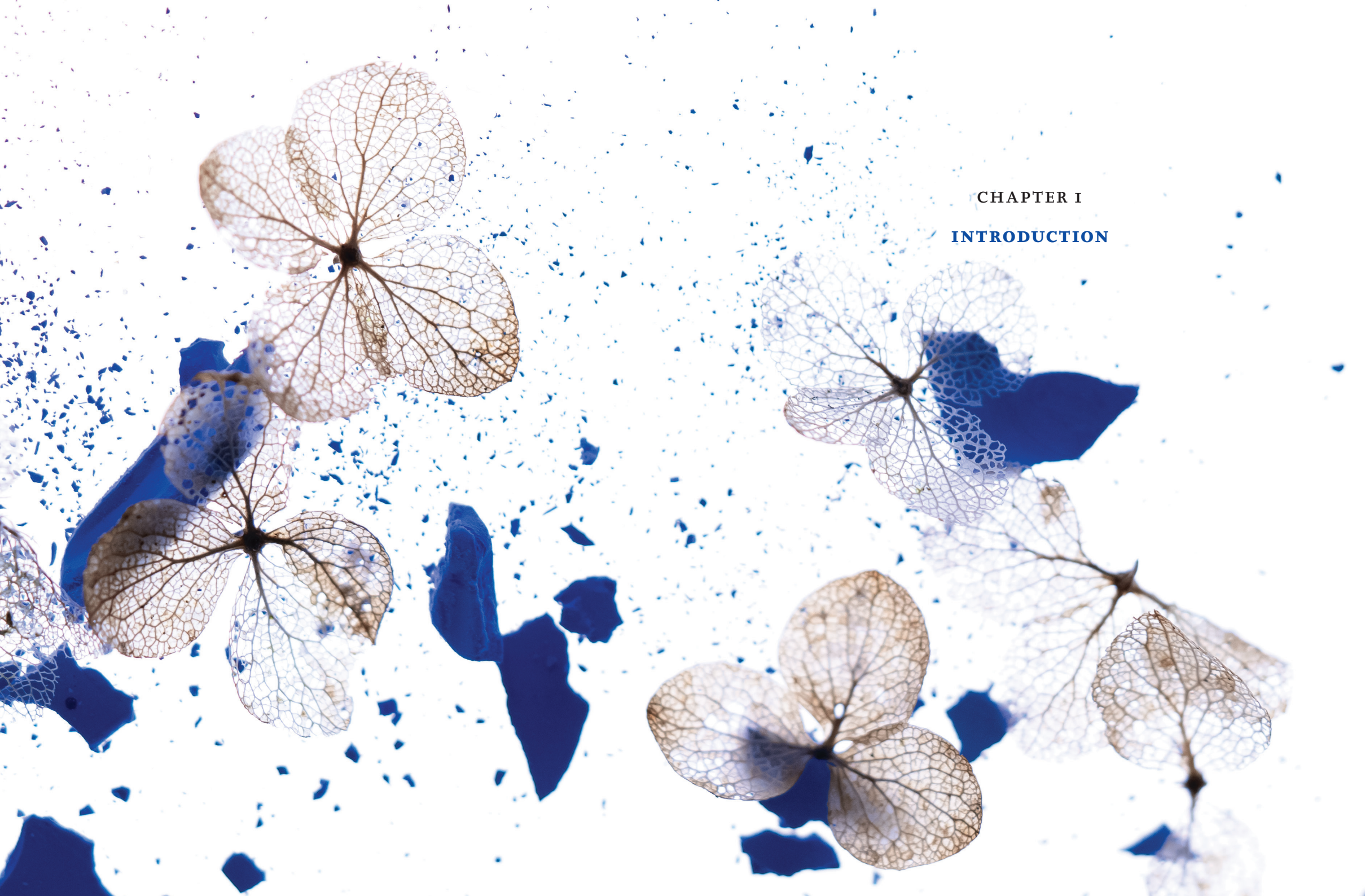
Dr. M.R. Tannemaat

Prof. Dr. G.J.M. Zijlmans (Universitair Medisch Centrum Utrecht)

Prof. Dr. Ir. M.J.A.M. van Putten (Universiteit Twente)

7	CHAPTER 1 Introduction
19	CHAPTER 2 Transcranial magnetic stimulation as biomarker of excitability in drug development: a randomized, double-blind, placebo-controlled, cross-over study
47	CHAPTER 3 Effects of pharmacological AMPA-receptor potentiation on TMS-EEG evoked potentials: a randomized, double-blind, placebo-controlled, crossover study in healthy subjects
69	CHAPTER 4 Effects of mexiletine and lacosamide on nerve excitability in healthy subjects: a randomized, double-blind, placebo-controlled, crossover study
101	CHAPTER 5 Muscle velocity recovery cycles as pharmacodynamic biomarker: effects of mexiletine in a randomized double-blind placebo-controlled cross-over study
131	CHAPTER 6 Safety, pharmacokinetics, and pharmacodynamics of a ClC-1 inhibitor – a first-in-class compound that enhances muscle excitability: a Phase I, single- and multiple-ascending dose study
163	CHAPTER 7 First in class ClC-1 inhibitor improves skeletal muscle function in animal models and patients with myasthenia gravis
205	CHAPTER 8 Discussion and conclusions
219	Nederlandse samenvatting
225	Curriculum vitae
227	List of publications

CHAPTER I
INTRODUCTION



EXCITABILITY OF THE CORTEX, PERIPHERAL NERVES, AND SKELETAL MUSCLES

The human cortex, peripheral nerves and skeletal muscles are excitable tissues. Excitability is defined as the characteristic of certain cells to react to stimuli through fluctuations in membrane potential,³⁹ thereby allowing our cell membranes to carry electrical signals throughout the body.¹ These electrical signals facilitate the transmission of impulses and are therefore critical to the function of neuronal and muscular tissues. Membrane potential changes are caused by fluctuations in permeability to sodium-, potassium-, calcium- and chloride-ions.¹ Ion channels are responsible for those changes in membrane permeability and the function of electrically excitable cells therefore largely relies on those channels. Voltage-gated ion channels open and close due to changes in membrane potential, neurotransmitter-gated ion channels function in response to neurotransmitters.² A wide range of neurological, (neuro-)muscular, and psychiatric diseases is related to abnormalities in excitability. For example, abnormalities in cortical excitability are found in epilepsy;³ abnormalities in cortical⁴⁻⁸ and nerve excitability⁹⁻¹³ in amyotrophic lateral sclerosis (ALS); and abnormalities in skeletal muscle excitability in myotonia congenita.¹⁴ Potential treatments for disorders related to excitability of neurons and muscle cells lie in the modulation of these voltage-gated and neurotransmitter-gated ion channels, which makes these proteins highly interesting as pharmacological targets.²

For development of novel drugs targeting excitability, it is critical to have biomarkers for pharmacodynamic effects in the early phase of drug development. Conventional clinical drug development relies on four different phases, starting with testing of safety and tolerability in healthy human subjects. For novel compounds with pioneering biological or therapeutic mechanisms, this linear approach may be unsuitable. Although assessment of safety is crucial, a pharmacological approach to early phase drug development can greatly improve the developmental process.¹⁵ A drug can be confirmed safe and tolerable in a small group of healthy subjects, but the administered dose range may not be pharmacologically active, leading to negative therapeutic findings in patient studies. Alternatively, when a drug is dosed above the therapeutic window, the early studies may show serious safety concerns, leading to discontinuation of further development, although the pharmacological mechanism may

have been of great therapeutic value. Solely testing safety and tolerability in early phase studies, without evaluation of pharmacological action of the drug, may therefore lead to risks for study participants and increased developmental costs.¹⁶ Valid biomarkers of pharmacodynamic effects could help determine the likely pharmacologically active dose range. Firstly, such a measure could help translation from preclinical studies to the first administration in humans. Pharmacokinetic-pharmacodynamic modelling then could assist in the prediction of (minimally) pharmacologically active dose between species. Secondly, a pharmacodynamic biomarker could show target engagement in healthy subjects, and thereby provide proof-of-pharmacology, in studies with novel biological mechanisms. Early detection of pharmacological effects could reduce uncertainty and could thereby improve the safety of study participants and add financial value. If such a biomarker responds in a dose-dependent manner, it could also guide dose-escalation studies in healthy subjects alongside safety measures. Lastly, a biomarker for pharmacodynamic effects may assist adequate dose-finding in the translation to patient studies.

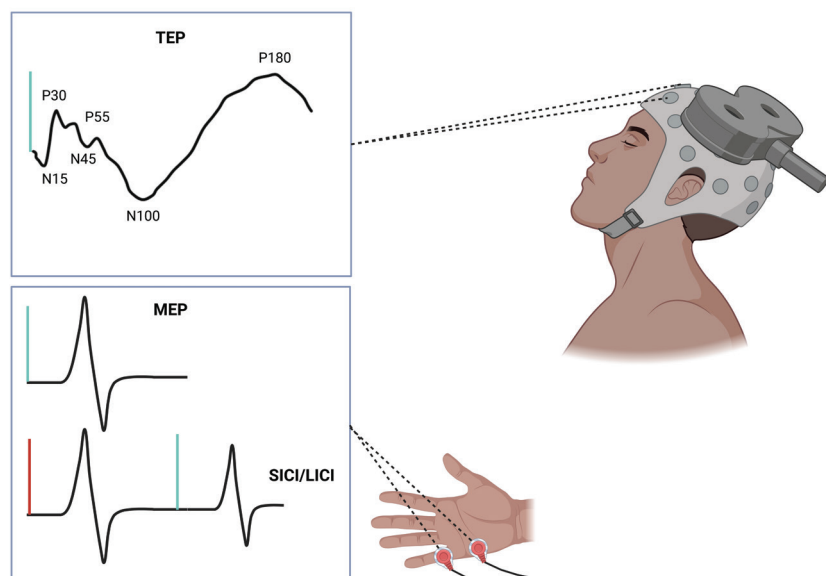
Clinical drug research focused on the field of neuronal and skeletal muscle excitability currently lacks reliable (translational) biomarkers for pharmacological target engagement and would therefore benefit greatly from development of these tools. This thesis describes the validation and implementation of three existing clinical measurements of excitability for use in clinical drug development: transcranial magnetic stimulation (TMS) combined with electromyography (EMG) and electroencephalography (EEG) for the evaluation of cortical excitability; nerve excitability threshold tracking (NETT) to determine peripheral nerve excitability; and muscle velocity recovery cycles (MVRC) to explore skeletal muscle membrane excitability.

CORTICAL EXCITABILITY

TMS is a non-invasive brain stimulation technique (Figure 1). Strong electrical currents in the TMS coil generate a magnetic pulse, which can generate a cortical action potential by activation of voltage-gated sodium channels.¹⁷ When directed at the motor cortex, this action potential can lead to muscle activation in a target muscle. To quantify this response, TMS-EMG can be used to measure a motor-evoked potential (MEP), as a measure of cortico-spinal excitability.¹⁸ The MEP is quantified

by measuring the peak-to-peak amplitude of the muscle action potential. Moreover, long- and short intracortical inhibition (LICI and sICI) can be evaluated by measuring the MEP amplitude after paired TMS pulses at different interstimulus intervals (ISI). Alternatively, TMS-EEG can be used to assess the direct brain response as a TMS-evoked potential (TEP).¹⁹ These responses are quantified using amplitudes of positive (P) and negative (N) deflections in the TEP, at set timepoints after stimulation. N15, P30, N45, P55, N100 and P180 therefore reflect positive and negative amplitudes 15, 30, 45, 55 100 and 180 ms after the test pulse.

FIGURE 1 Transcranial magnetic stimulation (TMS) combined with electro-encephalography to explore the cortical response using a TMS-evoked potential (TEP) (upper graph). TMS combined with electromyography to evaluate the motor-evoked potential (MEP) and short- and long intracortical inhibition (sICI/LICI) at the abductor digiti minimi (lower graph). Created with Biorender.com.



A multitude of studies has been performed evaluating pharmacological effects on cortico-spinal excitability using TMS-EMG.¹⁷ Drug targets investigated using TMS-EMG include (but are not limited to) sodium channel blockers, potassium channel modulators, and γ -aminobutyric acid-A ($GABA_A$) and $GABA_B$ agonists.²⁰ These studies show that TMS-EMG is

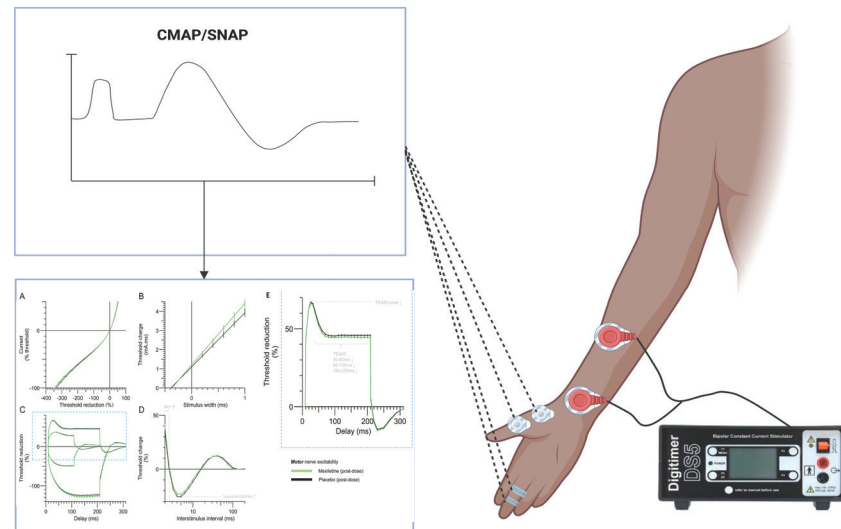
sensitive to pharmacological effects of drug targeting cortical excitability. Studies to investigate pharmacodynamic effects on TMS-EEG are more limited, and the knowledge of the neurophysiology behind the TEP is yet largely unclear. Pharmacological challenges using registered drugs, such as benzodiazepines and levetiracetam/brivaracetam, help to identify the meaning of the different TEP components.²¹ To our knowledge, studies using TMS-EMG/EEG as biomarker in early phase drug development with novel compounds are scarce. However, effects of a novel potassium channel opener²² and a $\alpha 5$ - $GABA_A$ receptor antagonist²³ were investigated in the early development phase using TMS-EMG/EEG, and these studies support the use of this biomarker for this purpose.

The first study that we performed using TMS, contributes to the growing body of evidence by repeating results from previous TMS-EMG/EEG studies on pharmacodynamic effects of levetiracetam and lorazepam, and adds to existing literature as the first study to evaluate effects of valproic acid on TMS-EEG. Moreover, we evaluated the variability of the measure and feasibility for use in studies to investigate novel drug molecules. The second study applies the technique in early-phase drug development, by exploring effects of a novel α -amino-3-hydroxy-5-methyl-4-isoxazolepropionic acid (AMPA) glutamate receptor positive allosteric modulator on TMS-EEG. The latter study also included TMS-EMG, of which the results are published separately.²⁴ This study demonstrates that TMS-EMG may also be used as translational biomarker of pharmacological effects in animals to humans.

PERIPHERAL NERVE EXCITABILITY

NETT provides information on axonal membrane excitability and ion channel properties at the site of stimulation (Figure 2).²⁵ In our study, the median nerve was stimulated using electrical currents at the wrist. For evaluation of motor nerve excitability, compound muscle action potentials (CMAP) were recorded in the abductor pollicis brevis; for sensory nerve excitability, sensory nerve action potentials (SNAP) were measured at digit two or three. The technique uses a 'threshold tracking' stimulation paradigm, which means that the stimulus intensity is adjusted based on a set threshold.²⁵ Threshold is defined as 40% of the maximum CMAP. Using four different stimulation protocols, the method explores different properties of the axonal membrane potential.²⁶

FIGURE 2 Nerve excitability threshold tracking (NETT) uses electrical stimulation of the median nerve (red electrodes) to measure the amplitude of the compound muscle action potentials (CMAP) at the abductor pollicis brevis; and peak-to-peak amplitude of the sensory nerve action potentials (SNAP) at digit three (upper graph). A stimulation paradigm is used to evaluate different excitability properties (lower graph shows NETT recording). Created with Biorender.com.



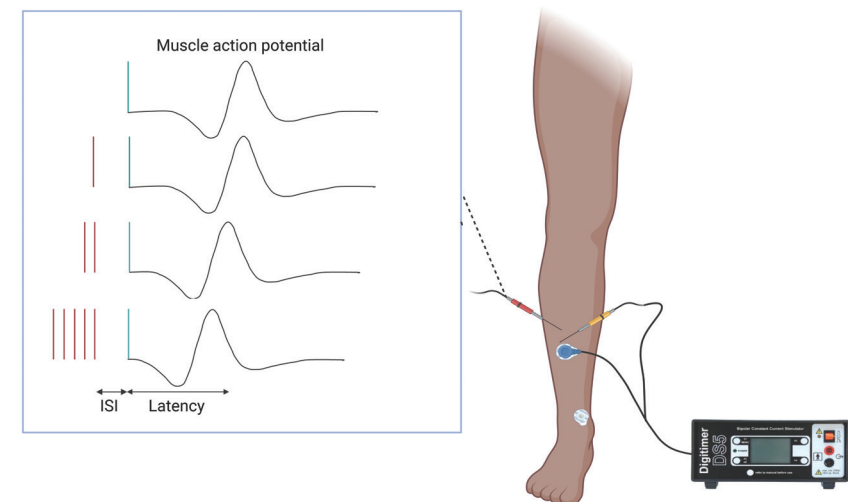
In contrast to the extensive literature describing drug effects on TMS-EMG, only a handful of studies describe pharmacological effects on NETT in humans. Previous studies describe the effects of sodium channel blockers, namely tetrodotoxin due to accidental puffer fish intoxication;²⁷ effects of a regional nerve block by lidocaine;²⁸ and effects of mexiletine in patients with chronic pain²⁹ and Machado-Joseph disease.³⁰ Moreover, acute pharmacological effects of retigabine and riluzole in patients with ALS have been described.^{31,32} In healthy subjects, neuronal excitability during general anaesthesia using propofol and sevoflurane have been studied.³³ Another example where NETT has been used to measure treatment effects, was with nusinersen in patients with spinal muscular atrophy.³⁴ To our knowledge NETT has not been used as biomarker in early phase drug development. No previous study compared acute, systemic, sodium blocking effects on NETT to placebo in healthy subjects. Therefore, our study evaluates the test-retest reliability, and effects of two registered sodium channel blockers-mexiletine and lacosamide- on both motor- and

sensory nerve excitability. Such a study is crucial as proof-of-concept, to explore whether NETT would be valuable as pharmacodynamic biomarker in early phase drug development.

SKELETAL MUSCLE EXCITABILITY

The measurement of MVRC provides a surrogate measure of muscle cell membrane excitability (Figure 3).³⁵ By direct electrical stimulation of the tibial muscle using a needle electrode, the muscle fibres are activated independent of neuromuscular transmission. The method uses the latency from stimulus to muscle action potential as a measure of velocity. A stimulation paradigm is applied with single stimuli, as well as (1, 2 and 5) conditioning pulses, followed by a test pulse at different ISIs. The physiological muscle action potential consists of a refractory period, followed by two periods of depolarization and increased excitability. MVRC can be used to quantify these two periods of supernormality as an increase in velocity due to conditioning pulses.³⁵

FIGURE 3 For muscle velocity recovery cycles (MVRC) electrical stimulation of the tibial anterior muscle fibres using a needle electrode (yellow) creates a muscle action potential, which is recorded using a second needle electrode (red). The latency of the muscle action potential is measured after single test pulses (blue), and (1, 2 and 5) conditioning pulses (red) followed by a test pulse (blue) at different interstimulus intervals (ISI). Created with Biorender.com.



MVRC has been used in previous research to discriminate between health and disease, such as myotonic dystrophy³⁶ and myotonia congenita.¹⁴ No previous studies report the use of MVRC as a pharmacological biomarker. The only article to secondarily describe treatment effects, compares patients with myotonia congenita using sodium channel blocking medication, to patients off treatment, with significant findings.¹⁴ Therefore, this thesis is the first to describe the capabilities of MVRC as pharmacodynamic biomarker and its implementation in an early phase drug study. First, we performed a study to evaluate the variability of MVRC, and to explore whether effects of mexiletine – a sodium channel blocker – can be detected in healthy subjects using MVRC. Mexiletine was chosen as proof-of-concept because it is known to decrease muscle excitability by inhibition of voltage-gated sodium channel subtype α_1 in muscle fibres.^{37,38} After validation of the method, we used MVRC as a pharmacodynamic biomarker in a Phase I trial with a muscle-specific ClC-1 inhibitor – a novel drug developed to enhance muscle excitability in patients with neuromuscular disease. MVRC was implemented in the first-in-human single- and multiple-ascending dose study in healthy subjects to confirm target engagement. After that, effects of ClC-1 inhibition on muscle excitability were evaluated using MVRC in the first-in-patient trial in patients with myasthenia gravis.

AIMS OF THIS THESIS

In conclusion, with the research presented in this thesis we evaluate the potential of TMS-EMG/EEG, NETT, and MVRC, as measures of excitability in early phase clinical drug development. For this purpose, each of the three measurements is first tested in a proof-of-concept study using registered drugs, that are known to influence excitability through ion channel modulation. We assessed whether significant treatment effects could be detected using these techniques. Moreover, we evaluated feasibility and test-retest reliability of the measurements. Secondly, after validation of the methods, and confirmation of their sensitivity to pharmacodynamic effects, we implemented the measurements in early-phase clinical drug studies, which are described in this thesis.

REFERENCES

- Neumann E. Chemical representation of ion flux gating in excitable biomembranes. *Neurochem Int.* 1980;2C:27-43. doi:10.1016/0197-0186(80)90009-1
- Camerino DC, Tricarico D, Desaphy JF. Ion channel pharmacology. *Neurotherapeutics.* 2007;4(2):184-198. doi:10.1016/j.nurt.2007.01.013
- de Goede AA, Ter Braack EM, van Putten MJAM. Single and paired pulse transcranial magnetic stimulation in drug naïve epilepsy. *Clin Neurophysiol.* 2016;127(9):3140-3155. doi:10.1016/j.clinph.2016.06.025
- Zanette G, Tamburin S, Manganotti P, Refatti N, Forgiione A, Rizzuto N. Different mechanisms contribute to motor cortex hyperexcitability in amyotrophic lateral sclerosis. *Clin Neurophysiol.* 2002;113(11):1688-1697. doi:10.1016/S1388-2457(02)00288-2
- Menon P, Geevasinga N, van den Bos M, Yiannikas C, Kiernan MC, Vucic S. Cortical hyperexcitability and disease spread in amyotrophic lateral sclerosis. *Eur J Neurol.* 2017;24(6):816-824. doi:10.1111/ene.13295
- Dharmadasa T, Matamala JM, Howells J, Vucic S, Kiernan MC. Early focality and spread of cortical dysfunction in amyotrophic lateral sclerosis: A regional study across the motor cortices. *Clin Neurophysiol.* 2020;131(4):958-966. doi:10.1016/j.clinph.2019.11.057
- Ziemann U, Winter M, Reimers CD, Reimers K, Tergau F, Paulus W. Impaired motor cortex inhibition in patients with amyotrophic lateral sclerosis. Evidence from paired transcranial magnetic stimulation. *Neurology.* 1997;49(5):1292-1298. doi:10.1212/wnl.49.5.1292
- Vucic S, Ziemann U, Eisen A, Hallett M, Kiernan MC. Transcranial magnetic stimulation and amyotrophic lateral sclerosis: pathophysiological insights. *J Neurol Neurosurg Psychiatry.* 2013;84(10):1161-1170. doi:10.1136/jnnp-2012-304019
- Geevasinga N, Menon P, Howells J, Nicholson GA, Kiernan MC, Vucic S. Axonal ion channel dysfunction in c9orf72 familial amyotrophic lateral sclerosis. *JAMA Neurol.* 2015;72(1):49-57. doi:10.1001/JAMANEUROL.2014.2940
- Menon P, Kiernan MC, Vucic S. ALS pathophysiology: insights from the split-hand phenomenon. *Clin Neurophysiol.* 2014;125(1):186-193. doi:10.1016/j.clinph.2013.07.022
- Kanai K, Kuwabara S, Misawa S, et al. Altered axonal excitability properties in amyotrophic lateral sclerosis: impaired potassium channel function related to disease stage. *Brain.* 2006;129(Pt 4):953-962. doi:10.1093/brain/awo24
- Park SB, Kiernan MC, Vucic S. Axonal Excitability in Amyotrophic Lateral Sclerosis : Axonal Excitability in ALS. *Neurotherapeutics.* 2017;14(1):78-90. doi:10.1007/s13311-016-0492-9
- Vucic S, Kiernan MC. Axonal excitability properties in amyotrophic lateral sclerosis. *Clin Neurophysiol.* 2006;117(7):1458-1466. doi:10.1016/j.clinph.2006.04.016
- Tan SV, Z'Graggen WJ, Boërio D, et al. Chloride channels in myotonia congenita assessed by velocity recovery cycles. *Muscle Nerve.* 2014;49(6):845-857. doi:10.1002/mus.24069
- Cohen AF, Burggraaf J, van Gerven JMA, Moerland M, Groeneveld GJ. The use of biomarkers in human pharmacology (Phase I) studies. *Annu Rev Pharmacol Toxicol.* 2015;55:55-74. doi:10.1146/annurev-pharmtox-011613-135918
- Cohen AF. Developing drug prototypes: pharmacology replaces safety and tolerability? *Nat Rev Drug Discov.* 2010;9(11):856-865. doi:10.1038/nrd3227
- Barker AT, Jalinous R, Freeston IL. Non-invasive magnetic stimulation of human motor cortex. *Lancet.* 1985;1(8437):1106-1107. doi:10.1016/S0140-6736(85)92413-4
- Abbruzzese G, Trompetto C. Clinical and research methods for evaluating cortical excitability. *J Clin Neurophysiol.* 2002;19(4):307-321. doi:10.1097/00004691-200208000-00005
- Ilmoniemi RJ, Virtanen J, Ruohonen J, et al. Neuronal responses to magnetic stimulation reveal cortical reactivity and connectivity. *Neuroreport.* 1997;8(16):3537-3540. doi:10.1097/00001756-199711000-00024
- Ziemann U, Reis J, Schwenkreis P, et al. TMS and drugs revisited 2014. *Clin Neurophysiol.* 2015;126(10):1847-1868. doi:10.1016/j.clinph.2014.08.028
- Darmani G, Ziemann U. Pharmacophysiology of TMS-evoked EEG potentials: A mini-review. *Brain Stimul.* 2019;12(3):829-831. doi:10.1016/j.brs.2019.02.021
- Premoli I, Rossini PG, Goldberg PY, et al. TMS as a pharmacodynamic indicator of cortical activity of a novel anti-epileptic drug, XEN1101. *Ann Clin Transl*

- Neurol. 2019;6(11):2164-2174. doi:10.1002/acn3.50896
- 23 Darmani G, Zipser CM, Böhmer GM, et al. Effects of the Selective α_5 -GABA_AR Antagonist S44819 on Excitability in the Human Brain: A TMS-EMG and TMS-EEG Phase I Study. *J Neurosci*. 2016;36(49):12312-12320. doi:10.1523/JNEUROSCI.1689-16.2016
 - 24 O'Donnell P, Dijkstra FM, Damar U, et al. Transcranial magnetic stimulation as a translational biomarker for AMPA receptor modulation. *Transl Psychiatry*. 2021;11(1):325. doi:10.1038/s41398-021-01451-2
 - 25 Bostock H, Cikurel K, Burke D. Threshold tracking techniques in the study of human peripheral nerve. *Muscle Nerve*. 1998;21(2):137-158. doi:10.1002/(sici)1097-4598(199802)21:2<137::aid-mus1>3.0.co;2-c
 - 26 Kiernan MC, Bostock H, Park SB, et al. Measurement of axonal excitability: Consensus guidelines. *Clin Neurophysiol*. 2020;131(1):308-323. doi:10.1016/j.clinph.2019.07.023
 - 27 Kiernan MC, Isbister GK, Lin CSY, Burke D, Bostock H. Acute tetrodotoxin-induced neurotoxicity after ingestion of puffer fish. *Ann Neurol*. 2005;57(3):339-348. doi:10.1002/ana.20395
 - 28 Moldovan M, Lange KHW, Aachmann-Andersen NJ, Kjær TW, Olsen NV, Krarup C. Transient impairment of the axolemma following regional anaesthesia by lidocaine in humans. *J Physiol*. 2014;592(13):2735-2750. doi:10.1113/jphysiol.2014.270827
 - 29 Kuwabara S, Misawa S, Tamura N, et al. The effects of mexiletine on excitability properties of human median motor axons. *Clin Neurophysiol*. 2005;116(2):284-289. doi:10.1016/j.clinph.2004.08.014
 - 30 Kanai K, Kuwabara S, Arai K, Sung JY, Ogawara K, Hattori T. Muscle cramp in Machado-Joseph disease: altered motor axonal excitability properties and mexiletine treatment. *Brain*. 2003;126(Pt 4):965-973. doi:10.1093/brain/awg073
 - 31 Kovalchuk MO, Heuberger JAAC, Sleutjes BTHM, et al. Acute Effects of Riluzole and Retigabine on Axonal Excitability in Patients With Amyotrophic Lateral Sclerosis: A Randomized, Double-Blind, Placebo-Controlled, Crossover Trial. *Clin Pharmacol Ther*. 2018;104(6):1136-1145. doi:10.1002/cpt.1096
 - 32 Wainger BJ, Macklin EA, Vucic S, et al. Effect of Ezogabine on Cortical and Spinal Motor Neuron Excitability in Amyotrophic Lateral Sclerosis: A Randomized Clinical Trial. *JAMA Neurol*. 2021;78(2):186-196. doi:10.1001/JAMANEUROL.2020.4300
 - 33 Maurer K, Wacker J, Vastani N, Seifert B, Spahn DR. Changes in axonal excitability of primary sensory afferents with general anaesthesia in humans. *Br J Anaesth*. 2010;105(5):648-656. doi:10.1093/bja/aeq218
 - 34 Kariyawasam DST, D'Silva AM, Herbert K, et al. Axonal excitability changes in children with spinal muscular atrophy treated with nusinersen. *J Physiol*. 2022;600(1):95-109. doi:10.1113/JP282249
 - 35 Z'Graggen WJ, Bostock H. Velocity recovery cycles of human muscle action potentials and their sensitivity to ischemia. *Muscle Nerve*. 2009;39(5). doi:10.1002/mus.21192
 - 36 Tan SV, Z'Graggen WJ, Boërio D, Turner C, Hanna MG, Bostock H. In vivo assessment of muscle membrane properties in myotonic dystrophy. *Muscle Nerve*. 2016;54(2). doi:10.1002/mus.25025
 - 37 Wang GK, Russell C, Wang SY. Mexiletine block of wild-type and inactivation-deficient human skeletal muscle hNav1.4 Na⁺ channels. *J Physiol*. 2004;554(3):621-633. doi:https://doi.org/10.1113/jphysiol.2003.054973
 - 38 Logigian EL, Martens WB, Moxley RT 4th, et al. Mexiletine is an effective antimyotonia treatment in myotonic dystrophy type 1. *Neurology*. 2010;74(18):1441-1448. doi:10.1212/WNL.0b013e3181dca3a
 - 39 Excitability - Latest research and news | Nature. Accessed January 18, 2024. <https://www.nature.com/subjects/excitability>





CHAPTER 2

**TRANSCRANIAL MAGNETIC
STIMULATION AS BIOMARKER OF
EXCITABILITY IN DRUG DEVELOPMENT:
A RANDOMIZED, DOUBLE-BLIND,
PLACEBO-CONTROLLED, CROSS-OVER STUDY**

Br J Clin Pharmacol. 2022; 88(6): 2926-2937. doi:10.1111/bcp.15232

Titia Q. Ruijs^{1,3}, Jules A.A.C. Heuberger¹, Annika A. de Goede^{1,2}, Dimitrios Ziagos¹,
Marije E. Otto¹, Robert J. Doll¹, Michel J.A.M. van Putten², Geert Jan Groeneveld^{1,3}

1. Centre for Human Drug Research, Leiden, NL
2. University of Twente, Enschede, NL
3. Leiden University Medical Centre, Leiden, NL

ABSTRACT

The purpose of this study was to investigate pharmacodynamic effects of drugs targeting cortical excitability using transcranial magnetic stimulation (TMS) combined with electromyography (EMG) and electroencephalography (EEG) in healthy subjects, to further develop TMS outcomes as biomarkers for proof-of-mechanism in early phase clinical drug development. Anti-epileptic drugs presumably modulate cortical excitability. Therefore, we studied effects of levetiracetam, valproic acid and lorazepam on cortical excitability in a double-blind, placebo-controlled, four-way cross-over study. In 16 healthy male subjects, single- and paired-pulse TMS-EMG/EEG measurements were performed pre-dose and 1.5, 7, and 24 hours post-dose. Treatment effects on motor-evoked potential (MEP), short (sICI) and long intra-cortical inhibition (LICI) and TMS-evoked potential (TEP) amplitudes, were analysed using a mixed model ANCOVA and cluster-based permutation analysis. We show that MEP amplitudes decreased after administration of levetiracetam (estimated difference (ED) -378.4 μ V; 95% confidence interval (95%CI): -644.3 μ V, -112.5 μ V; $p < 0.01$), valproic acid (ED -268.8 μ V; 95%CI: -532.9 μ V, -4.6 μ V; $p = 0.047$) and lorazepam (ED -330.7 μ V; 95%CI: -595.6 μ V, -65.8 μ V; $p = 0.02$) when compared with placebo. LICI was enhanced by levetiracetam (ED -60.3%; 95%CI: -87.1%, -33.5%; $p < 0.001$) and lorazepam (ED -68.2%; 95%CI: -94.7%, -41.7%; $p < 0.001$) at a 50 ms interstimulus interval. Levetiracetam increased TEP-component N45 ($p = 0.004$) in a central cluster and decreased N100 ($p < 0.001$) in a contralateral cluster.

In conclusion, this study shows that levetiracetam, valproic acid and lorazepam decrease cortical excitability, which can be detected using TMS-EMG/EEG in healthy subjects. These findings provide support for the use of TMS excitability measures as biomarkers to demonstrate pharmacodynamic effects of drugs that influence cortical excitability.

INTRODUCTION

Transcranial magnetic stimulation (TMS) is a non-invasive technique which can be used to investigate corticospinal excitability. Stimulation targeted at the motor cortex generates motor evoked potentials (MEP) and TMS-evoked potentials (TEP), that can be quantified by electromyography (EMG)¹ and electroencephalography (EEG),^{2,3} respectively. TMS-EMG and TMS-EEG facilitate assessment of different measures of cortical excitability, using a single pulse (sp) and paired pulse (pp) stimulation paradigm, of which the latter facilitates assessment of intra-cortical inhibition.^{4,5} This study is intended to broaden and deepen the knowledge about effects of anti-epileptic drugs (AEDs) on TMS-EMG/EEG outcomes, to further develop these outcomes as biomarkers for pharmacodynamic effects on cortical excitability. Although TMS-EMG has been widely used to assess the effects of drugs targeted at cortical excitability,⁶ the number of research groups investigating pharmacological effects on TEPs is limited.⁷⁻¹³ There is abundant space for further progress in replicating and extending the current knowledge about cortical excitability and in showing the value of TMS to measure biomarkers for pharmacodynamic effects in early phase drug development.⁷ Before being able to use TMS-related outcomes in clinical drug development with new pharmacological targets, it is of importance to determine the sensitivity of the measurement to detect pharmacological effects in healthy subjects, and the typical effect size of regularly used drugs administered at a dose within the therapeutic range. A reliable biomarker is a valuable investigative tool in clinical drug development, particularly in the development of new pharmacological treatments for diseases with underlying pathology related to cortical excitability, such as epilepsy^{14,15} and amyotrophic lateral sclerosis.¹⁶ The goal would be to use TMS-EMG/EEG outcomes as biomarkers for proof-of-mechanism.

Therefore, the primary objective of this study was to evaluate effects of three commonly prescribed AEDs (levetiracetam, valproic acid, and lorazepam) on cortical excitability in a placebo-controlled, cross-over fashion in healthy subjects. These AEDs are expected to decrease cortical excitability with distinct mechanisms of action. The secondary objective was to evaluate intra- and inter-subject variability of cortical excitability measures.

MATERIALS AND METHODS

This study was approved by the Ethics Committee ‘Stichting Beoordeling Ethiek Biomedisch Onderzoek’, Assen, The Netherlands. The trial was executed in accordance to the Declaration of Helsinki at the Centre for Human Drug Research (CHDR), Leiden, The Netherlands, between September 2017 and February 2018. The study is registered in the Dutch Trial Registry (NTR) under NL6638.

SUBJECTS Subjects gave written informed consent. Healthy male subjects between 18 and 45 years were recruited using online advertisements and CHDR’s subject database. Eligibility was confirmed by a medical screening up to 30 days before the first dose, consisting of evaluation of medical history, physical examination, electrocardiogram, blood chemistry, haematology, and urinalysis. Subjects with contra-indications according to the TMS safety questionnaire¹⁷ were excluded, as well as subjects with an abnormal sleeping pattern, (history of) illicit drug or alcohol abuse or a positive test for such substances, nicotine use a month before dosing, or a resting motor threshold (rMT) of >83% of the maximum stimulator output (MSO). Use of medication was prohibited from 14 days prior to the first dose. Use of caffeine was prohibited from 24 hours before dosing.

EXPERIMENTAL DESIGN This is a randomized, double-blind, double-dummy, placebo-controlled, cross-over study. On four visits, subjects received a single dose of levetiracetam 2000 mg (Levetiracetam, oral solution 100mg/mL, Aurobindo) and placebo capsules; valproic acid 1000 mg (Depakine sugarfree oral solution 200 mg/5mL, Sanofi-aventis) and placebo capsules; lorazepam 2 mg (Lorazepam, 2 tablets of 1 mg, Apotex Europe BV) and placebo solution; or placebo solution and placebo capsules. Lorazepam tablets were encapsulated, and matching placebo capsules and solutions were produced. Drug doses were chosen within the therapeutic range. A Williams design was used to balance first-order carry-over effects.¹⁸ The randomization of the treatment order was generated in SAS (version 9.4, SAS Institute Inc., Cary, USA) by a statistician uninvolved with data collection. The randomization remained blinded for all staff, apart from the statistician and the pharmacy preparing the medication. Subjects were enrolled by a blinded physician.

Subjects remained fasted from minimally eight hours before until two hours after dosing. TMS-EMG-EEG measurements were performed before dosing and 1.5, 7 and 24 hours after dosing, based on the pharmacokinetic (PK) profile of the study drugs. The first post-dose measurement was performed around T_{max} , the second when an intermediate plasma concentration was expected, and the third at low concentrations. Measurements were performed at approximately the same clock time for all subjects, to minimize potential effects of diurnal variation on TMS outcomes. Samples for PK analysis were drawn directly before all TMS measurements and directly after the measurement at 1.5 hours post-dose. Additionally, samples were obtained at 0.5, and 3.5 hours post-dose. Between each study visit was a wash-out of at least seven days. There was a safety follow-up seven to ten days after the last dose.

TRANSCRANIAL MAGNETIC STIMULATION Sp and ppTMS were applied according to guidelines by Rossi and colleagues,¹⁹ using a MagPro R30 with MagOption stimulator and a MCF-B65 butterfly coil (MagVenture GmbH, Hückelhoven, Germany).

Stimulation was performed at the motor hotspot of the dominant abductor digiti minimi (ADM) muscle as determined by the Edinburgh Handedness questionnaire.²⁰ The TMS coil was fixated using a frame at an angle of 45° from the midline, in direct contact with the EEG cap. At the start of each measurement, rMT was determined as the lowest stimulus intensity at which a minimum of 5 out of 10 TMS pulses elicited a MEP with a peak-to-peak amplitude of at least 50 μ V.^{21,22} Hereafter, 50 single pulses were applied at 120% rMT. This was followed by 50 paired pulses at different inter-stimulus intervals (ISI), namely 2, 5, 50, 100, 150, 200, 250 and 300 ms, applied in randomized order (total 400 paired pulses). Conditioning and test pulses were applied at 120% rMT, except for ISIs 2 and 5 ms, where conditioning pulses were applied at an intensity of 80% rMT. The duration between single pulses and pairs of paired pulses was randomized between 3.5 and 4.5 seconds.

EMG and EEG acquisition EMG and EEG were registered simultaneously during TMS stimulation using NeuroCenter software (Clinical Science Systems, Leiden, The Netherlands). EMG was recorded with Ag/AgCl surface electrodes (Blue Sensor N, AMBU, Denmark) on the ADM and corresponding tendon. TEPs were registered using a TMS-compatible 32-leads EEG cap (ANT Neuro, Enschede, The Netherlands) and EEG amplifier

(TMSi, Oldenzaal, The Netherlands). The ground electrode, used for both EEG and EMG, was located between CZ and Fpz. Electrode impedances were below 5 k Ω and signals were amplified at a frequency of 2048 Hz. During the TMS measurements, subjects received in-ear headphones with masking noise to minimize auditory evoked potentials.²³ Adapted noise, based on the frequencies of the TMS click, was played at an intensity individualized for each subject with a maximum volume of 95 dB. Masking of auditory components appears to be sufficient as represented by lateralized responses in the topographical plots even at late latencies,²⁴ see Supplementary Figure 1.

DATA PROCESSING AND ANALYSIS The following parameters were extracted from the TMS-EMG data: single pulse rMT (% of M50) and mean peak-to-peak MEP amplitude (μ V); long intra-cortical inhibition (LICI) at ISIs of 50-300 ms, defined as the percentage ratio of the mean MEP amplitude after the test pulse and the mean MEP amplitude after the conditioning pulse; short intra-cortical inhibition (SICI) at ISIs of 2 and 5 ms, defined as the percentage ratio of the mean MEP amplitude after the test pulse and the mean amplitude of the unconditioned spMEPs.

MEP amplitude, SICI and LICI were calculated using in-house written MATLAB (version R2015a, The Mathworks, Natick, USA) scripts. To correct for pre-existing muscle activation, responses were excluded if muscle activity was $>50 \mu$ V in the 50 ms before each single or conditioning pulse.

TEPs were determined at all 32 EEG leads. EEG responses were analysed in common average montage and were baseline corrected by subtracting the average EEG amplitude 500-50 ms before applying the single or conditioning pulse. Individual EEG trials were defined from 100 ms before until 650 ms after each single or conditioning pulse. Principal component analysis (PCA) was used to reduce artefacts caused by TMS stimulation and muscle activation on the scalp.²⁵ The first four of 25 principal components were removed, after which individual trials were filtered (4th order Butterworth bandpass filter; 1-35 Hz) and averaged over 50 repetitions to create the TEP for each EEG lead. Per condition (placebo, levetiracetam, valproic acid and lorazepam) TEP responses after artefact removal are shown for each individual subject in the Supplementary Figures 2-5.

After all data was collected, review of the blinded TMS-EMG data was

performed as per standard operating procedure at CHDR. Measurements with technical errors were removed from analysis.

PK ANALYSIS Serum concentrations of levetiracetam were measured by a validated high-performance liquid chromatography diode array detection method at the ISO 15189 certified Clinical Pharmaceutical Laboratory of the Leiden University Medical Centre. Serum concentration of valproic acid were measured using an in vitro chemiluminescent microparticle immunoassay (CMIA) using an Abbott Architect system. The lower limit of quantification (LLOQ) was determined at 2.5 μ g/mL for levetiracetam and 2 μ g/mL for valproic acid. Serum lorazepam concentrations were analysed using an immunoassay at University Medical Centre Groningen. The LLOQ was 5.21 ng/mL. All assays were validated in accordance to the EMA bioanalytical method development guideline (all coefficients of variation (CV%) below 15%).

STATISTICAL ANALYSES Treatment effects were analysed up to 7 hours post-dose. We predefined that measurements performed at 24 hours after dosing would not be included due to the expected low drug concentrations at this time point but were measured for pharmacokinetic-pharmacodynamic (PKPD) modelling. Due to the exploratory nature of the study, no calculation of sample size was performed. Sample size was based on a previous pharmaco-TMS study in 15 healthy subjects.¹⁰

Statistical analysis of rMT, MEP and TEP endpoints was performed using a mixed model analysis of covariance (ANCOVA), with treatment, time, period, and treatment by time as fixed factors and subject, subject by treatment and subject by time as random factors, and the baseline measurement per period as covariate. Estimated differences between placebo and the AEDs were reported and statistical significance was defined at the 5% level. Analysis of effects on TMS-EMG endpoints was performed in SAS (version 9.4, SAS Institute Inc., Cary, USA).

Statistical analysis of TMS-EEG outcomes was performed using cluster-based permutation analysis (CBPA) incorporating all leads. CBPA was performed in Fieldtrip (Nijmegen, The Netherlands, downloaded 13-08-2015; <http://fieldtrip.fcdonders.nl>).²⁶ Comparison of drug versus placebo was performed using dependent samples t-tests, for each EEG

lead and time sample between 0-300 ms after the test pulse (both for sp- and ppTMS). To compensate for handedness, topographical plots of left-handed subjects were mirrored. Clusters were formed by t-values with a p-value <0.05, based on neighbouring leads ($n \geq 2$) and adjacent time samples. A permutation test (1500 times) was used to determine significance at the 5% level.²⁶ Additionally, we applied a Bonferroni correction ($N=3$) to compensate for multiple testing (three active conditions). Besides analysing the entire time sample of 300 ms after the test pulse, we applied the same analysis to time periods of interest (TOIs) around the TEP components (N15: 0-20 ms; P30: 20-40 ms; N45: 40-55 ms; P60: 55-80 ms; N100: 80-130 ms; P180: 130-230 ms).

For the purpose of evaluating repeatability, intra- and inter-subject variability were calculated, represented by CV%. CV% were calculated within the placebo visit, including measurements up to 7 hours post-dose, using estimates of covariance parameters produced by the mixed model analysis. The serum concentration of the AEDs was analysed using a non-compartmental analysis.

PKPD ANALYSIS Concentration-effect relationships between MEP amplitude and treatments (including all timepoints up to 24 hours post-dose) were investigated with non-linear mixed effects (NLME) modelling, using PK data linked to the closest available pharmacodynamic measurement in time. Tested PKPD-model structures included intercept (no effect), linear and non-linear (E_{max}) relationships, with additional inter-individual variability (IV) and/or between-occasion variability (BOV) for the baseline parameter. Initial analysis was performed in R (version 4.0.3, R Foundation for Statistical Computing, Vienna, Austria), where models were compared with an analysis of variance for nested models (p-value < 0.05) or with the Akaike Information Criterion (AIC, lowest value is favoured) for non-nested models. Treatments for which concentration-effect relationships other than intercept were selected, were also analysed using NONMEM (version 7.4, ICON Development Solutions, Hanover, USA), where models were compared based on drop in objective function value (DOFV > 3.84, $p < 0.05$) for one additional parameter for nested models or AIC for non-nested models.

NOMENCLATURE OF TARGETS AND LIGANDS Key protein targets and ligands in this article are hyperlinked to corresponding entries in <http://www.guidetopharmacology.org>, and are permanently archived in the Concise Guide to Pharmacology 2021/22.²⁷⁻²⁹

RESULTS

Seventeen subjects were enrolled in the study, of whom sixteen completed all study visits, for demographics see Table 1. One subject was excluded after one study visit, due to positive illicit drugs testing.

TABLE 1 Sample characteristics.

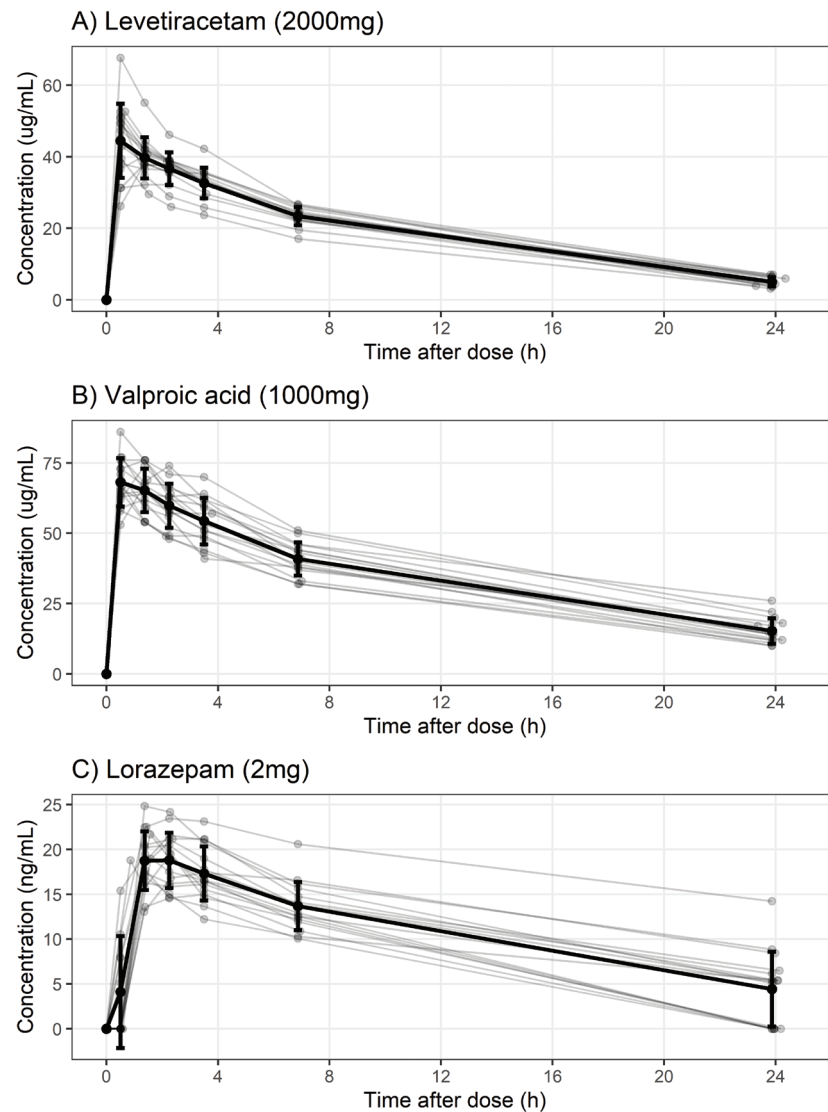
N=17	Mean	SD	Median	Range
Age (years)	25	6	24	20-44
Height (cm)	183	8	184	167-194
Weight (kg)	75	13	74	54-109
BMI (kg/m ²)	22	4	21	19-32

BMI = body mass index; SD = standard deviation.

The AEDs and TMS measurements were well tolerated. Individual, and mean \pm standard deviation serum concentrations of the AEDs are shown in Figure 1. Mean maximum concentrations (C_{max}) were 45.92 $\mu\text{g/mL}$ (range 32.10 – 67.60) for levetiracetam, 70.69 $\mu\text{g/mL}$ (range 58.00 – 86.00) for valproic acid and 19.79 ng/mL (range 14.99-24.84) for lorazepam. Mean serum concentrations per timepoint are also listed in Supplementary Table 1. Median T_{max} was 0.51 hours for levetiracetam (range 0.5-1.47 hours), and 0.53 hours for valproic acid (range 0.5-2.25 hours), corresponding to the first sampling point. The median T_{max} was 1.91 h (range 1.37-3.52 hours) for lorazepam, with 10 of 16 subjects showing a lag time of 30 minutes.

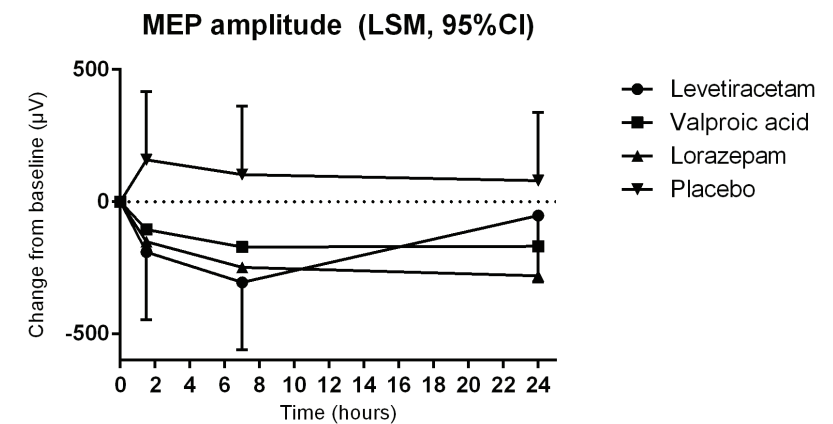
CORTICAL EXCITABILITY ASSESSED BY TMS-EMG In total, 192 measurements were recorded up to 7 hours post-dose. During blinded data review, six EMG recordings were excluded because of absence of MEPs (indicating there was no motor hotspot stimulation) or clipping of the EMG signal.

FIGURE 1 Individual and mean \pm standard deviation (SD) serum concentrations of levetiracetam, valproic acid and lorazepam.



Estimated mean post-dose MEP amplitudes were 889.3 μ V (placebo), 510.9 μ V (levetiracetam), 620.5 μ V (valproic acid) and 558.6 μ V (lorazepam). All AEDs significantly decreased MEP amplitude after spTMS when compared to placebo, with an estimated difference of -378.4 μ V (95%CI: -644.3, -112.5; $p < 0.01$) for levetiracetam, -268.8 μ V (95%CI: -532.9, -4.6; $p = 0.047$) for valproic acid, and -330.7 μ V (95%CI: -595.6, -65.8; $p = 0.02$) for lorazepam, see Figure 2. Intra-subject CV% of MEP amplitude was 35%, inter-subject CV% 84%.

FIGURE 2 Change from baseline of the least square means (LSM) of the MEP amplitude (μ V), using single pulse TMS, for levetiracetam, valproic acid, lorazepam and placebo.



Estimated mean post-dose rMT was 55.3%, 55.7%, 54.3% and 55.5% of MSO for placebo, levetiracetam, valproic acid and lorazepam, respectively. No significant treatment effects on rMT were detected when compared to placebo, with estimated differences of 0.4% for levetiracetam (95%CI: -1.1%, 1.9%; $p = 0.61$), -1.0% for valproic acid (95%CI: -2.5%, 0.5%; $p = 0.19$) and 0.2% for lorazepam (95%CI: -1.3%, 1.7%; $p = 0.78$). Intra-subject CV% of rMT was 4%, inter-subject CV% 14%.

Levetiracetam and lorazepam both significantly enhanced LIC1 compared to placebo at ISI 50 ms (i.e. the percentage ratio decreased, indicating more intra-cortical inhibition). No significant effects on LIC1 were detected at the other ISIs, nor on SIC1. Results and CV% for SIC1 and LIC1 are listed in Table 2.

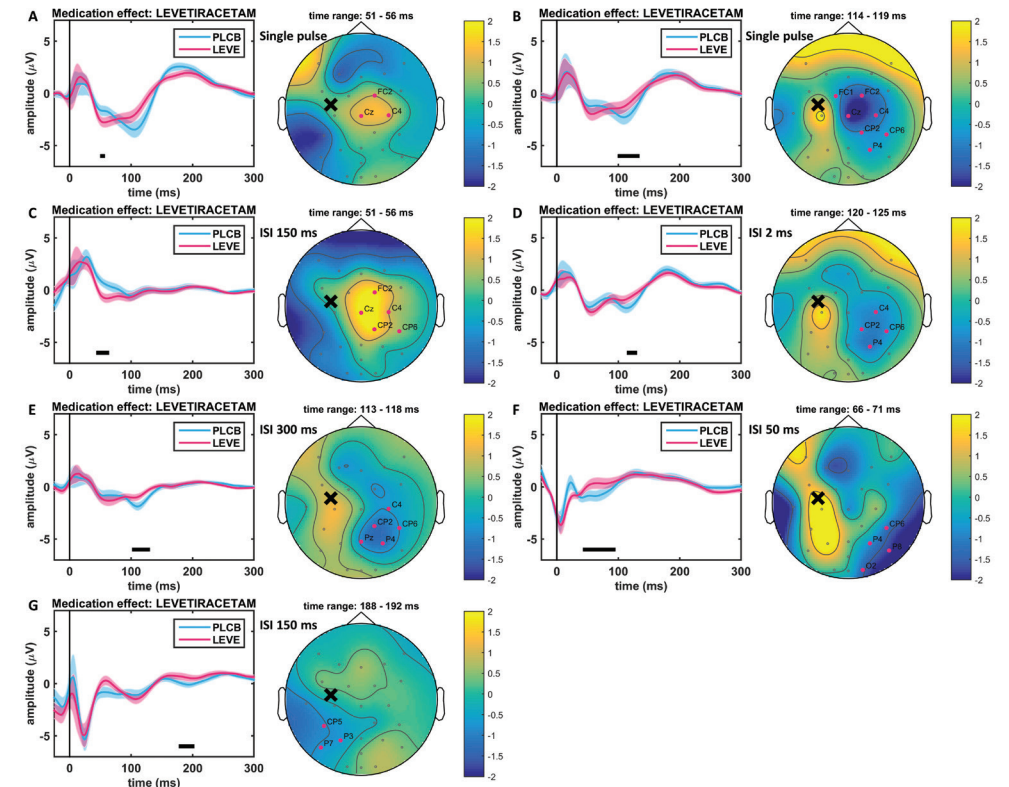
TABLE 2 Estimated mean (%) up to 7 hours of placebo, levetiracetam, valproic acid and lorazepam for long intra-cortical inhibition (LICI) and short intra-cortical inhibition (SICI) using paired-pulse TMS-EMG at 8 different interstimulus intervals (ISI). Estimated difference of placebo versus treatment (%), with 95% confidence interval (CI) and p-value. Intra-subject cv% (%) and inter-subject cv% (%) within the placebo occasion are listed.

ISI (ms)		Estimated mean relative amplitude of conditioned pulse to unconditioned pulse (%)	Estimated difference with placebo (%) (95% CI), p-value	Intra-subject cv%	Inter-subject cv%
2	Placebo	35.7		50%	58%
	Levetiracetam	42.4	6.7 (-6.5, 20.0), p= 0.31		
	Valproic Acid	48.5	12.8 (-0.4, 26.0), p= 0.06		
	Lorazepam	47.4	11.7, (-1.5, 24.9), p= 0.08		
5	Placebo	74.0		45%	48%
	Levetiracetam	78.5	4.5 (-20.9, 29.9), p= 0.72		
	Valproic Acid	88.7	14.7 (-10.4, 39.8), p=0.24		
	Lorazepam	90.4	16.4 (-9.1, 41.8), p= 0.20		
50	Placebo	102.9		85%	103%
	Levetiracetam	42.6	-60.3 (-87.1, -33.5), p<.001		
	Valproic Acid	78.0	-24.9 (-51.2, 1.4), p= 0.06		
	Lorazepam	34.7	-68.2 (-94.7, -41.7), p <.001		
100	Placebo	9.9		134%	172%
	Levetiracetam	7.3	-2.6 (-10.9, 5.6), p= 0.52		
	Valproic Acid	8.9	-1.0 (-9.2, 7.2), p= 0.81		
	Lorazepam	4.9	-5.0 (-13.3, 3.2), p= 0.22		
150	Placebo	19.9		92%	121%
	Levetiracetam	21.0	1.1 (-11.2, 13.5), p= 0.86		
	Valproic Acid	18.1	-1.8 (-14.0, 10.4), p= 0.77		
	Lorazepam	14.7	-5.2 (-17.6, 7.2), p= 0.40		
200	Placebo	64.4		38%	60%
	Levetiracetam	70.6	6.2 (-10.3, 22.8), p= 0.45		
	Valproic Acid	63.4	-1.0 (-17.6, 15.6), p= 0.91		
	Lorazepam	56.8	-7.6 (-24.1, 8.8), p= 0.36		
250	Placebo	64.7		47%	45%
	Levetiracetam	73.8	9.0 (-8.5, 26.6), p=0.31		
	Valproic Acid	77.7	13.0 (-4.3, 30.3), p= 0.14		
	Lorazepam	78.9	14.2 (-3.3, 31.6), p= 0.11		
300	Placebo	55.3		34%	49%
	Levetiracetam	54.4	-0.9 (-12.7, 10.9), p= 0.88		
	Valproic Acid	52.9	-2.4 (-14.0, 9.3), p= 0.68		
	Lorazepam	66.6	11.3 (-0.4, 23.1), p= 0.06		

CORTICAL EXCITABILITY ASSESSED BY TMS-EEG Of 192 TMS-EEG recordings, three were excluded after blinded data review of the EMG data, because of absence of MEPs.

For spTMS, levetiracetam significantly increased the N45 compared to placebo (p=0.004) in a centrally located cluster (Figure 3A). Furthermore, levetiracetam significantly decreased the N100 in a contralateral centro-parietal cluster (p<0.001) (Figure 3B).

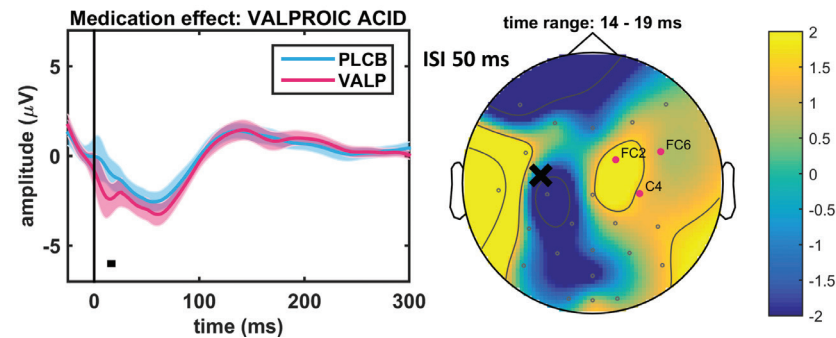
FIGURE 3 Significant clusters found using CBPA of TEPs, comparing placebo (PLCB; in blue) to levetiracetam (LEVE; in red). A) single pulse (N45 cluster), B) single pulse (N100 cluster), C) ISI 150 ms (N45/P60 cluster), D) ISI 2 ms (N100 cluster), E) ISI 300 ms (N100 cluster), F) ISI 50 ms (N45/P60/N100 cluster), and G) ISI 150 ms (P180 cluster). For each cluster the grand average (mean ± standard error of the mean (SEM)) over all significant electrodes is presented, as well as the difference in topographical distribution at the time of the cluster. The colors of the topographical plot of the cortex show the increase or decrease of amplitude (µV) of the response. The black cross represents the stimulation site, the red dots significant electrodes and the thick black bar below the average TEP response corresponds to the time interval with significant differences.



In line with the results for spTMS, levetiracetam significantly increased the N45 and P60 in a similar centro-parietal cluster at ISI 150 ms ($p < 0.001$ and $p = 0.004$, respectively) (Figure 3C). In addition, we found that levetiracetam significantly decreased N100 clusters at ISIs 2 and 300 ms ($p = 0.003$ and $p = 0.003$, respectively) (Figure 3D and 3E), these clusters are comparable to the N100 cluster found using spTMS. Furthermore, we found a significant N45, P60 and N100 cluster ($p = 0.004$, $p < 0.001$ and $p = 0.004$, respectively) at ISI 50 ms (Figure 3F). A significant P180 cluster ($p = 0.006$) was detected at ISI 150 ms (Figure 3G).

Valproic acid significantly increased the N15 amplitude ($p = 0.005$) at ISI 50 ms in a contralateral cluster (Figure 4). Lorazepam significantly decreased the N100 ($p = 0.001$) at ISI 300 ms in a contralateral parietal cluster (Figure 5).

FIGURE 4 Significant N15 cluster comparing paired pulse TEPs of placebo (PLCB; in blue) with valproic acid (VALP; in red) for ISI 50 ms. The grand average (mean \pm SEM) over all significant electrodes is presented, as well as the difference in topographical distribution at the time of the cluster. The colors of the topographical plot of the cortex show the increase or decrease of amplitude (μ V) of the response. The black cross represents the stimulation site, the red dots significant electrodes and the thick black bar below the average TEP response corresponds to the time interval with significant differences.

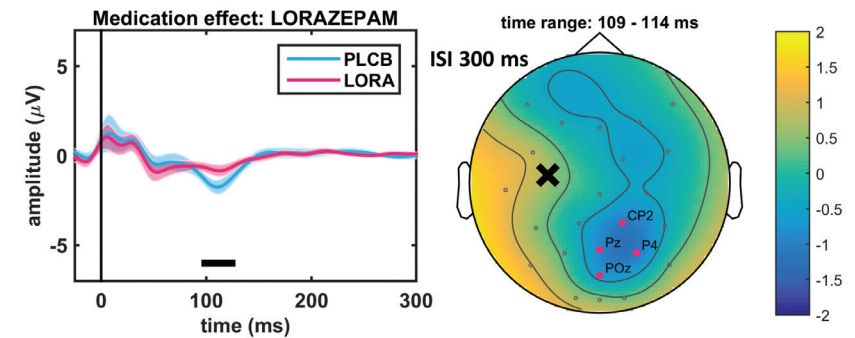


CONCENTRATION-EFFECT RELATIONSHIP OF MEP AMPLITUDE

A concentration-effect relationship between MEP amplitude and levetiracetam could be characterized with a proportional effect on baseline, described with an E_{\max} -equation ($p < 0.001$ compared to intercept only). IIV and BOV on the baseline parameter was log-normally distributed and statistically preferred over either IIV or BOV alone, although shrinkage

for BOV was moderate (25% and 33%). Parameters were estimated with small uncertainty (i.e. relative standard error, $RSE < 50\%$), except for EC_{50} which was estimated with an RSE of 90.38%. Inclusion of IIV for EC_{50} or E_{\max} did not improve the model in terms of OFV nor $RSE\%$. Residual unexplained variability (RUV) was best described with a proportional error structure. Model parameters from analysis in NONMEM are listed in Supplementary Table 2 and a model simulation for the typical individual is shown in Supplementary Figure 6. Based on available data, no concentration-effect relationships could be found for valproic acid and lorazepam on MEP amplitude.

FIGURE 5 Significant N100 cluster comparing paired-pulse TEPs of placebo (PLCB; in blue) with lorazepam (LORA; in red) for ISI 300 ms. The grand average (mean \pm SEM) over all significant electrodes is presented, as well as the difference in topographical distribution at the time of the cluster. The colors of the topographical plot of the cortex show the increase or decrease of amplitude (μ V) of the response. The black cross represents the stimulation site, the red dots significant electrodes and the thick black bar below the average TEP response corresponds to the time interval with significant differences.



DISCUSSION

In this study, the effects of three AEDs on cortical excitability were assessed using sp- and ppTMS-EMG and TMS-EEG. All drugs decreased cortical excitability. Levetiracetam, valproic acid and lorazepam all significantly decreased MEP amplitude. Additionally, levetiracetam and lorazepam enhanced LIC1 at ISI 50 ms. Levetiracetam affected the amplitude of TEP components N45 and N100 in EEG clusters after spTMS. The mechanism through which these drugs inhibit cortical excitability

differ, which is reflected by the distinguishing fingerprints that were detected on TEP components. This finding gives new insights into pharmacological effects on TEPs, in addition to the existing literature.³⁰ In this discussion, we compared our results to placebo-controlled trials, to facilitate accurate comparison to our results.

TMS AS A PHARMACODYNAMIC BIOMARKER We assessed the variability of TMS-EMG and the feasibility of TMS-EMG/EEG for the purpose of using it in early phase clinical drug development. The main goal would be to use TMS-EMG/EEG outcomes as pharmacodynamic biomarkers for proof-of-mechanism of novel compounds that modulate cortical excitability. In our opinion, TMS-EMG and TMS-EEG are suitable to be used for this purpose. This is supported by our observed significant effects of single doses of three AEDs with different mechanisms of action, in a sample size that is typically used in early phase proof-of-mechanism-like drug studies. Moreover, TMS-EMG/EEG embodies certain qualities that are favourable to pharmacodynamic biomarkers: the method is non-invasive and relatively quick to perform, which allows for multiple measurements at different drug concentrations.

Although it should be noted that the variability of the outcome parameters is relatively high, the effect size was large enough to generate significant results in a small number of subjects. Therefore, we consider TMS-EMG/EEG outcomes as useful biomarkers for proof-of-mechanism of new compounds. In our opinion TMS-EMG can be used in Phase I dose escalation study designs, to evaluate target engagement and to aid in dose finding for further studies. Because the inter-subject variability of TMS-EMG was higher than the intra-subject variability, we would propose to use TMS to demonstrate pharmacological effects in a cross-over rather than a parallel study design.

As an exploratory outcome of this study, we have evaluated the concentration-effect relationship between the study drugs and MEP amplitude. A significant PKPD relationship was detected for levetiracetam, but not for valproic acid and lorazepam. It should be noted that the design of our study was not ideal for the assessment of PKPD relationships, because the concentration range observed in this study is relatively small and the number of post-dose measurements is limited. This is also demonstrated

by the high uncertainty around the estimated EC₅₀ parameter for levetiracetam. Whether TMS-EMG/EEG, despite the high variability of the outcomes, can be used for evaluation of concentration-effect relations therefore remains to be confirmed in future studies. Administration of multiple dose levels of the same compound can inform this concentration-effect relationship across a wider range of concentrations which would lower the parameter uncertainty currently observed in the model.

EFFECTS OF LEVETIRACETAM Levetiracetam targets synaptic vesical glycoprotein SV2A, which decreases central neurotransmitter release³¹ and therefore theoretically decreases cortical excitability. We showed a significant decrease of MEP amplitude induced by levetiracetam, indicating reduced excitability, in line with previously reported results.³² Other studies showed a non-significant decrease of MEP amplitude after administration of levetiracetam,^{33,34} and brivaracetam, an AED with a closely related mechanism of action.⁷

With use of CBPA of spTEPs, our study demonstrated that levetiracetam increased the amplitude of the N₄₅ component in a central cluster and decreased the N₁₀₀ amplitude contralateral to the stimulation site. The decrease in N₁₀₀ is consistent with changes caused by brivaracetam.⁷ The increase in N₄₅ is also in line with literature.¹⁰ We found the effect in a contralateral cluster, whereas the N₄₅ component showed widespread negativity in the study by Premoli *et al.*, with the maximum effect in the ipsilateral hemisphere.¹⁰

To our knowledge, our study is the first to evaluate effects of levetiracetam on paired pulse TMS-EEG. Interestingly, the effect we observe on the N₁₀₀ cluster following spTMS, is very similar in shape and localization to the significant N₁₀₀ clusters detected at ISIs 2 and 300 ms.

There is substantial evidence that the N₄₅ component represents γ -aminobutyric acid-A (GABA_A) mediated inhibition, whereas GABA_B receptor activity is reflected by the N₁₀₀ component.¹¹ Our findings on the N₄₅ component may therefore provide further indication that levetiracetam indirectly affects GABA_Aergic inhibition.^{10,35} The effect of levetiracetam on N₁₀₀ in the contralateral hemisphere may be caused by inhibition of cortico-cortical connections, as previously suggested for brivaracetam.⁷

EFFECTS OF VALPROIC ACID The anti-epileptic mechanism of action of valproic acid has not been completely clarified. It induces inhibition through the increase of GABA availability. Furthermore, valproic acid blocks voltage-gated sodium channels, affects neuronal potassium and calcium regulation, and inhibits N-methyl-D-aspartate (NMDA) transmission.³⁶

To our knowledge this is the first study to report that valproic acid decreased MEP amplitude in healthy volunteers. A previous study did not report an effect on MEP amplitude, but this study was not placebo-controlled.³⁷ The effect on MEP amplitude confirms that valproic acid decreases cortical excitability, as can be expected based on the mechanism of action.

To the best of our knowledge, no previous studies using TMS-EEG were performed to investigate the effect of valproic acid in healthy volunteers. Using TMS-EEG, we detected a significant N15 cluster at ISI 50 ms. Interestingly, considering the proposed mechanisms of action of the drug, our results indicate that valproic acid does not induce the same effect on the N45 and N100 components as lorazepam and other positive allosteric modulators (PAM) of GABA_A receptors.¹¹ The effect also does not bear resemblance to the effect of sodium channel blockers, such as lamotrigine which increased N45 and decreased P180,¹⁰ nor NMDA-receptor antagonists, such as dextromethorphan which increases the N45 component.³⁸ The effects of valproic acid on TEPs will need to be repeated to confirm if the effects on N15 can be reproduced.

EFFECTS OF LORAZEPAM Lorazepam is a GABA_A receptor PAM and stimulates GABAergic inhibition.³⁹ Our study demonstrated a decrease in MEP amplitude by lorazepam, in line with previous findings on stimulus response curves,^{40,41} indicating reduced excitability. LICI at ISI 50 ms was enhanced by lorazepam, which is associated with GABA_B receptor mediated inhibition,⁴² similar to the N100 component. No effect on SICI was detected, corresponding to results of other studies.^{40,43}

Previous studies using spTMS showed effects of other GABA_A-PAMS on N45 and N100, leading to the hypothesis that the N45 component is correlated to GABA_A receptor mediated inhibition.¹¹ It is therefore unexpected that we did not replicate these findings with lorazepam, which may be explained by a smaller number of subjects and relatively large variability in the measurements, indicating that our study is possibly

underpowered for demonstrating this effect. In our study, lorazepam did induce a significant cluster with a decrease of N100 using ppTMS (ISI 300 ms).

RECOMMENDED STATISTICAL ANALYSIS IN PLACEBO CONTROLLED TMS TRIALS Previous studies often assessed drug effects on cortical excitability by comparing pre-dose and post-dose outcomes in treatment and placebo condition separately. However, in a placebo-controlled trial, a more appropriate analysis would be to compare the treatment effect to placebo.⁴⁴ In the current study, an ANCOVA was used, because it can provide a comparison between treatment and placebo, using the baseline measurement per period as covariate. This analysis takes into account the inter-subject variability by introducing a random subject effect, while the intra-subject variability is given by the residual error term. Time effects, such as diurnal variation, are taken into account by including time effect in the model, while the subject by time interaction allows for different time effect between subjects. Similarly, the subject by treatment interaction included in the model allows for different treatment effect across subjects. Finally, potential pre-treatment differences are corrected by including the baseline as covariate. Due to these advantages over pre-dose versus post-dose comparison, we strongly recommend direct comparison of treatment versus placebo in future placebo-controlled pharmaco-TMS studies.

POSSIBLE LIMITATIONS The use of a 32-lead EEG cap, as opposed to 64-leads, could have impacted results and could explain why certain treatment-induced EEG clusters detected in previous studies were not confirmed in this study. A cluster, consisting of a minimum of three leads with significant signal changes in the same direction, covers a relatively larger area using 32-lead EEG and therefore needs to be more extensive than with 64-lead EEG.

Single trial PCA was applied to reduce artefacts caused by TMS stimulation and muscle activation on the scalp. PCA has shown to be an effective method to reduce both artefacts simultaneously, as seen for example in subjects 4, 5 and 8 in the Supplementary Figures 7-10. However, in others (e.g. subjects 2, 6 and 11) the final TEP is still contaminated by residual artefacts. Since no consensus has been reached within the TMS-EEG community on a common 'gold standard' analysis approach,

numerous alternative artefact rejection methods exist with each their own advantages and disadvantages.⁴⁵ As the final TEP is most likely largely influenced by the applied preprocessing pipeline,⁴⁶ we chose to use PCA making our results comparable with previous own findings, although this method may not always perform optimally.

Although not a limitation on itself, it should be noted that the stimulation intensity was adjusted prior to each TMS session, based on the rMT at the start of each measurement. This is in contrast to some previous studies, such as a study analysing levetiracetam effects on TMS-EEG.¹⁰ We chose this approach to make sure that stimulation intensity was always related to the rMT, and that changes in rMT (e.g., due to drug effects) would not lead to subthreshold stimulation. Importantly, we did not observe a significant change in rMT and therefore this should not have impacted the comparison of the results of our study to previous studies.

CONCLUSIONS

The aim of this study was to show the value of TMS-EMG and TMS-EEG in determining effects of drugs targeting cortical excitability, for the purpose of developing these measurements as pharmacodynamic biomarkers for use in early phase clinical drug development. Pharmacodynamic effects on TMS-EMG have been intensively studied, but studies that assess drug effects on TMS-EEG are limited. Therefore, we investigated the sensitivity of TMS-EMG/EEG to detect effects of three commonly prescribed AEDs on cortical excitability in a double-blind, placebo-controlled, four-way cross-over study in healthy subjects. Our study shows that a single doses of levetiracetam, valproic acid and lorazepam decrease cortical excitability, as expected from anti-epileptic drugs. These findings support the development of TMS-EMG and TMS-EEG as a suitable biomarkers for proof-of-mechanism of new treatments in the early clinical phase.

SUPPLEMENTARY INFORMATION

SUPPLEMENTARY TABLE 1 Mean serum concentrations of levetiracetam, valproic acid and lorazepam at the scheduled sampling times.

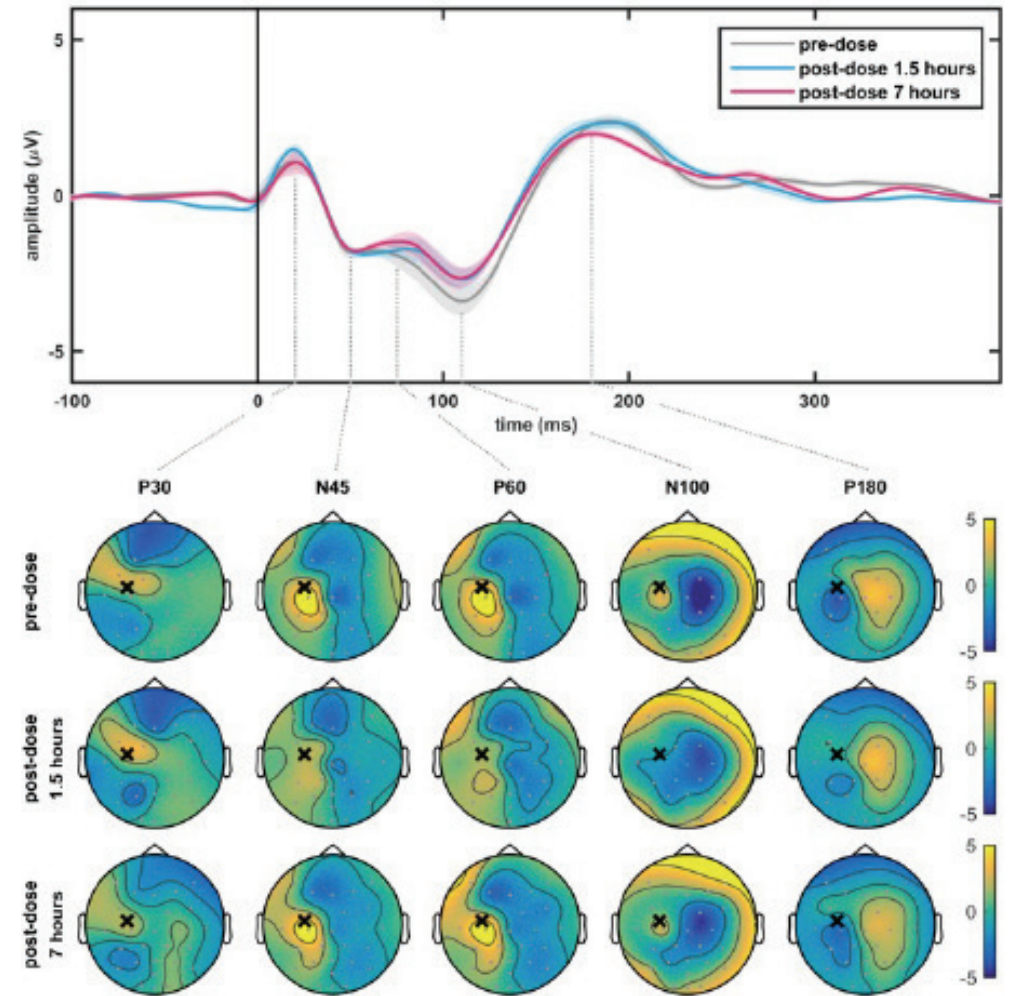
Treatment	Time after dosing	Mean serum concentration	SD	Median
Levetiracetam (2000mg)	0	0 µg/mL	0	0
	30 min	44.45 µg/mL	10.37	46.25
	1 h 22 min	39.68 µg/mL	5.76	39.4
	2 h 15 min	36.64 µg/mL	4.6	37.95
	3 h 30 m	32.61 µg/mL	4.28	32.95
	6 h 52 min	23.37 µg/mL	2.53	23.5
Valproic acid (1000mg)	0	0 µg/mL	0	0
	30 min	68.12 µg/mL	8.59	66.5
	1 h 22 min	65.25 µg/mL	7.73	65
	2 h 15 min	59.81 µg/mL	7.84	60
	3 h 30 m	54.31 µg/mL	8.26	54
	6 h 52 min	40.88 µg/mL	5.88	40.5
Lorazepam (2mg)	0	0 ng/mL	0	0
	30 min	4.11 ng/mL	6.24	0
	1 h 22 min	18.75 ng/mL	3.27	18.76
	2 h 15 min	18.79 ng/mL	3.09	19.2
	3 h 30 m	17.32 ng/mL	3.01	16.56
	6 h 52 min	13.69 ng/mL	2.69	13.35
	23 h 52 min	4.42 ng/mL	4.17	5.31

SUPPLEMENTARY TABLE 2 PKPD-model parameters to describe the proportional effect of levetiracetam on MEP amplitude.

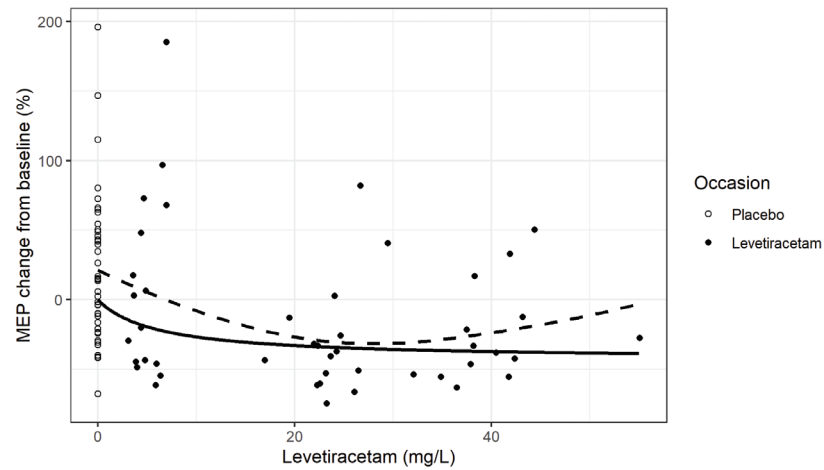
Parameter	Estimate	RSE(%)
POPULATION PARAMETERS		
Baseline (μV)	633.5	18.35
EC ₅₀ (mg/L)	6.069	90.38
E _{max} (%)	-43.35	26.35
VARIABILITY ON BASELINE (VARIANCE)		
IIV	0.1287	41.13
BOV	0.4290	35.25
RESIDUAL UNEXPLAINED VARIABILITY (RUV, σ^2)		
Proportional error	0.1246	20.97

RSE = relative standard error, EC₅₀ = concentration at which 50% of the maximum effect is achieved, E_{max} = maximum effect, IIV = inter-individual variability, BOV = between-occasion variability.

SUPPLEMENTARY FIGURE 1 Average single pulse TEP and topographical plots of the characteristic TEP components at pre-dose (in grey and top row) and post-dose 1.5 hours (in blue and middle row) and 7 hours (in red and bottom row) for the placebo condition. Masking of auditory components appears to be sufficient as represented by lateralized responses in the topographical plots even at late latencies. Each TEP is the average over all subjects (mean \pm SEM) at electrodes CZ, C4, FC2, CP2, CP6 and P4 (similar to significant clusters found for levetiracetam). The topographical plots show the distribution of the P30, N45, P60, N100 and P180 components, where the black cross represents the stimulation site and the grey dots the 32 electrodes. The colours of the topographical plot of the cortex show a positive (in yellow) or negative (in blue) amplitude (μV) of the response.



SUPPLEMENTARY FIGURE 6 PKPD-relationship between levetiracetam and MEP amplitude change from baseline. Measured data is shown as dots. The solid line shows the E_{\max} -model simulation for a typical individual and the dotted line is a smooth curve (loess-regression, span width = 1).



MEP = motor-evoked potential



SUPPORTING INFORMATION

Additional supporting information may be found in the online version of the article at the publisher's website.

REFERENCES

- Barker AT, Jalinous R, Freeston IL. Non-invasive magnetic stimulation of human motor cortex. *The Lancet*. 1985;325(8437):1106-1107.
- Ilmoniemi RJ, Kičić D. Methodology for combined TMS and EEG. *Brain topography*. 2010;22(4):233.
- Ilmoniemi RJ, Virtanen J, Ruohonen J, et al. Neuronal responses to magnetic stimulation reveal cortical reactivity and connectivity. *Neuroreport*. 1997;8(16):3537-3540.
- Kujirai T, Caramia M, Rothwell JC, et al. Corticocortical inhibition in human motor cortex. *The Journal of physiology*. 1993;471(1):501-519.
- Valls-Solé J, Pascual-Leone A, Wassermann EM, Hallett M. Human motor evoked responses to paired transcranial magnetic stimuli. *Electroencephalography and Clinical Neurophysiology/ Evoked Potentials Section*. 1992;85(6):355-364.
- Ziemann U, Reis J, Schwenkreis P, et al. TMS and drugs revisited 2014. *Clinical neurophysiology*. 2015;126(10):1847-1868.
- Darmani G, Bergmann TO, Zipser C, Baur D, Müller-Dahlhaus F, Ziemann U. Effects of anti-epileptic drugs on cortical excitability in humans: A TMS-EMG and TMS-EEG study. *Human brain mapping*. 2019;40(4):1276-1289.
- Darmani G, Zipser CM, Böhmer GM, et al. Effects of the selective α_5 -GABA_AR antagonist S44819 on excitability in the human brain: a TMS-EMG and TMS-EEG phase I study. *Journal of Neuroscience*. 2016;36(49):12312-12320.
- Koenig F, Belardinelli P, Liang C, et al. TMS-EEG signatures of glutamatergic neurotransmission in human cortex. *bioRxiv*. 2019;55920.
- Premoli I, Biondi A, Carlesso S, Rivolta D, Richardson MP. Lamotrigine and levetiracetam exert a similar modulation of TMS-evoked EEG potentials. *Epilepsia*. Jan 2017;58(1):42-50. doi:10.1111/epi.13599
- Premoli I, Castellanos N, Rivolta D, et al. TMS-EEG signatures of GABAergic neurotransmission in the human cortex. *The Journal of neuroscience; the official journal of the Society for Neuroscience*. Apr 16 2014;34(16):5603-12. doi:10.1523/JNEUROSCI.5089-13.2014
- Premoli I, Rivolta D, Espenhahn S, et al. Characterization of GABA_B-receptor mediated neurotransmission in the human cortex by paired-pulse TMS-EEG. *NeuroImage*. Dec 2014;103:152-62. doi:10.1016/j.neuroimage.2014.09.028
- Premoli I, Rossini PG, Goldberg PY, et al. TMS as a pharmacodynamic indicator of cortical activity of a novel anti-epileptic drug, XEN1101. *Annals of Clinical and Translational Neurology*. 2019;6(11):2164-2174.
- de Goede AA, ter Braack EM, van Putten MJ. Single and paired pulse transcranial magnetic stimulation in drug naïve epilepsy. *Clinical neurophysiology*. 2016;127(9):3140-3155.
- Tsuboyama M, Kaye HL, Rotenberg A. Biomarkers Obtained by Transcranial Magnetic Stimulation of the Motor Cortex in Epilepsy. *Frontiers in integrative neuroscience*. 2019;13
- Vucic S, Ziemann U, Eisen A, Hallett M, Kiernan MC. Transcranial magnetic stimulation and amyotrophic lateral sclerosis: pathophysiological insights. *J Neurol Neurosurg Psychiatry*. 2013;84(10):1161-1170.
- Rossi S, Hallett M, Rossini PM, Pascual-Leone A. Screening questionnaire before TMS: an update. *Clinical neurophysiology: official journal of the International Federation of Clinical Neurophysiology*. Aug 2011;122(8):1686. doi:10.1016/j.clinph.2010.12.037
- Williams E. Experimental designs balanced for the estimation of residual effects of treatments. *Australian Journal of Chemistry*. 1949;2(2):149-168.
- Rossi S, Hallett M, Rossini PM, Pascual-Leone A. Safety, ethical considerations, and application guidelines for the use of transcranial magnetic stimulation in clinical practice and research. *Clinical neurophysiology; official journal of the International Federation of Clinical Neurophysiology*. Dec 2009;120(12):2008-39. doi:10.1016/j.clinph.2009.08.016
- Oldfield RC. The assessment and analysis of handedness: the Edinburgh inventory. *Neuropsychologia*. 1971;9(1):97-113.
- Groppa S, Oliviero A, Eisen A, et al. A practical guide to diagnostic transcranial magnetic stimulation: report of an IFCN committee. *Clinical Neurophysiology*. 2012;123(5):858-882.
- Rossini PM, Burke D, Chen R, et al. Non-invasive electrical and magnetic stimulation of the brain, spinal cord, roots and peripheral nerves: basic principles and procedures for routine clinical and research application. An updated report from an IFCN Committee. *Clinical Neurophysiology*. 2015;126(6):1107-1107.

- 23 Ter Braack, de Vos, Van Putten. Masking the auditory evoked potential in TMS-EEG: a comparison of various methods. *Brain topography*. 2015;28(3):520-528.
- 24 Rocchi L, Di Santo A, Brown K, et al. Disentangling EEG responses to TMS due to cortical and peripheral activations. *Brain Stimul*. Jan-Feb 2021;14(1):4-18. doi:10.1016/j.brs.2020.10.011
- 25 Ter Braack, de Jonge, Putten v. Reduction of TMS induced artifacts in EEG using principal component analysis. *IEEE Trans Neural Syst Rehabil Eng*. May 2013;21(3):376-82. doi:10.1109/TNSRE.2012.2228674
- 26 Maris E, Oostenveld R. Nonparametric statistical testing of EEG- and MEG-data. *J Neurosci Methods*. Aug 15 2007;164(1):177-90. doi:10.1016/j.jneumeth.2007.03.024
- 27 Alexander SP, Christopoulos A, Davenport AP, et al. The Concise Guide To Pharmacology 2021/22: G protein-coupled receptors. *British Journal of Pharmacology*. 2021;178(S1):S27-S156. doi:https://doi.org/10.1111/bph.15538
- 28 Alexander SP, Kelly E, Mathie A, et al. The Concise Guide To Pharmacology 2021/22: Transporters. *British Journal of Pharmacology*. 2021;178(S1):S412-S513. doi:https://doi.org/10.1111/bph.15543
- 29 Alexander SP, Mathie A, Peters JA, et al. The Concise Guide To Pharmacology 2021/22: Ion channels. *British Journal of Pharmacology*. 2021;178(S1):S157-S245. doi:https://doi.org/10.1111/bph.15539
- 30 Darmani G, Ziemann U. Pharmacophysiology of TMS-evoked EEG potentials: A mini-review. *Brain Stimulation: Basic, Translational, and Clinical Research in Neuromodulation*. 2019;12(3):829-831.
- 31 Abou-Khalil B. Levetiracetam in the treatment of epilepsy. *Neuropsychiatric disease and treatment*. 2008;4(3):507.
- 32 Epstein CM, Girard-Siqueira L, Ehrenberg JA. Prolonged neurophysiologic effects of levetiracetam after oral administration in humans. *Epilepsia*. 2008;49(7):1169-1173.
- 33 Reis J, Wentrup A, Hamer HM, et al. Levetiracetam influences human motor cortex excitability mainly by modulation of ion channel function—a TMS study. *Epilepsy research*. 2004;62(1):41-51.
- 34 Sohn YH, Kaelin-Lang A, Jung HY, Hallett M. Effect of levetiracetam on human corticospinal excitability. *Neurology*. 2001;57(5):858-863.
- 35 Poulain P, Margineanu DG. Levetiracetam opposes the action of GABA_A antagonists in hypothalamic neurones. *Neuropharmacology*. Mar 2002;42(3):346-52. doi:10.1016/S0028-3908(01)00185-X
- 36 Johannessen CU. Mechanisms of action of valproate: a commentary. *Neurochemistry international*. 2000;37(2-3):103-110.
- 37 Zunhammer M, Langguth B, Landgrebe M, et al. Modulation of human motor cortex excitability by valproate. *Psychopharmacology*. 2011;215(2):277-280.
- 38 Belardinelli P, König F, Liang C, et al. TMS-EEG signatures of glutamatergic neurotransmission in human cortex. *Scientific reports*. 2021/04/14 2021;11(1):8159. doi:10.1038/s41598-021-87533-z
- 39 Griffin CE, Kaye AM, Bueno FR, Kaye AD. Benzodiazepine pharmacology and central nervous system-mediated effects. *Ochsner Journal*. 2013;13(2):214-223.
- 40 Boroojerdi B, Battaglia F, Muellbacher W, Cohen L. Mechanisms influencing stimulus-response properties of the human corticospinal system. *Clinical Neurophysiology*. 2001;112(5):931-937.
- 41 Kimiskidis V, Papagiannopoulos S, Kazis D, et al. Lorazepam-induced effects on silent period and corticomotor excitability. *Experimental brain research*. 2006;173(4):603-611.
- 42 McDonnell MN, Orekhov Y, Ziemann U. The role of GABA(B) receptors in intracortical inhibition in the human motor cortex. *Experimental brain research*. Aug 2006;173(1):86-93. doi:10.1007/s00221-006-0365-2
- 43 Di Lazzaro V, Oliviero A, Meglio M, et al. Direct demonstration of the effect of lorazepam on the excitability of the human motor cortex. *Clinical Neurophysiology*. 2000;111(5):794-799.
- 44 Gliner JA, Morgan GA, Harmon RJ. Pretest-posttest comparison group designs: Analysis and interpretation. *Journal of the American Academy of Child and Adolescent Psychiatry*. 2003;42(4):500-503.
- 45 Tremblay S, Rogasch NC, Premoli I, et al. Clinical utility and prospective of TMS-EEG. *Clinical neurophysiology; official journal of the International Federation of Clinical Neurophysiology*. May 2019;130(5):802-844. doi:10.1016/j.clinph.2019.01.001
- 46 Bertazzoli G, Esposito R, Mutanen TP, et al. The impact of artifact removal approaches on TMS-EEG signal. *NeuroImage*. Oct 1 2021;239:118272. doi:10.1016/j.neuroimage.2021.118272



The background of the page is a light blue gradient with several dried, pressed leaves scattered across it. The leaves are in various shades of brown and tan, showing their intricate vein structures. There are also numerous small, dark blue particles or specks scattered throughout the background, giving it a textured, almost crystalline appearance.

CHAPTER 3

EFFECTS OF PHARMACOLOGICAL AMPA-RECEPTOR POTENTIATION ON TMS-EEG EVOKED POTENTIALS: A RANDOMIZED, DOUBLE-BLIND, PLACEBO-CONTROLLED, CROSSOVER STUDY IN HEALTHY SUBJECTS

**THIS CHAPTER (PAGES 48 TO 67) IS SUBJECT TO AN EMBARGO
AND IS THEREFORE NOT INCLUDED IN THIS FILE**

Titia Q. Ruijs^{1,3*}, Annika A. de Goede^{1*}, Francis M. Dijkstra^{1,3}, Jules A.A.C. Heuberger¹,
Brian Tracey², Fahimeh Mamashli², Patricio O'Donnell², Laura B. Rosen²,
Mahnaz Asgharnejad², Gabriel E. Jacobs^{1,3}, Derek L. Buhl² *These authors share first authorship

1. Centre for Human Drug Research, Leiden, NL
2. Takeda Pharmaceuticals International, Inc., Cambridge, USA
3. Leiden University Medical Centre, Leiden, NL

The background of the page is a light blue color with scattered dark blue particles. Several dried, pressed leaves are visible, showing their intricate vein structures. The leaves are arranged in a way that they appear to be floating or scattered across the page. The overall aesthetic is clean and scientific, with a touch of natural beauty.

CHAPTER 4

**EFFECTS OF MEXILETINE AND LACOSAMIDE
ON NERVE EXCITABILITY IN HEALTHY SUBJECTS:
A RANDOMIZED, DOUBLE-BLIND,
PLACEBO-CONTROLLED, CROSSOVER STUDY**

Clin Pharmacol Ther, 112: 1008-1019. <https://doi.org/10.1002/cpt.2694>

Titia Q. Ruijs^{1,2}, Ingrid W. Koopmans^{1,2}, Marieke L. de Kam¹, Michiel J. van Esdonk¹, Martin Koltzenburg³,
Geert Jan Groeneveld^{1,2}, Jules A.A.C. Heuberger¹

1. Centre for Human Drug Research, Leiden, NL
2. Leiden University Medical Centre, Leiden, NL
3. National Hospital for Neurology and Neurosurgery, London, UK

ABSTRACT

Selective voltage-gated sodium channel blockers are of growing interest as treatment for pain. For drug development of such compounds, it would be critical to have a biomarker that can be used for proof-of-mechanism. We aimed to evaluate whether drug-induced changes in sodium conductance can be detected in the peripheral nerve excitability profile in 18 healthy subjects. In a randomized, double-blind, three-way crossover study, effects of single oral doses of 333 mg mexiletine and 300 mg lacosamide were compared to placebo. On each study visit, motor- and sensory nerve excitability measurements of the median nerve were performed (pre-dose; 3- and 6-hours post-dose) using Qtrac. Treatment effects were calculated using an ANCOVA with baseline as covariate. Mexiletine and lacosamide had significant effects on multiple motor- and sensory nerve excitability variables. Depolarizing threshold electrotonus (TE_{d40} (40-60ms)) decreased by mexiletine (estimated difference (ED) -1.37% (95% confidence interval: -2.20, -0.547); p=0.002) and lacosamide (ED -1.27% (-2.10, -0.443); p=0.004) in motor nerves. Moreover, mexiletine and lacosamide decreased superexcitability (less negative) in motor nerves (ED 1.74% (0.615, 2.87); p=0.004, and 1.47% (0.341, 2.60); p=0.013, respectively). Strength-duration time constant decreased after lacosamide in motor- (ED -0.0342 ms (-0.0571, -0.0112); p=0.005) and sensory nerves (ED -0.0778 ms (-0.116, -0.0399); p<0.001).

Concluding, mexiletine and lacosamide significantly decrease excitability of motor- and sensory nerves, in line with their suggested mechanism of action. Results of this study indicate that nerve excitability threshold tracking can be an effective pharmacodynamic biomarker. The method could be a valuable tool in clinical drug development.

INTRODUCTION

Selective voltage-gated sodium channel (Na_v) blockers are subject to growing interest as treatment for pain.¹ It is of importance that pharmacodynamic (PD) effects of such treatments are detected in the early phase of clinical development, preferably in healthy subjects. Detection of PD effects early in the development program is useful as proof-of-mechanism, to show target engagement, to aid in dose escalation study designs and to assist dose finding for the translation to patient studies. A reliable clinical biomarker for effects of drugs that target Na_v-channels is lacking, so development of such a PD biomarker would be highly valuable.

Nerve excitability threshold tracking (NETT), also called nerve excitability testing, is a non-invasive peripheral nerve stimulation technique, which can be used to estimate axonal excitability of motor- and sensory nerves.^{2,3} Excitability of the axonal membrane is largely dependent on Na_v and potassium channel conductance,⁴ and pharmacological modulation of these channels influences axonal excitability. Therefore, we performed a study aimed to evaluate whether pharmacologically induced changes in Na_v-conductance can be detected using NETT in healthy subjects. As a proof-of-concept, effects of a single dose of mexiletine and lacosamide, two Na_v-blockers that are expected to decrease axonal excitability based on their mechanism of action, were compared to placebo in double-blind fashion. To our knowledge, this is the first placebo-controlled study in which effects of Na_v-blockers were investigated on NETT in healthy human subjects and our results encourage the use of NETT as a biomarker in early phase clinical drug development.

METHODS

The study (Netherlands Trial Registry: NL7327) was conducted at Centre for Human Drug Research, Leiden, The Netherlands, in accordance with the Declaration of Helsinki after approval by Ethics Committee Stichting 'Beoordeling Ethiek Biomedisch Onderzoek', The Netherlands.

SUBJECTS Subjects gave signed informed consent before commencement of study activities. Medical screening was performed to determine eligibility. Healthy, male subjects, 18 to 45 years old, with body mass index (BMI) between 18-30 kg/m², were included. Health status was

confirmed by evaluation of medical history, physical examination, and laboratory tests. Nicotine users and subjects with a history of drug or alcohol abuse, or a positive test for these substances, were excluded. Subjects with conditions considered to influence electrophysiological measurements were excluded. Use of medication, dietary supplements, CYP450 iso-enzyme modulating products, alcohol, caffeine, and nicotine was prohibited. Strenuous physical activity was prohibited from 48 hours before each study day.

STUDY DESIGN This was a randomized, double-blind, double-dummy, placebo-controlled, three-way crossover study. On three separate study visits, subjects received a single dose of mexiletine, lacosamide or placebo in randomized order. Between each visit was a wash-out period of seven days. On each visit, three motor- and sensory NETT measurements were performed: pre-dose, and three- and six-hours post-dose. Blood samples for pharmacokinetic (PK) analysis were drawn pre-dose, and before and after each post-dose NETT measurement. Evoked pain tests, and intraepidermal electrical stimulation, were performed before and after dosing, these results will be reported separately. Measurements and meals were at approximately the same clock-time, to prevent influence of diurnal variation or food.

Primary objectives were to evaluate the sensitivity of NETT to detect effects of mexiletine and lacosamide, and to evaluate the test-retest reliability of NETT. These outcomes were evaluated with motor- and sensory NETT endpoints, and variability was expressed in coefficients of variation (CV%), respectively. The exploratory objective was to determine concentration-effect relations between the drug concentrations and NETT variables.

No important changes to study methods or trial outcomes were made after first subject, first dose.

STUDY DRUGS Mexiletine (Namuscla, 167 mg, Lupin Europe GmbH) capsules and lacosamide (Vimpat, 100 mg, UCB Pharma S.A.) filmcoated tablets were over-encapsulated. For both treatments, matching placebo was produced, enabling double-blind and double-dummy drug administration.

A dose of 300 mg of mexiletine hydrochloride for a duration of three months has been reported to exhibit significant effects on nerve ex-

citability in patients with neuropathic pain.⁵ Therefore, a similar dose of 333 mg mexiletine was selected for this study, to reach therapeutic plasma concentrations with a single dose. Moreover, 333 mg mexiletine was deemed to have an acceptable safety profile, as single doses up to 600 mg mexiletine have been administered to healthy subjects.⁶

A single dose of 300 mg lacosamide was chosen, because it would lead to therapeutic concentrations for the treatment of epilepsy and was considered safe for healthy subjects. The suggested reference range based on effect and tolerability is 10-40 $\mu\text{mol/L}$, or 2.5-10 mg/L.^{7,8} Mean C_{max} after a single dose of 300 mg lacosamide was 7.366 mg/L.⁹

Study staff and subjects remained blinded until database lock. The block-randomization was produced using SAS version 9.4 by a statistician uninvolved in the clinical study conduct. Subjects were randomly assigned to one of six treatment sequences in a balanced study design. Randomisation numbers were assigned to participants sequentially after medical screening by blinded study staff.

PK ANALYSIS Plasma concentrations of the study drugs were analysed using a validated LC-MS/MS method. Mexiletine concentrations were evaluated by Leiden University Medical Centre (Leiden, The Netherlands) laboratory; lacosamide concentrations by the laboratory of Apotheek Haagse Ziekenhuizen (The Hague, The Netherlands). Lower limit of quantification (LLOQ) was 0.06 mg/L for mexiletine and 0.75 mg/L for lacosamide. Reproducibility of the assays was in line with the EMA bioanalytical method development guideline, with CV%<15%.

NERVE EXCITABILITY THRESHOLD TRACKING Motor- and sensory nerve excitability of the median nerve was measured using NETT. The nerve was stimulated using surface electrodes (Red Dot, 3M, St. Paul, USA), with the active electrode located at the wrist and the reference 10 cm proximal to the active electrode on the radial side. Electrical stimulation was induced using an isolated bipolar constant current stimulator (DS5, Digitimer, Hertfordshire, UK). Compound muscle action potentials (CMAP) were recorded from the abductor pollicis brevis, using a belly-tendon montage (Disposable Tab Electrodes, Natus Medical, Pleasanton, USA). Sensory nerve action potentials (SNAP) were recorded antidromically using ring electrodes (Disposable Wide Ring Electrode, Natus Medical, Pleasanton, USA) on digit three. When no

SNAP could be recorded from digit three, digit two was used. CMAP and SNAP signals were amplified using an EMG amplifier (D440-2, DigiTimer, Hertfordshire, UK), gain 10,000 for sensory measurements and 300 for motor measurements, bandpass filter 3 to 3000 Hz. Signals were digitized using an analog-digital convertor (NI-USB-6341, National Instruments, Austin, USA). Hum Bug (Quest Scientific Instruments, North Vancouver, Canada) was used to minimize 50 Hz noise. To maintain stable temperature conditions, the hand and forearm were warmed using a heat blanket (Norm-O-Temp with Maxi-Therm Lite infant hyper-hypothermia blanket, Cincinnati, USA) programmed at 35°C, from 30 minutes prior stimulation until the end of the measurement. Skin temperature was registered before and after the measurement using a temperature probe (BioSignals Plux, Arruda dos Vinhos, Portugal).

Stimulation was guided by QTRAC-S software (version 28-5-2018, Institute of Neurology, London, UK) with the TRONDNF stimulation paradigm (Institute of Neurology, London, UK). This paradigm and corresponding variables were described previously.^{2,3} Each NETT measurement consists of four protocols:¹⁰ stimulus response curve (relationship between stimulus current and amplitude of the muscle/sensory action potential); strength-duration relationship (relationship between stimulus duration and stimulus charge); threshold electrotonus (threshold changes during a depolarizing or hyperpolarizing conditioning currents of 10-300 ms, the current set to 20% or 40% of the current needed for the unconditioned target response); current-voltage (I/V) relationship (threshold changes due to conditioning currents, currents are between +50% depolarizing and -100% hyperpolarizing); and recovery cycle (threshold changes due to supramaximal conditioning pulses at interstimulus intervals (ISI) of 200 to 2 ms between the conditioning- and test pulse). For this study, the following changes were made to TRONDNF. First, for motor- and sensory measurements the maximal delay in threshold electrotonus was increased from 200 to 300 ms, to evaluate the full accommodation to hyperpolarization. Additionally, changes were made to allow for direct comparison between the motor- and sensory nerve endpoints. Test-stimulus duration of sensory measurements was increased from 0.5 to 1 ms (with exception of the strength-duration paradigm) and for sensory recovery cycles measurements the conditioning width was changed from 0.5 to 1 ms. Stimulus duration in the sensory strength-duration

measurements was programmed to decrease with steps of 0.2 ms instead of 0.1 ms. Finally, fraction of the peak (window fraction) was set from 40% to 10%.

QTRAC-P (version 26-10-2018, Institute of Neurology, London, UK) was used to process data and generate the following endpoints (description based on previous publications):^{10,11} threshold for 50% CMAP/SNAP (current required for 50% of maximal CMAP/SNAP), rheobase (slope of strength-duration relation), strength-duration time constant (SDTC) (negative x-intercept of the strength-duration relation), TED₄₀ peak and TED₂₀ peak (peak threshold decrease due to depolarizing currents set to 40% and 20% of the resting threshold), TED₄₀ (X-X ms) and TED₂₀ (X-X ms) (mean threshold decrease due to 40% and 20% depolarizing currents, with conditioning stimulus latency between brackets (X-X ms)), S₂-accommodation (difference between TED₄₀ peak and TED₄₀ (90-100ms)), accommodation half-time (time when TED₄₀ is halfway between TED₄₀ peak and TED₄₀ (90-100ms)), TEH₄₀ (X-Xms) (mean threshold decrease due to 40% and 20% hyperpolarizing currents, with conditioning stimulus latencies between brackets (X-Xms)), fanning (sum of values of TED₄₀ (190-200ms) and TEH₄₀ (190-200ms)), hyperpolarizing I/V-slope (slope between 100% and 80% hyperpolarizing currents), minimum I/V slope (smallest slope in the I/V curve), resting I/V slope (slope between -10% and +10% conditioning stimuli), relative refractory period (ISI at which threshold returns to baseline), refractoriness at 2 ms (threshold change due to conditioning stimulus with ISI 2 ms), subexcitability (peak threshold change (highest value) after superexcitability), superexcitability (peak threshold change (lowest value) after refractory period).

A blind data review was performed before statistical analysis, to exclude measurements with technical errors.

STATISTICAL ANALYSIS Treatment effects (placebo vs. mexiletine; placebo vs. lacosamide) on NETT outcomes were calculated using a mixed model analysis of variance (ANCOVA), with baseline as covariate. Time, period, treatment, treatment by time were used as fixed factors. Subject, subject by treatment and subject by time were implemented as random factors. Normal distribution of the residuals was checked graphically, and in case of log-normal distribution variables were log transformed before analysis. The between-day intra-subject variability

and inter-subject variability of NETT, expressed in CV%, were calculated from the baseline values of each visit, and were derived from the model covariate variables (the random factors subject, subject by time and subject by treatment). For statistical significance, 5% level was used. Sample size was based on a previous NETT study,¹⁰ which showed significant PD effects of retigabine in ALS patients in a similar cross-over design.

CONCENTRATION-EFFECT RELATIONSHIPS For analysis of concentration-effect relationships, PK data was linked to PD measurements, based on closest available clock-time. Each variable was modelled with an intercept only, a linear concentration-effect relationship and non-linear (E_{max}) concentration-effect relationship in a mixed effects model with random effects by subject and subject by treatment on baseline to evaluate the potential concentration-effect relationships. Linear and non-linear relationships were compared with the intercept only model with an analysis of variance, fits of linear and non-linear relationship were compared based on the Akaike information criterion (AIC), in which the model with the lowest AIC or a p-value of <0.05 was selected. Concentration-effect models were estimated in R (version 3.6.1).

RESULTS

The clinical phase of the study ran from September 2019 to February 2020. Eighteen subjects were enrolled, demographics are listed in *Supplementary Table 1*. *Supplementary Figure 1* shows individual – and mean \pm standard deviation-plasma concentrations of mexiletine and lacosamide. No observations in the absorption phase are available. Mean concentrations ranged between 5.88 mg/L and 4.83 mg/L for lacosamide, and 0.903 mg/L and 0.639 mg/L for mexiletine. The summary plasma concentrations by protocol time are listed in *Supplementary Table 2*. All adverse events in this study were mild and transient.

EXCITABILITY MEASUREMENTS A total of 162 motor and 162 sensory NETT measurements were performed. As a result of the blinded data review, subexcitability was excluded from 19 measurements; super-excitability, accommodation half-time and minimum- and hyperpolarizing I/V

slope from one measurement; refractoriness from three measurements; and all threshold electrotonus variables from five measurements.

Raw baseline excitability variables before administration of the study drugs, and post-dose estimated means, are shown in *Supplementary Table 3*. Test-retest reliability (CV%) is listed in *Supplementary Table 4*.

PHARMACODYNAMIC EFFECTS ON MOTOR NERVE EXCITABILITY

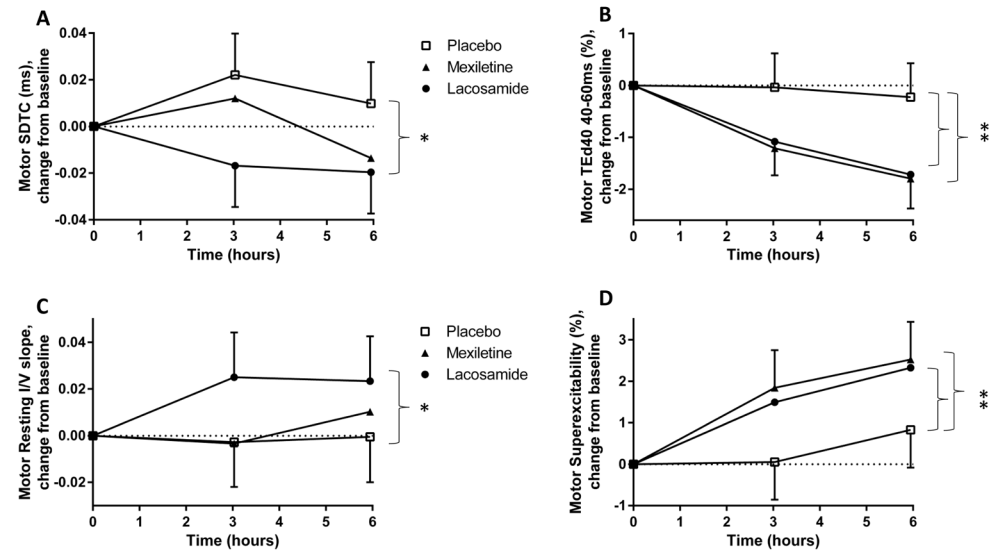
Effects of mexiletine and lacosamide on motor nerve excitability are listed in *Table 1*. A representative selection of significant variables from each NETT paradigm is shown in *Figure 1*, depicted as the estimated mean change from baseline. Furthermore, to visualize effects on NETT recordings, average recordings of three- and six-hours post-dose (treatment vs. placebo, without baseline correction) are shown in *Figure 2* and *Figure 3*, for mexiletine and lacosamide respectively.

MEXILETINE Significant effects of mexiletine were observed on threshold electrotonus with depolarizing conditioning currents 40% of threshold (TEd_{40}). Mexiletine decreased the peak in threshold reduction due to the depolarizing currents (TEd_{40} peak). Furthermore, it lowered the threshold reduction induced by depolarizing conditioning pulses of 40-200 ms (TEd_{40} (40-60ms) (*Figure 1B*); TEd_{40} (90-100ms); TEd_{40} (190-200ms)). Thus, there was a shift to lower values for the TEd_{40} curve without s2-accommodation.

In the recovery cycles, different phases of excitability after an action potential are measured, namely the relative refractory period (RRP), followed by a period of superexcitability (increased excitability, characterized by a threshold reduction) and subexcitability (decreased excitability, characterized by a threshold increase). Superexcitability significantly decreased (less negative) after mexiletine administration (*Figure 1D*). Moreover, a small, but significant increase in RRP duration was observed when comparing mexiletine to placebo.

LACOSAMIDE SDTC was significantly shortened by lacosamide compared to placebo (*Figure 1A*). Additionally, similar to mexiletine, lacosamide induced a shift to lower values for TEd_{40} : it lowered TEd_{40} peak and decreased TEd_{40} with conditioning stimulus durations 10-200 ms (TEd_{40} (10-20ms); TEd_{40} (40-60ms) (*Figure 1B*); TEd_{40} (90-100ms); TEd_{40} (190-200ms)).

FIGURE 1 Estimated mean change from baseline of motor nerve excitability threshold tracking variables. Every graph shows one selected variable with significant treatment effects from each threshold tracking paradigm: A) strength duration time constant (SDTC), B) TED₄₀ (40-60ms), C) Resting I/V slope, D) Superexcitability. Error bars indicate the 95% confidence interval. The time after dosing (hours) is indicated on the x-axis. Significant effects of mexiletine and/or lacosamide versus placebo in the treatment period are highlighted with an asterisk. N=18.

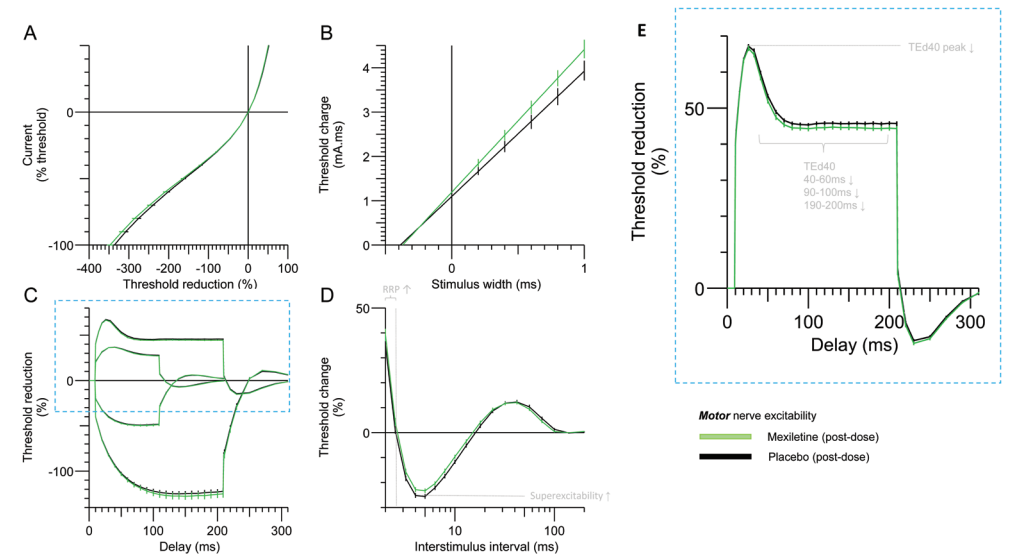


Accommodation half-time and s₂-accommodation were significantly reduced by lacosamide. Furthermore, lacosamide had significant effects on threshold electrotonus with 20% depolarizing currents (TED₂₀): TED₂₀ peak and TED₂₀ (10-20ms) were lowered compared to placebo.

Lacosamide induced a significant increase in resting I/V-slope (Figure 1C) and lastly, we found a significantly reduced superexcitability (less negative) (Figure 1D) and refractoriness at ISI 2 ms by lacosamide.

DRUG EFFECTS ON SENSORY NERVE EXCITABILITY Effects of mexiletine and lacosamide on sensory nerve excitability are shown in Table 1. Estimated mean change from baseline of one representative variable from each stimulation paradigm is shown in Figure 4. Moreover, average post-dose NETT recordings (treatment vs. placebo, without baseline correction), are shown in Figure 5 and Figure 6, for mexiletine and lacosamide respectively.

FIGURE 2 The average post-dose (three and six hours) motor nerve excitability threshold tracking recordings of placebo (black) vs. mexiletine (green). Variables that were significantly affected by mexiletine are highlighted with ↑ (for increase) and ↓ (for decrease). Subgraphs of excitability recordings are as follows: A) I/V relationship; B) strength-duration relationship; C) threshold electrotonus; D) recovery cycles. Graph E) is zoomed in on the depolarizing threshold electrotonus with 40% depolarizing currents. Indication of variables is reproduced from Kiernan et al.³ Note that these graphs show mean combined post-dose measurements for placebo vs. active treatment and baseline measurements are not considered, therefore these do not exactly match the statistical analysis. Moreover, these figures include all measurements including the minimal amount of data excluded in the blinded data review.



MEXILETINE Mexiletine significantly reduced SNAP amplitudes. Consistent with motor nerves, mexiletine decreased superexcitability (less negative) (Figure 4D). Moreover, hyperpolarizing I/V slope was significantly increased by mexiletine (Figure 4C).

LACOSAMIDE Lacosamide significantly shortened SDTC (Figure 4A). Additionally, lacosamide significantly reduced TED₄₀ peak, TED₄₀ (10-20ms) (Figure 4B), accommodation half-time and s₂-accommodation. These results are in line with our findings in motor nerves. Hyperpolarizing I/V-slope (Figure 4C) and minimum I/V-slope were significantly increased by lacosamide. Furthermore, lacosamide decreased refractoriness at ISI 2ms and subexcitability.

FIGURE 3 The average post-dose (three and six hours) motor nerve excitability threshold tracking recordings of placebo (black) vs. lacosamide (red). Variables that were significantly affected by lacosamide are highlighted with ↑ (for increase) and ↓ (for decrease). Subgraphs of excitability recordings are as follows: A) I/v relationship; B) strength-duration relationship; C) threshold electrotonus; D) recovery cycles. Graph E) is zoomed in on the depolarizing threshold electrotonus with 40% depolarizing currents. Indication of variables is reproduced from Kiernan *et al.*³ Note that these graphs show mean combined post-dose measurements for placebo vs. active treatment and baseline measurements are not considered, therefore these do not exactly match the statistical analysis. Moreover, these figures include all measurements including the minimal amount of data excluded in the blinded data review.

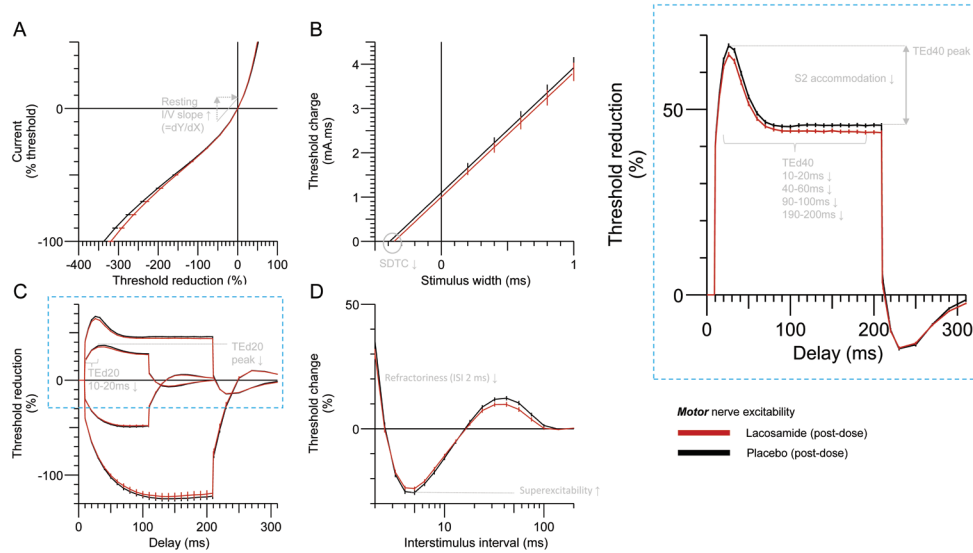


FIGURE 4 Estimated mean change from baseline of sensory nerve excitability threshold tracking variables. Every graph shows one selected variable with significant treatment effects from each threshold tracking paradigm: A) strength duration time constant (SDTC), B) TE_{d40} (10-20ms), C) Hyperpolarizing I/v slope, D) Superexcitability. Error bars indicate the 95% confidence interval. The time after dosing (hours) is indicated on the x-axis. Significant effects of mexiletine and/or lacosamide versus placebo in the treatment period are highlighted with an asterisk. N=18.

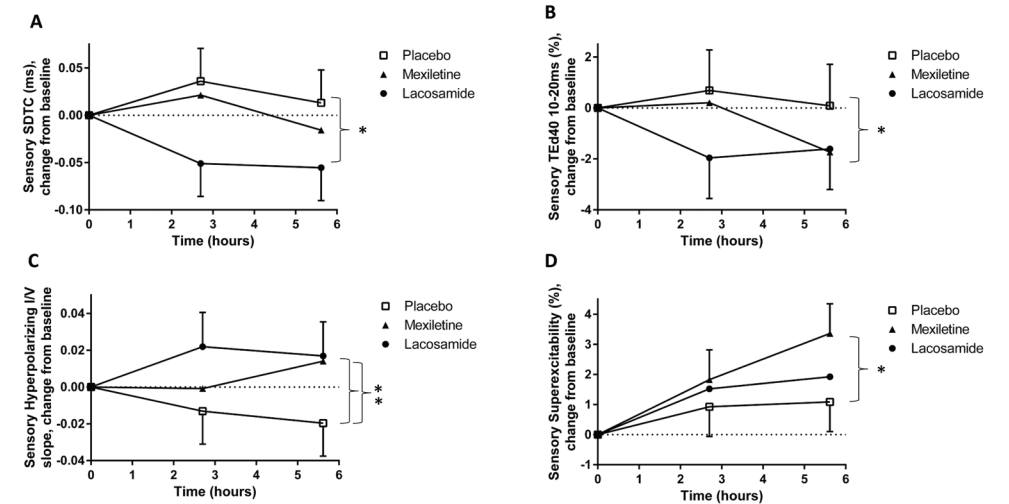


FIGURE 5 The average post-dose (three and six hours) sensory nerve excitability threshold tracking recordings of placebo (black) vs. mexiletine (green). Variables that were significantly affected by mexiletine are highlighted with ↑ (for increase) and ↓ (for decrease). Subgraphs of excitability recordings are as follows: A) I/V relationship; B) strength-duration relationship; C) threshold electrotonus; D) recovery cycles. Graph E) is zoomed in on the depolarizing threshold electrotonus with 40% depolarizing currents. Indication of variables is reproduced from Kiernan *et al.*³ Note that these graphs show mean combined post-dose measurements for placebo vs. active treatment and baseline measurements are not considered, therefore these do not exactly match the statistical analysis. Moreover, these figures include all measurements including the minimal amount of data excluded in the blinded data review.

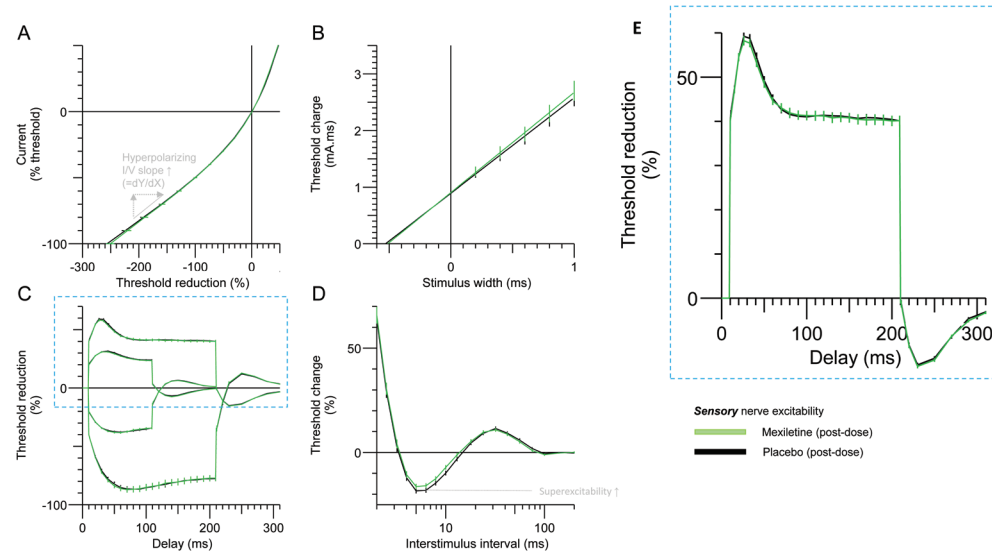


FIGURE 6 The average post-dose (three and six hours) sensory nerve excitability threshold tracking recordings of placebo (black) vs. lacosamide (red). Variables that were significantly affected by lacosamide are highlighted with ↑ (for increase) and ↓ (for decrease). Subgraphs of excitability recordings are as follows: A) I/V relationship; B) strength-duration relationship; C) threshold electrotonus; D) recovery cycles. Graph E) is zoomed in on the depolarizing threshold electrotonus with 40% depolarizing currents. Indication of variables is reproduced from Kiernan *et al.*³ Note that these graphs show mean combined post-dose measurements for placebo vs. active treatment and baseline measurements are not considered, therefore these do not exactly match the statistical analysis. Moreover, these figures include all measurements including the minimal amount of data excluded in the blinded data review.

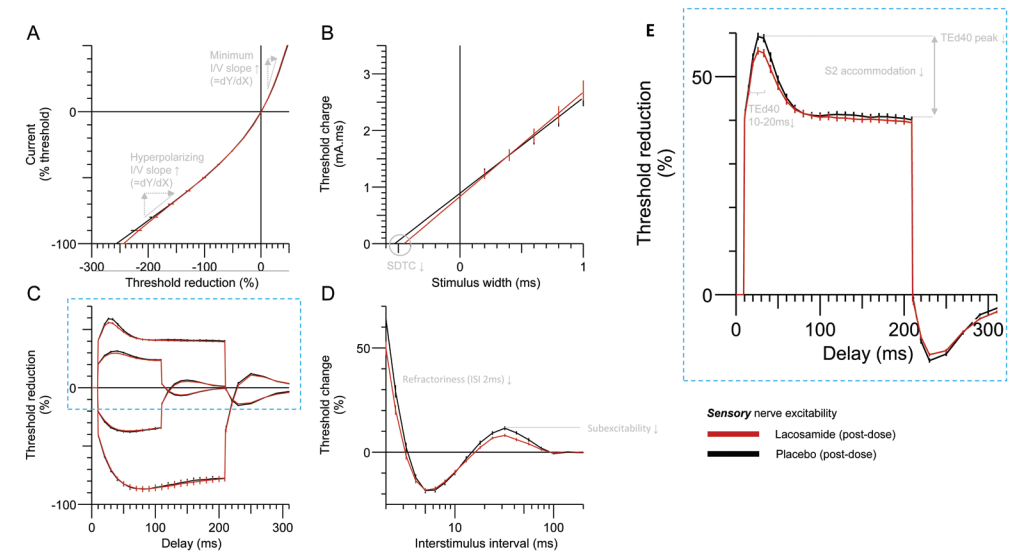


TABLE 1 Treatment effects of mexiletine vs. placebo, and lacosamide vs. placebo, on motor- and sensory nerve excitability threshold tracking endpoints (estimated mean difference with placebo, 95% CI, p-value).

		Motor nerve excitability			Sensory nerve excitability		
		Estimated mean treatment period	Estimated difference treatment vs. placebo (95%CI)	P value	Estimated mean treatment period	Estimated difference treatment vs. placebo (95%CI)	P value
CMAP (mV)/ SNAP (µV)	Placebo	13.4			44.2		
	Mexiletine	13.1	-0.351 (-1.05, 0.346)	0.312	39.2	-4.95 (-8.62, -1.29)	0.010
	Lacosamide	13.7	0.249 (-0.447, 0.946)	0.469	44.1	-0.0664 (-3.74, 3.61)	0.971
Threshold for 50% CMAP/ SNAP (mA)	Placebo	4.18			2.64		
	Mexiletine	4.33	0.147 (-0.128, 0.423)	0.285	2.74	3.7% (-5.6%, 14.0%)	0.434
	Lacosamide	4.14	-0.0406 (-0.312, 0.231)	0.763	2.77	4.8% (-4.6%, 15.2%)	0.314
Rheobase (mA)	Placebo	2.57			1.54		
	Mexiletine	2.63	0.164 (-0.0422, 0.370)	0.115	1.67	8.0% (-4.0%, 21.5%)	0.190
	Lacosamide	2.54	0.0609 (-0.143, 0.265)	0.547	1.72	11.6% (-0.8%, 25.6%)	0.065
Strength-duration time constant (ms)	Placebo	0.394			0.537		
	Mexiletine	0.378	-0.0167 (-0.0397, 0.0062)	0.147	0.516	-0.0218 (-0.0597, 0.0161)	0.251
	Lacosamide	0.360	-0.0342 (-0.0571, -0.0112)	0.005	0.460	-0.0778 (-0.116, -0.0399)	<0.001
TEd ₄₀ (10-20ms) (%)	Placebo	66.0			58.1		
	Mexiletine	64.9	-1.11 (-2.33, 0.0997)	0.070	56.9	-1.15 (-3.05, 0.747)	0.225
	Lacosamide	63.8	-2.21 (-3.41, -1.00)	0.001	55.9	-2.17 (-4.09, -0.247)	0.028
TEd ₄₀ (40-60ms) (%)	Placebo	49.4			45.8		
	Mexiletine	48.0	-1.37 (-2.20, -0.547)	0.002	45.0	-0.816 (-2.70, 1.07)	0.382
	Lacosamide	48.1	-1.27 (-2.10, -0.443)	0.004	45.5	-0.285 (-2.19, 1.62)	0.761
TEd ₄₀ (90-100ms) (%)	Placebo	45.5			41.5		
	Mexiletine	44.4	-1.06 (-1.95, -0.179)	0.020	40.7	-0.784 (-2.74, 1.17)	0.419
	Lacosamide	44.2	-1.28 (-2.16, -0.395)	0.006	41.4	-0.0998 (-2.08, 1.88)	0.919
TEd ₄₀ (190-200ms) (%)	Placebo	45.8			40.7		
	Mexiletine	44.4	-1.35 (-2.25, -0.452)	0.005	39.9	-0.782 (-2.73, 1.17)	0.418
	Lacosamide	43.7	-2.04 (-2.94, -1.14)	<0.001	39.7	-0.968 (-2.94, 1.00)	0.322
TEd ₄₀ peak (%)	Placebo	65.1			58.1		
	Mexiletine	63.9	-1.19 (-2.18, -0.195)	0.023	56.6	-1.46 (-3.36, 0.446)	0.128
	Lacosamide	62.8	-2.35 (-3.34, -1.36)	<0.001	55.9	-2.16 (-4.10, -0.222)	0.030
TEd ₄₀ accommodation half-time (ms)	Placebo	19.9			16.7		
	Mexiletine	19.6	-0.27 (-1.19, 0.64)	0.547	16.0	-0.75 (-1.78, 0.27)	0.144
	Lacosamide	18.7	-1.25 (-2.15, -0.34)	0.009	14.5	-2.21 (-3.26, -1.16)	<0.001
S ₂ accommodation (%)	Placebo	19.6			16.5		
	Mexiletine	19.5	-0.182 (-1.14, 0.778)	0.702	15.9	-0.682 (-1.77, 0.402)	0.209
	Lacosamide	18.6	-1.04 (-2.00, -0.0893)	0.033	14.4	-2.12 (-3.22, -1.01)	0.001
TEd ₂₀ (10-20ms) (%)	Placebo	34.0			-32.0		
	Mexiletine	33.8	-0.13 (-0.81, 0.55)	0.700	-31.4	-0.61 (-2.11, 0.88)	0.410
	Lacosamide	33.0	-0.95 (-1.62, -0.28)	0.008	-31.6	-1.13 (-2.65, 0.38)	0.136

(Continuation Table 1)

		Motor nerve excitability			Sensory nerve excitability		
		Estimated mean treatment period	Estimated difference treatment vs. placebo (95%CI)	P value	Estimated mean treatment period	Estimated difference treatment vs. placebo (95%CI)	P value
TEd ₂₀ peak (%)	Placebo	36.4			31.7		
	Mexiletine	35.9	-0.521 (-1.23, 0.186)	0.1406	30.7	-1.02 (-2.62, 0.569)	0.198
	Lacosamide	34.9	-1.57 (-2.26, -0.868)	<0.001	30.2	-1.55 (-3.17, 0.0739)	0.061
TEh ₄₀ (10-20ms) (%)	Placebo	-73.7			-66.0		
	Mexiletine	-74.0	-0.323 (-2.03, 1.39)	0.702	-65.9	0.0958 (-2.04, 2.24)	0.928
	Lacosamide	-72.3	1.34 (-0.368, 3.05)	0.120	-64.8	1.25 (-0.910, 3.41)	0.247
TEh ₄₀ (90-100ms) (%)	Placebo	-124			-85.2		
	Mexiletine	-123	0.386 (-4.23, 5.00)	0.865	-87.1	-1.84 (-4.92, 1.24)	0.233
	Lacosamide	-122	1.98 (-2.61, 6.57)	0.384	-85.6	-0.349 (-3.48, 2.78)	0.821
TEh ₄₀ (190-200ms) (%)	Placebo	-123			-78.7		
	Mexiletine	-124	-0.299 (-4.88, 4.29)	0.894	-78.9	-0.164 (-2.98, 2.65)	0.906
	Lacosamide	-121	2.64 (-1.92, 7.20)	0.244	-77.9	0.813 (-2.04, 3.67)	0.565
Fanning, sum of TEd ₄₀ -and TEh ₄₀ (190-200 ms)	Placebo	169			119		
	Mexiletine	168	-1.14 (-6.07, 3.80)	0.638	119	-0.443 (-4.64, 3.76)	0.831
	Lacosamide	164	-4.65 (-9.56, 0.258)	0.062	118	-1.86 (-6.12, 2.40)	0.380
Hyperpolarizing I/V-slope	Placebo	0.345			0.322		
	Mexiletine	0.330	-4.2% (-9.6%, 1.5%)	0.138	0.345	0.0230 (0.0033, 0.0427)	0.024
	Lacosamide	0.347	0.5% (-5.2%, 6.6%)	0.851	0.358	0.0358 (0.0158, 0.0558)	0.001
Minimum I/V-slope	Placebo	0.240			0.309		
	Mexiletine	0.234	-0.0063 (-0.0152, 0.0025)	0.153	0.318	0.0084 (-0.0038, 0.0206)	0.171
	Lacosamide	0.248	0.0072 (-0.0017, 0.0161)	0.107	0.328	0.0182 (0.0056, 0.0307)	0.006
Resting I/V-slope	Placebo	0.580			0.768		
	Mexiletine	0.586	0.0051 (-0.0164, 0.0265)	0.630	0.778	1.3% (-5.1%, 8.1%)	0.688
	Lacosamide	0.606	0.0258 (0.0043, 0.0474)	0.021	0.760	-0.9% (-7.3%, 5.8%)	0.771
Relative refractory period (ms)	Placebo	2.57			3.33		
	Mexiletine	2.63	0.0532 (0.0013, 0.105)	0.045	3.35	0.0188 (-0.142, 0.180)	0.812
	Lacosamide	2.54	-0.0323 (-0.0840, 0.0193)	0.211	3.18	-0.152 (-0.313, 0.0089)	0.063
Refractoriness at ISI 2 ms (%)	Placebo	35.0			64.6		
	Mexiletine	38.1	3.06 (-0.568, 6.69)	0.095	62.9	-1.70 (-8.77, 5.37)	0.626
	Lacosamide	31.0	-4.02 (-7.64, -0.395)	0.031	50.9	-13.71 (-20.75, -6.66)	0.001
Subexcitability (%)	Placebo	11.6			10.4		
	Mexiletine	12.1	0.480 (-1.05, 2.01)	0.520	10.6	0.280 (-1.30, 1.86)	0.718
	Lacosamide	11.1	-0.483 (-2.06, 1.10)	0.533	7.74	-2.62 (-4.21, -1.03)	0.002
Superexcitability (%)	Placebo	-24.3			-18.5		
	Mexiletine	-22.6	1.74 (0.615, 2.87)	0.004	-16.9	1.58 (0.609, 2.56)	0.002
	Lacosamide	-22.8	1.47 (0.341, 2.60)	0.013	-17.8	0.714 (-0.260, 1.69)	0.145

CI, confidence interval; CMAP, compound muscle action potential; ISI, interstimulus interval; SNAP, sensory nerve action potential.

DISCUSSION

This study was performed to evaluate whether NETT is a useful tool to determine PD effects of Na_V-blockers in early phase clinical drug development. As a proof-of-concept, we evaluated effects of mexiletine and lacosamide on motor- and sensory NETT. We found a significant reduction of nerve excitability by both study drugs, indicating that NETT is sensitive to detect drug-induced changes in Na_V-conductance.

EFFECTS OF Na_V-BLOCKERS ON NETT To our knowledge this is the first study to demonstrate effects of oral Na_V-blockers on NETT in healthy subjects. However, proposed effects of reduced Na_V-conductance by tetrodotoxin (TTX) on NETT have been evaluated previously using theoretical nerve modelling.¹² Kiernan *et al.* concluded that TTX-effects are mainly caused by a threshold increase and flattening of the threshold/potential relationship. This in turn results in a decrease in SDTC and an increase in rheobase. SDTC is a membrane-time constant derived from the rate of decline of current strength required at increasing stimulus durations, thought to be dependent on persistent Na_V-channel properties.⁴ Our study, with Na_V-blockers with different modes of action than TTX, also showed a decrease of SDTC by lacosamide, but interestingly not by mexiletine. Rheobase was unaffected. Threshold electrotonus examines the threshold reduction due to depolarizing and hyperpolarizing conditioning currents, to demonstrate internodal membrane properties.⁴ The model by Kiernan *et al.* also predicts a clear decrease in depolarizing threshold electrotonus and an increase in hyperpolarizing threshold electrotonus. Our results are in line with the TTX-effect on depolarizing threshold electrotonus, but not with the TTX-effect on hyperpolarizing threshold electrotonus. Furthermore, the nerve model by Kiernan *et al.* shows a reduction of all phases of the recovery cycles by Na_V-blockade, resulting in a flattening of the recovery cycles curve, corroborating our findings. Lastly, the model predicts an increased hyperpolarizing I/V-slope, which is explained by Kiernan *et al.* as activation of hyperpolarization mediated I_H currents, corresponding to our findings for both mexiletine and lacosamide.

Based on the resemblance between the theoretical nerve model with TTX¹² and our findings, we conclude that the significant effects

of mexiletine and lacosamide on nerve excitability are in line with expected effects of Na_V-blockade. Above-described differences between the TTX-model and mexiletine and lacosamide (rheobase, hyperpolarizing threshold electrotonus), may be explained by the difference in mechanism of action. TTX binds to Na_V extracellularly at the outer pore, preventing access of cations,¹² whereas mexiletine binds to the inner pore and exhibits a state-dependent Na_V-block.¹³ The binding site and action mechanism of lacosamide is much less clear. Lacosamide was originally suggested to selectively enhance slow Na_V-inactivation without affecting fast inactivation, through an unknown binding site.^{14,15} More recent findings suggest that lacosamide does bind to fast-inactivated state of sodium channels, but with slow binding and unbinding kinetics.¹⁶ Another possible explanation for the lack of effects of mexiletine and lacosamide on rheobase and hyperpolarizing threshold electrotonus, may be a larger reduction of Na_V-conductance by TTX. Overall, this data supports the hypothesis that the observed effects are a result of direct Na_V-blockade, however, it should be noted that additional (indirect) effects for example on membrane potential or other ion channels could also contribute to the observed pattern of NETT effects, as was described for lidocaine.¹⁷ To better understand the exact mechanisms for the observed NETT effects, in future work it would be of interest to perform nerve modeling with our data to clarify this further, as described above for TTX.¹²

When comparing effects between the Na_V-blockers – mexiletine and lacosamide – within our study, many observed effects are similar, such as effects on depolarizing threshold electrotonus and superexcitability. However, lacosamide affected a more extensive set of variables than mexiletine, often with larger effect sizes. Difference in target site concentration and/or potency at the relevant involved ion-channels are potential causes for these discrepancies. A difference in mechanism of action or binding kinetics of the drugs is another possible explanation.

Apart from theoretical model simulations, there is a limited amount of prior clinical data investigating Na_V-blocking effects on NETT in humans available to place our findings into context. Effects of a high dose of lidocaine (5-6 ml of a 50 mM solution lidocaine) administered as local nerve block (not placebo-controlled)¹⁷ and human intoxication with TTX¹² have been previously evaluated. After the conduction block of anaesthetic lidocaine perfusion, when force had recovered, profound effects on nerve excitability were still measured. Consistent results between lidocaine

and TTX were a decreased depolarizing threshold electrotonus, SDTC, and superexcitability, which is in line with our findings on these variables. It should be noted however, that at high concentrations lidocaine decreased hyperpolarizing electrotonus and left-shifted the depolarizing I/V relationship, which was opposite to effects of TTX poisoning. This discrepancy indicates there may be other factors than Na_v blockade driving these changes, and the authors indeed showed with nerve modelling that (indirect) effects on membrane potential and other channels contributed to the observed lidocaine effect.^{12,17} Of course, this setting with high local drug concentrations might not be fully comparable to our setting with oral administrations.

A final relevant study examined chronic effects of mexiletine in patients with neuropathic pain: mexiletine decreased refractoriness and SDTC after three months of use,⁵ in line with our reported effects of lacosamide but not mexiletine.

DIFFERENT EFFECTS ON MOTOR- AND SENSORY NERVES We found different effects of Na_v-blockade on motor vs. sensory nerve excitability. In general, effects we found on depolarizing threshold electrotonus were more apparent in motor nerves, whereas effects on I/V (hyperpolarizing and minimum I/V slope) were only significantly affected in sensory nerves. These disparate effects may be explained by a physiological difference in nerve excitability profile between motor- and sensory axons of the median nerve.^{18,19} There are differences in expression of persistent Na_v-channels between motor- and sensory nerves.²⁰ Moreover, within each group there are further differences of motor axons innervating fast or slow muscles, whereas cutaneous sensory neurons contain 4 types of afferents which could be differentially affected by Na_v-blockade. This could include:

- differences in resting membrane potential
- expression differences of transporters such as the sodium/potassium ATPase pump
- qualitative and quantitative differential ion-channel expression profiles.¹⁹

There may also be technical limitations that could explain these differences: recording of SNAPS is more challenging than CMAPs. However, the CV%s were not much higher in sensory- than motor recordings and it is therefore likely that the observed excitability changes reflect mechanistic differences.

CONCENTRATION-EFFECT RELATIONSHIPS The majority (90%) of variables with significant treatment effects also have significant concentration-effect relationships, pointing towards concentration-dependent treatment effects in the studied concentration-range. The fact that we prove drug concentration to be the driver for detected treatment effects encourages the use of NETT as biomarker for pharmacological effects of Na_v modulators. A substantial additional set of 25 variables that did not show significant treatment effects, also had a significant linear concentration-effect relationship. This may hint at an underlying concentration-dependent effect, although not sufficiently robust to be demonstrated in the treatment effect analysis and a larger sample size might be required to identify significant treatment effects on these variables.

NERVE EXCITABILITY THRESHOLD TRACKING AS PD BIOMARKER

A reliable biomarker of Na_v blocking effects for use in early phase clinical drug development is lacking. Given the results of this study, we conclude that NETT is a suitable biomarker for PD effects of Na_v-blockers. Most importantly, in a relatively small number of healthy subjects, significant effects of Na_v-blockade can be detected at plasma concentrations within the therapeutic range. Moreover, NETT has favourable characteristics for a PD biomarker. It is non-invasive and relatively quick to perform, allowing evaluation of nerve excitability several times a day at different drug plasma concentrations. Intrasubject variability is low, as CV%s (estimated from the statistical model) were below 10% for most variables, which indicates high test-retest reliability (Supplementary Table 4). These characteristics indicate that NETT can be considered a valuable tool for determining target engagement in early phase clinical studies in a healthy population. Furthermore, the significant concentration-effect relations found in our study could indicate that the method is suitable for detecting dose-related effects in first-in-human ascending dose studies, as a signal for receptor occupancy. This should be confirmed in future studies. Moreover, the biomarker could potentially be used as a translational tool, for the translation from preclinical (animal) data to human effective doses, as also suggested previously for local anaesthetic nerve blocks.²¹ Also, NETT could aid dose finding in the translation from healthy subjects to patients.

POSSIBLE LIMITATIONS A limitation for the concentration-effect relationship analysis, was the limited number of PD measurements and corresponding PK samples. Because of the long half-life of the study drugs, both measurements were performed at high plasma concentrations. To confirm the potential of NETT to detect concentration-effect relationships, a wider range of plasma concentrations would be desirable.

Statistical analysis performed in our study was not corrected for multiple testing, because of the exploratory nature of the study. However, there is a clear consistency in the significant effects and most significant effects are accompanied by a significant linear concentration-effect relationship, strongly indicating that pharmacological effects are underlying these results.

CONCLUSION To our knowledge, this is the first published randomized, placebo-controlled trial to evaluate acute effects of Na_v-blockers (mexiletine and lacosamide) on NETT in healthy subjects. This study shows that NETT can be used to detect a decrease in peripheral nerve excitability exhibited by both mexiletine and lacosamide. Therefore, NETT can be considered a valuable PD biomarker for effects of Na_v-modulation. This could be a useful tool in early phase clinical drug development for proof-of-mechanism, and potentially to assist in dose finding for patient studies.

SUPPLEMENTARY INFORMATION

SUPPLEMENTARY TABLE 1 Demographics.

Demographics	N	18
Age (years)	Mean	25
	SD	5
	Median	24
	Range	19, 36
Height (cm)	Mean	184
	SD	8
	Median	184
	Range	170, 202
Weight (kg)	Mean	80
	SD	13
	Median	80
	Range	60, 100
BMI (kg/m ²)	Mean	23
	SD	3
	Median	23
	Range	19, 30

BMI = body mass index; SD = standard deviation.

SUPPLEMENTARY TABLE 2 Plasma concentrations (mg/L) of mexiletine and lacosamide at the scheduled sampling times (minutes after dosing). Additionally, this table lists median concentration in μ M, based on molecular weight 250.29 g/mol for lacosamide¹ and molecular weight 179.26 g/mol for mexiletine.²

	Time after dosing (minutes)	Mean plasma concentration (mg/L)	Standard deviation	Median plasma concentration (mg/L)	Median plasma concentration (μ M)
Lacosamide (300 mg)	0	0	0	0	0
	160	5.88	1.18	5.89	23.51
	204	5.69	1.12	5.70	22.75
	335	4.98	1.01	4.94	19.72
	379	4.83	0.988	4.87	19.44
Mexiletine (333 mg)	0	0.00	0.00	0.00	0.00
	160	0.903	0.214	0.855	4.77
	204	0.835	0.195	0.787	4.39
	335	0.653	0.155	0.618	3.45
	379	0.639	0.187	0.590	3.29

1. National Center for Biotechnology Information. PubChem Compound Summary for CID 219078, Lacosamide. 2005-08-09 updated 2022-01-29. Available from: <https://pubchem.ncbi.nlm.nih.gov/compound/Lacosamide>.

2. National Center for Biotechnology Information. PubChem Compound Summary for CID 4178, Mexiletine. 2005-06-24 updated 2022-01-29. Available from: <https://pubchem.ncbi.nlm.nih.gov/compound/Mexiletine>.

SUPPLEMENTARY TABLE 3 Raw baseline and estimated means (three- and six-hours post-dose) of excitability variables for placebo, mexiletine and lacosamide.

		Motor nerve excitability			Sensory nerve excitability		
		Raw mean baseline	Estimated mean +3h	Estimated mean +6h	Raw mean baseline	Estimated mean +3h	Estimated mean +6h
CMAP (mV)/ SNAP (µV)	Placebo	13.0	13.5	13.4	37.8	43.8	44.6
	Mexiletine	12.5	13.1	13.0	40.3	41.7	36.8
	Lacosamide	12.6	13.7	13.7	41.3	46.0	42.3
Threshold for 50% CMAP/ SNAP (mA)	Placebo	4.34	4.16	4.20	3.02	2.65	2.63
	Mexiletine	4.81	4.20	4.45	2.88	2.77	2.71
	Lacosamide	4.23	4.14	4.14	2.96	2.74	2.80
Rheobase (mA)	Placebo	3.06	2.59	2.56	1.86	1.54	1.55
	Mexiletine	3.41	2.65	2.61	1.74	1.67	1.67
	Lacosamide	2.94	2.56	2.52	1.81	1.71	1.74
Strength-duration time constant (ms)	Placebo	0.379	0.401	0.388	0.520	0.549	0.526
	Mexiletine	0.374	0.390	0.365	0.514	0.534	0.497
	Lacosamide	0.383	0.362	0.359	0.505	0.462	0.457
TEd ₄₀ 10-20ms (%)	Placebo	65.7	66.2	65.7	58.1	58.4	57.8
	Mexiletine	66.5	65.3	64.5	57.9	57.9	55.9
	Lacosamide	65.6	63.9	63.6	57.0	55.7	56.1
TEd ₄₀ 40-60ms (%)	Placebo	49.6	49.5	49.3	46.9	46.1	45.5
	Mexiletine	49.6	48.3	47.7	45.9	45.6	44.4
	Lacosamide	49.4	48.4	47.8	45.7	45.3	45.7
TEd ₄₀ 90-100ms (%)	Placebo	45.8	45.3	45.6	42.4	41.6	41.5
	Mexiletine	45.7	44.3	44.5	42.0	40.9	40.6
	Lacosamide	45.7	44.0	44.4	41.8	40.7	42.2
TEd ₄₀ 190-200ms (%)	Placebo	45.6	45.7	45.9	41.5	40.4	41.0
	Mexiletine	45.6	44.5	44.4	40.6	40.3	39.6
	Lacosamide	45.7	43.7	43.8	41.6	39.5	39.9
TEd ₄₀ peak (%)	Placebo	64.9	65.3	64.9	58.4	58.4	57.8
	Mexiletine	65.5	64.4	63.5	58.1	57.6	55.6
	Lacosamide	64.7	63.0	62.5	56.9	55.7	56.1
TEd ₄₀ accommodation half-time (ms)	Placebo	19.4	20.2	19.6	16.1	17.1	16.3
	Mexiletine	20.1	20.1	19.2	16.2	16.6	15.3
	Lacosamide	19.3	19.0	18.3	15.2	14.9	14.1
S ₂ accommodation (%)	Placebo	19.1	20.0	19.2	16.1	16.8	16.3
	Mexiletine	19.8	20.0	18.9	16.1	16.8	15.0
	Lacosamide	19.0	19.1	18.1	15.2	15.0	13.9
TEd ₂₀ 10-20ms (%)	Placebo	33.8	33.9	34.0	29.7	-32.2	-31.9
	Mexiletine	34.3	33.9	33.7	29.6	-32.0	-30.9
	Lacosamide	34.0	33.0	33.1	29.1	-31.0	-32.2
TEd ₂₀ peak (%)	Placebo	36.2	36.5	36.4	31.4	31.8	31.6
	Mexiletine	37.0	36.1	35.7	31.2	31.4	30.0
	Lacosamide	36.3	35.0	34.8	30.7	30.0	30.4

(Continuation Supplementary Table 3)

		Motor nerve excitability			Sensory nerve excitability		
		Raw mean baseline	Estimated mean +3h	Estimated mean +6h	Raw mean baseline	Estimated mean +3h	Estimated mean +6h
TEh ₄₀ 10-20ms (%)	Placebo	-73.0	-73.9	-73.4	-66.5	-66.5	-65.5
	Mexiletine	-73.6	-74.4	-73.6	-66.3	-66.5	-65.3
	Lacosamide	-73.7	-72.2	-72.5	-66.2	-63.7	-65.8
TEh ₄₀ 90-100ms (%)	Placebo	-123	-125	-122	-89.7	-85.8	-84.7
	Mexiletine	-124	-124	-123	-87.4	-86.9	-87.2
	Lacosamide	-122	-121	-122	-89.0	-84.6	-86.5
TEh ₄₀ 190-200ms (%)	Placebo	-124	-124	-123	-81.0	-78.7	-78.8
	Mexiletine	-127	-124	-123	-79.9	-78.6	-79.1
	Lacosamide	-123	-121	-121	-81.3	-76.8	-79.1
Fanning sum of TEd ₄₀ - and TEh ₄₀ 190-200 ms	Placebo	169	170	168	122	119	120
	Mexiletine	173	169	167	121	119	119
	Lacosamide	169	164	165	123	116	119
Hyper- polarizing 1/v-slope	Placebo	0.347	0.356	0.334	0.334	0.325	0.318
	Mexiletine	0.356	0.338	0.323	0.330	0.337	0.352
	Lacosamide	0.364	0.346	0.348	0.349	0.360	0.355
Minimum 1/v-slope	Placebo	0.240	0.241	0.240	0.304	0.311	0.307
	Mexiletine	0.236	0.236	0.232	0.305	0.316	0.319
	Lacosamide	0.249	0.249	0.246	0.316	0.335	0.320
Resting 1/v-slope	Placebo	0.588	0.579	0.582	0.725	0.771	0.765
	Mexiletine	0.585	0.579	0.592	0.742	0.777	0.779
	Lacosamide	0.575	0.607	0.605	0.775	0.779	0.742
Relative refractory period (ms)	Placebo	2.52	2.59	2.56	3.18	3.38	3.28
	Mexiletine	2.56	2.65	2.61	3.24	3.37	3.33
	Lacosamide	2.52	2.56	2.52	3.15	3.27	3.09
Refractor-iness at 1S1 2 ms (%)	Placebo	32.2	36.5	33.6	55.2	66.5	62.6
	Mexiletine	33.8	40.6	35.6	56.3	65.2	60.5
	Lacosamide	31.1	33.2	28.8	53.2	54.2	47.5
Sub-excitability (%)	Placebo	11.9	11.7	11.5	9.72	10.5	10.2
	Mexiletine	11.1	12.1	12.1	8.87	10.7	10.6
	Lacosamide	10.4	11.5	10.8	9.20	8.09	7.40
Super-excitability (%)	Placebo	-24.9	-24.7	-23.9	-19.5	-18.6	-18.4
	Mexiletine	-24.4	-22.9	-22.2	-19.1	-17.7	-16.2
	Lacosamide	-24.9	-23.2	-22.4	-19.9	-17.6	-18.0

SUPPLEMENTARY TABLE 4 Inter- and intrasubject coefficient of variation (cv%) based pre-dose values at each visit, and intrasubject cv% based on the statistical model.

	Motor nerve excitability			Sensory nerve excitability		
	Inter-subject cv (%)	Intra-subject cv (%)	Model-based intrasubject cv (%)	Inter-subject cv (%)	Intra-subject cv (%)	Model-based intrasubject cv (%)
CMAP (mV)/SNAP (μ V)	26.7	12.8	8.9	34.3	16	16.9
Threshold for 50% CMAP/SNAP (mA)	32.9	31.2	12.7	33.9	32.9	18.20
Rheobase (mA)	35.8	34.4	14.1	38.9	37.5	22.10
Strength-duration time constant (ms)	22.9	13	10.1	19.7	16.2	13.9
TEd ₄₀ (10-20ms) (%)	6	3.7	3	8	5.5	5.4
TEd ₄₀ (40-60ms) (%)	7.3	3.6	2.7	9.8	5.1	6.6
TEd ₄₀ (90-100ms) (%)	8.1	4.1	3.2	10.1	5.4	7.9
TEd ₄₀ (190-200ms) (%)	8.2	4.2	3.2	10.9	5.4	7.6
TEd ₄₀ peak (%)	6	3.4	2.5	8.2	4.8	5.2
TEd ₄₀ accommodation half-time (ms)	12.3	6.5	7.9	16.1	10.6	11.4
S ₂ -accommodation (%)	12.4	7	8.4	16	9.7	12.1
TEd ₂₀ (10-20ms) (%)	6.6	4.6	3.2	9.1	6.8	8.6
TEd ₂₀ peak (%)	8	5	3.3	9.1	6	8.2
TEh ₄₀ (10-20ms) (%)	7.2	4.5	3.8	6.5	4.1	5.3
TEh ₄₀ (90-100ms) (%)	15.3	8.6	5.9	16.1	7.2	5.9
TEh ₄₀ (190-200ms) (%)	18.1	10.1	6.1	16.2	6.7	5.8
Fanning	14.6	7.7	4.8	13.5	5	5.6
Hyperpolarizing 1/v-slope	15.8	8.5	9.90	16.3	10.2	10.1
Minimum 1/v-slope	17.3	8.4	6.1	14.2	7.9	7.3
Resting 1/v-slope	12.7	6.5	5.8	15.5	9.3	11.60
Relative refractory period (ms)	8.2	4.3	3.5	15.9	6.3	7.7
Refractoriness at ISI 2 ms (%)	40.5	22.6	19.1	38.9	17.7	19.2
Subexcitability (%)	35.7	24	20.1	43.6	16.3	26.2
Superexcitability (%)	21	7.7	7.9	31.4	8.7	9.6

SUPPLEMENTARY TABLE 5 Concentration-effect relationship relationships of excitability threshold tracking endpoints. The slope and p-value of the linear effect relations are reported. Baseline was estimated as a separate variable in the model.

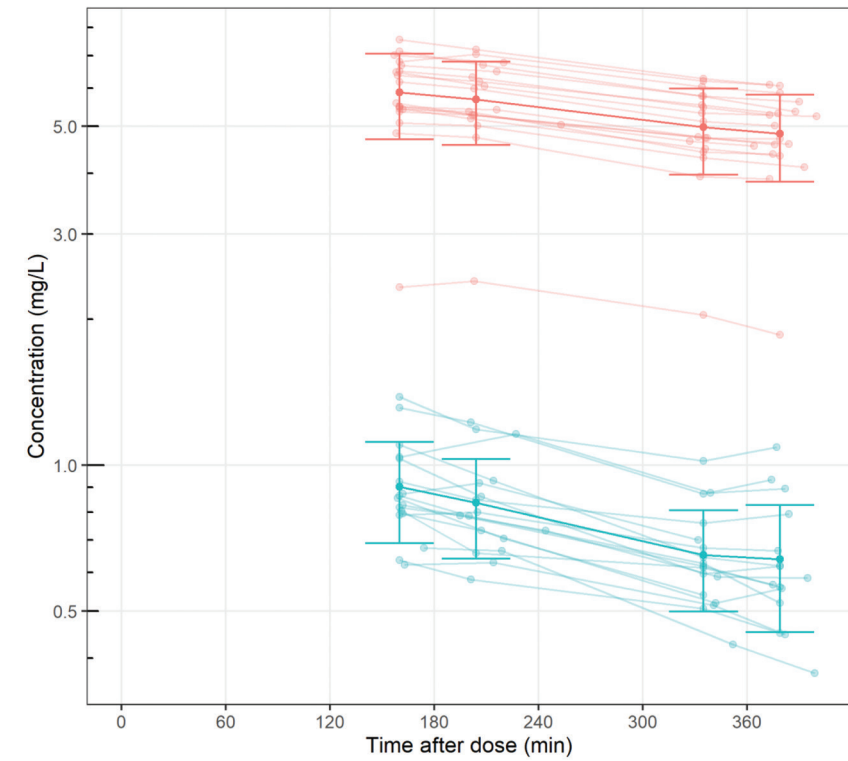
		Motor nerve			Sensory nerve		
		Estimated population baseline	Slope (/ug/L)	P value	Estimated population baseline	Slope (/ug/L)	P value
CMAP (mV)/SNAP (μ V)	Mexiletine	13.14			40.38		
	Lacosamide	13.13	0.15	0.001	40.9	0.862	0.004
Threshold for 50% CMAP/SNAP (mA)	Mexiletine	4.39			2.89		
	Lacosamide	4.12			2.92		
Rheobase (mA)	Mexiletine	3.08			1.75		
	Lacosamide	2.88			1.78		
Strength-duration time constant (ms)	Mexiletine	0.38			0.53		
	Lacosamide	0.39	-0.004	0.002	0.52	-0.011	<0.001
TEd ₄₀ (10-20ms) (%)	Mexiletine	65.68			57.8		
	Lacosamide*	65.7	1.02/-2.56	<0.001	57.8	-0.385	<0.001
TEd ₄₀ (40-60ms) (%)	Mexiletine	49.46	-1.732	<0.001	46.14	-1.508	0.037
	Lacosamide	49.43	-0.248	<0.001	45.87		
TEd ₄₀ (90-100ms) (%)	Mexiletine	45.61	-1.582	<0.001	41.84	-1.502	0.037
	Lacosamide	45.64	-0.282	<0.001	41.63		
TEd ₄₀ (190-200ms) (%)	Mexiletine	45.58	-1.39	<0.001	40.73	-1.487	0.038
	Lacosamide	45.7	-0.352	<0.001	41.2	-0.24	0.002
TEd ₄₀ peak (%)	Mexiletine	64.99	-0.893	0.043	57.84		
	Lacosamide	64.82	-0.40	<0.001	57.89	-0.433	<0.001
TEd ₄₀ accommodation half-time (ms)	Mexiletine	19.76			16.48		
	Lacosamide	19.44	-0.167	0.001	16.05	-0.285	<0.001
S ₂ -accommodation (%)	Mexiletine	19.5			16.38		
	Lacosamide	19.19	-0.122	0.022	15.99	-0.29	0.001
TEd ₂₀ (10-20ms) (%)	Mexiletine	33.93			29.29		
	Lacosamide	33.84	-0.171	<0.001	29.29		
TEd ₂₀ peak (%)	Mexiletine	36.35			31.32		
	Lacosamide*	36.29	1.57/-2.01	<0.001	31.37	-0.239	0.005
TEh ₄₀ (10-20ms) (%)	Mexiletine	-73.58			-66.23		
	Lacosamide	-73.41	0.193	0.025	-66.27	0.313	0.016
TEh ₄₀ (90-100ms) (%)	Mexiletine	-124.36			-87.01		
	Lacosamide	-122.07			-88.12	0.59	0.001
TEh ₄₀ (190-200ms) (%)	Mexiletine	-124.64			-79.81	2.37	0.037
	Lacosamide	-123	0.635	0.042	-80.27	0.503	<0.001
Fanning	Mexiletine	169.87			120.48	-3.721	0.017
	Lacosamide	168.71	-0.989	0.003	121.5	-0.763	<0.001
Hyperpolarizing 1/v-slope	Mexiletine	0.34			0.33		
	Lacosamide	0.35			0.33	0.004	0.002

(Continuation Supplementary Table 3)

		Motor nerve			Sensory nerve		
		Estimated population baseline	Slope (/ug/L)	P value	Estimated population baseline	Slope (/ug/L)	P value
Minimum 1/v-slope	Mexiletine	0.24	-0.008	0.025	0.31		
	Lacosamide	0.24	0.001	0.029	0.31	0.004	<0.001
Resting 1/v-slope	Mexiletine	0.59			0.75	0.051	0.025
	Lacosamide	0.58	0.004	0.002	0.76	0.007	0.019
Relative refractory period (ms)	Mexiletine	2.56	0.102	<0.001	3.29	0.155	0.007
	Lacosamide	2.54			3.23		
Refractoriness at 1s1 2 ms (%)	Mexiletine	34.14	5.963	0.007	60.05	5.675	0.035
	Lacosamide	32.21			57.85	-1.102	0.019
Subexcitability (%)	Mexiletine	11.95			9.91		
	Lacosamide	11.26			10.06	-0.443	<0.001
Superexcitability (%)	Mexiletine	-24.37	2.421	<0.001	-18.81	2.418	<0.001
	Lacosamide	-24.66	0.311	<0.001	-19.26	0.256	<0.001

*E_{max} variables presented as EC₅₀/E_{max}. EC₅₀ is reported as ug/L.

SUPPLEMENTARY FIGURE 1 Individual and mean ± standard deviation plasma concentrations of mexiletine and lacosamide, at all four post-dose sampling timepoints before and after the nerve excitability threshold tracking measurements at three and six hours after dosing. N=18.



REFERENCES

- 1 Alsalous M, Higerd GP, Effraim PR, Waxman SG. Status of peripheral sodium channel blockers for non-addictive pain treatment. *Nature reviews Neurology*. Dec 2020;16(12):689-705. doi:10.1038/s41582-020-00415-2
- 2 Bostock H, Cikurel K, Burke D. Threshold tracking techniques in the study of human peripheral nerve. *Muscle & nerve*. Feb 1998;21(2):137-58. doi:10.1002/(SICI)1097-4598(199802)21:2<137::aid-mus1>3.0.co;2-c
- 3 Kiernan MC, Bostock H, Park SB, et al. Measurement of axonal excitability: Consensus guidelines. *Clinical neurophysiology; official journal of the International Federation of Clinical Neurophysiology*. Jan 2020;131(1):308-323. doi:10.1016/j.clinph.2019.07.023
- 4 Burke D, Kiernan MC, Bostock H. Excitability of human axons. *Clinical neurophysiology; official journal of the International Federation of Clinical Neurophysiology*. Sep 2001;112(9):1575-85. doi:10.1016/S1388-2457(01)00595-8
- 5 Kuwabara S, Misawa S, Tamura N, et al. The effects of mexiletine on excitability properties of human median motor axons. *Clinical neurophysiology; official journal of the International Federation of Clinical Neurophysiology*. Feb 2005;116(2):284-9. doi:10.1016/j.clinph.2004.08.014
- 6 Pringle T, Fox J, McNeill JA, et al. Dose independent pharmacokinetics of mexiletine in healthy volunteers. *British journal of clinical pharmacology*. Mar 1986;21(3):319-21. doi:10.1111/j.1365-2125.1986.tb05196.x
- 7 Svendsen T, Brodtkorb E, Baftiu A, Burns ML, Johannessen SI, Johannessen Landmark C. Therapeutic Drug Monitoring of Lacosamide in Norway: Focus on Pharmacokinetic Variability, Efficacy and Tolerability. *Neurochemical research*. Jul 2017;42(7):2077-2083. doi:10.1007/s11064-017-2234-8
- 8 Reimers A, Berg JA, Burns ML, Brodtkorb E, Johannessen SI, Johannessen Landmark C. Reference ranges for antiepileptic drugs revisited: a practical approach to establish national guidelines. *Drug design, development and therapy*. 2018;12:271-280. doi:10.2147/dddt.s154388
- 9 Cawello W, Mueller-Voessing C, Fichtner A. Pharmacokinetics of lacosamide and omeprazole coadministration in healthy volunteers: results from a phase I, randomized, crossover trial. *Clinical drug investigation*. May 2014;34(5):317-25. doi:10.1007/s40261-014-0177-2
- 10 Kovalchuk MO, Heuberger J, Sleutjes B, et al. Acute Effects of Riluzole and Retigabine on Axonal Excitability in Patients With Amyotrophic Lateral Sclerosis: A Randomized, Double-Blind, Placebo-Controlled, Crossover Trial. *Clinical pharmacology and therapeutics*. Dec 2018;104(6):1136-1145. doi:10.1002/cpt.1096
- 11 Tomlinson S, Burke D, Hanna M, Koltzenburg M, Bostock H. In vivo assessment of HCN channel current (I_h) in human motor axons. *Muscle & nerve*. 2010;41(2):247-256. doi:https://doi.org/10.1002/mus.21482
- 12 Kiernan MC, Isbister GK, Lin CS, Burke D, Bostock H. Acute tetrodotoxin-induced neurotoxicity after ingestion of puffer fish. *Annals of neurology*. Mar 2005;57(3):339-48. doi:10.1002/ana.20395
- 13 Nakagawa H, Munakata T, Sunami A. Mexiletine Block of Voltage-Gated Sodium Channels: Isoform- and State-Dependent Drug-Pore Interactions. *Molecular pharmacology*. Mar 2019;95(3):236-244. doi:10.1124/mol.118.114025
- 14 Errington AC, Stöhr T, Heers C, Lees G. The investigational anticonvulsant lacosamide selectively enhances slow inactivation of voltage-gated sodium channels. *Molecular pharmacology*. Jan 2008;73(1):157-69. doi:10.1124/mol.107.039867
- 15 Curia G, Biagini G, Perucca E, Avoli M. Lacosamide: a new approach to target voltage-gated sodium currents in epileptic disorders. *CNS drugs*. 2009;23(7):555-68. doi:10.2165/00023210-200923070-00002
- 16 Jo S, Bean BP. Lacosamide Inhibition of Nav1.7 Voltage-Gated Sodium Channels: Slow Binding to Fast-Inactivated States. *Molecular pharmacology*. Apr 2017;91(4):277-286. doi:10.1124/mol.116.106401
- 17 Moldovan M, Lange KH, Aachmann-Andersen NJ, Kjær TW, Olsen NV, Krarup C. Transient impairment of the axolemma following regional anaesthesia by lidocaine in humans. *The Journal of physiology*. Jul 1 2014;592(13):2735-50. doi:10.1113/jphysiol.2014.270827
- 18 Kiernan MC, Lin CS, Andersen KV, Murray NM, Bostock H. Clinical evaluation of excitability measures in sensory nerve. *Muscle & nerve*. Jul 2001;24(7):883-92. doi:10.1002/mus.1085
- 19 Fujimaki Y, Kanai K, Misawa S, et al. Differences in excitability between median and superficial radial sensory axons. *Clinical neurophysiology; official journal of the International Federation of Clinical Neurophysiology*. Jul 2012;123(7):1440-5. doi:10.1016/j.clinph.2011.11.002
- 20 Bostock H, Rothwell JC. Latent addition in motor and sensory fibres of human peripheral nerve. *The Journal of physiology*. Jan 1 1997;498 (Pt 1)(Pt 1):277-94. doi:10.1113/jphysiol.1997.sp021857
- 21 Moldovan M, Alvarez S, Rothe C, et al. An in vivo Mouse Model to Investigate the Effect of Local Anesthetic Nanomedicines on Axonal Conduction and Excitability. *Frontiers in neuroscience*. 2018;12:494. doi:10.3389/fnins.2018.00494



CHAPTER 5

**MUSCLE VELOCITY RECOVERY CYCLES
AS PHARMACODYNAMIC BIOMARKER:
EFFECTS OF MEXILETINE IN A RANDOMIZED
DOUBLE-BLIND PLACEBO-CONTROLLED
CROSS-OVER STUDY**

Clin Transl Sci. 2022; 15: 2971-2981. doi: 10.1111/cts.13418

Titia Q. Ruijs^{1,2}, Ingrid W. Koopmans^{1,2},
Marieke L. de Kam¹, Martijn R. Tannemaat²,
Geert Jan Groeneveld^{1,2}, Jules A.A.C. Heuberger¹

1. Centre for Human Drug Research, Leiden, NL
2. Leiden University Medical Centre, Leiden, NL

ABSTRACT

Measuring muscle velocity recovery cycles (MVRC) is a method to obtain information on muscle cell excitability, independent of neuromuscular transmission. The goal was to validate MVRC as pharmacodynamic biomarker for drugs targeting muscle excitability. As proof-of-concept, sensitivity of MVRC to detect effects of mexiletine, a voltage-gated sodium channel (Na_v) blocker, was assessed. In a randomized, double-blind, two-way crossover study, effects of a single pharmacologically active oral dose of 333 mg mexiletine was compared to placebo in 15 healthy male subjects. MVRC was performed pre-dose, 3- and 5-hours post-dose using QTrac. Effects of mexiletine vs. placebo were calculated using a mixed effects model with baseline as covariate. Mexiletine had significant effects on MVRC when compared to placebo. Early supernormality after five conditioning stimuli was decreased by mexiletine (estimated difference (ED) -2.78% (95% confidence interval (CI): -4.16, -1.40); $p=0.0003$). Moreover, mexiletine decreased the difference in late supernormality after five vs. one conditioning stimuli (5XLSN) (ED -1.46% (95% CI: -2.26, -0.65); $p=0.001$). These results indicate that mexiletine decreases the percentage increase in velocity of the muscle fiber action potential after five conditioning stimuli, at long and short interstimulus intervals, which corresponds to a decrease in muscle membrane excitability. This is in line with the pharmacological activity of mexiletine, which leads to use-dependent $\text{Na}_v1.4$ blockade affecting muscle membrane potentials. This study shows that effects of mexiletine can be detected using MVRC in healthy subjects, thereby indicating that MVRC can be used as tool to demonstrate pharmacodynamic effects of drugs targeting muscle excitability in early phase drug development.

INTRODUCTION

Neuromuscular diseases (NMDs) have received growing attention in preclinical and clinical research in recent decades, which has led to increased understanding of these disorders. However, significant progress is still to be made where it comes to developing treatment options for these patients. An essential part of advancing treatments through (pre) clinical drug development towards therapy is the use of biomarkers, especially for these often complex disorders.¹ Such biomarkers should be tailored to specific NMDs, as they are a collection of rare disorders with a broad spectrum of underlying pathophysiology. However, despite their heterogeneity, a common feature for many of these diseases is direct or indirect muscle pathology, resulting in symptoms of muscle weakness and other muscle pathology. A biomarker that can characterize these defects and allows quantification of pharmacological effects, would therefore be of great value in drug development for a relevant subset of NMDs.

Muscle velocity recovery cycle (MVRC) measurements could be such a pharmacodynamic biomarker, as they evaluate muscle cell excitability *in vivo* and are considered to be independent of neuromuscular transmission.² The physiological muscle action potential is followed by early and late depolarizing afterpotentials, resulting in two periods of increased excitability. By applying one or more conditioning pulses before the test pulse, MVRC can indirectly quantify these afterpotentials as periods of increased velocity (supernormality).² Previous studies showed that MVRC was able to distinguish different types of NMD from healthy controls, indicating that the method has analytical and clinical validity. Abnormalities in MVRC endpoints were detected in critical illness neuropathy, Anderson Tawil syndrome, channelopathies, erythromelalgia, myotonic dystrophies, inclusion body myositis, hypo- and hyperkalemic periodic paralysis, sodium channel myotonias and myotonia congenita.³⁻¹²

However, to our knowledge, sensitivity of MVRC to detect (acute) pharmacodynamic effects has not been evaluated. Therefore, the primary aim of this study was to investigate whether MVRC could detect pharmacologically induced changes in muscle excitability in healthy subjects. As a proof-of-concept, we selected mexiletine as pharmacological intervention. Mexiletine is a use-dependent voltage-gated sodium (Na_v) channel blocker, thought to influence muscle excitability through blocking Na_v channels subtype 1.4 in skeletal muscle fibers.¹³⁻¹⁵ As a

secondary objective, this study was set up to evaluate the feasibility and repeatability of MVRC for use in an early phase clinical drug study.

MATERIALS AND METHODS

This trial was approved by the Foundation 'Beoordeling Ethiek Biomedisch Onderzoek', an independent Ethics Committee based in Assen, The Netherlands. The trial was executed between January 2020 and March 2020, in accordance with the Declaration of Helsinki. The study was registered in the Dutch Trial Registry (Nederlands Trial Register, registration number NL8084).

STUDY DESIGN This was a randomized, double-blind, placebo-controlled, two-way cross-over study in healthy subjects. Subjects received a single dose of mexiletine 333 mg and matching placebo in randomized order on two separate study visits. Drug administrations were separated by a wash-out period of seven days. MVRC measurements were performed pre-dose and at two post-dose timepoints based on the pharmacokinetic (PK) profile of mexiletine. The first post-dose measurement was performed three hours post-dose (approximately T_{max}), the second at five hours post-dose (another measurement at expected high plasma concentrations of mexiletine), maximizing the power to detect a pharmacodynamic effect. Measurement conditions and mealtimes were standardized, and measurements were performed at approximately the same clock time, to avoid interference of diurnal variation or effects of food. A follow-up visit was performed five to nine days after the last dose administration.

No important changes were made to the methods or trial outcomes after study commencement.

STUDY POPULATION All subjects signed written informed consent before participation in the study. To confirm eligibility and health status, subjects were screened before participation, based on an interview of medical history, physical examination (including vital signs and electrocardiogram), and laboratory tests. Subjects were aged between 18 and 45 years, with a BMI between 18 and 30 kg/m² and a minimum weight of 50 kg. Subjects with active or chronic disease that could interfere with the safety or conduct of the study were excluded, particularly

history of trauma to the lower extremities or other conditions that could interfere with the MVRC measurements. The use of medication, dietary supplements, CYP-enzyme containing products, alcohol and caffeine were prohibited during the study. Subjects with history of addictive substance abuse were excluded, and drug- and alcohol tests were performed to determine current use of these substances. Excessive exercise was prohibited within 72 hours before dosing.

STUDY DRUGS, RANDOMIZATION, AND BLINDING Mexiletine (Namuscla, 167 mg, Lupin Europe GMBH) and matching placebo were administered as capsules. The matching placebo was indistinguishable from the active drug. A dose of 333 mg mexiletine was chosen as it was thought to be pharmacodynamically active, because the recommended therapeutic dose for patients with myotonia congenita is between 200 and 600 mg mexiletine hydrochloride daily (167 – 500 mg mexiletine). Moreover, a dose of 333 mg mexiletine was considered safe for healthy subjects – doses up to 600 mg mexiletine have been administered.¹⁶

The randomization schedule was generated using SAS version 9.4 (SAS Institute, Inc., Cary, NC, USA) by an unblinded statistician, who was not involved in the clinical execution of the study. A balanced treatment allocation (two sequences, each for 6 subjects) was chosen to control for first-order carry-over effects. Blinded study staff enrolled subjects and assigned participants to interventions. All participants and study staff remained blinded during the study.

MUSCLE VELOCITY RECOVERY CYCLES Practical details of the MVRC procedure were described previously.^{2,17} We performed the measurements in the distal tibialis anterior muscle. A monopolar needle electrode (Natus Dantec DCN, 25mmx26G) for stimulation was inserted approximately one centimetre proximal to the distal end of the muscle. The anode surface electrode (BlueSensor NE, Ambu, Ballerup, Denmark) was placed distal to-and in near proximity of-the monopolar needle. A concentric recording needle electrode (25mmx30G, TECA elite, Natus, Middleton, USA) was placed two cm proximal to the monopolar electrode. Needles were inserted perpendicular to the skin, to a depth of approximately one cm. A ground electrode (Red dot, 3M, St. Paul, USA) was placed on the medial malleolus. Stimulation was computer guided by QTracS software (protocol M3REC6, Institute of Neurology, London, UK). Pulses

were applied by an isolated bipolar constant-current stimulator (DS5, Digitimer, Hertfordshire, UK). The recordings were amplified (gain 1000, bandpass filter 3 Hz to 3 kHz) using an EMG amplifier (D440-2, DigiTimer, Hertfordshire, UK). An analog-digital convertor (NI-USB-6341, National Instruments, Austin, Texas) digitized the signal at a sampling frequency of 20 kHz. Hum Bug (Quest Scientific Instruments, North Vancouver, Canada) was used to minimize 50 Hz noise. Skin temperature was held between 32-36° Celsius by an infrared lamp (Daylight heat lamp, General Electronic). Skin temperature was recorded at the beginning and end of the measurement.

Two stimulation paradigms were applied: recovery cycles with one, two, and five conditioning stimuli; and frequency ramp. In the first paradigm, conditioning pulses are applied at interstimulus intervals (ISIs) of 10 ms. After the last conditioning pulse, a test pulse is applied at a decreasing ISI between 1000 and 1.8 ms in 33 steps: 1000, 900, 800, 700, 600, 500, 450, 400, 350, 300, 260, 220, 180, 140, 110, 89, 71, 56, 45, 35, 28, 22, 18, 14, 11, 8.9, 7.1, 5.6, 4.5, 3.5, 2.8, 2.2, and 1.8 ms. In the frequency ramp paradigm, a train of conditioning pulses is applied with a frequency ranging between 1 and 30 Hz.¹¹

Moreover, 15-point repeated recovery cycles measurements before, during and after 5 minutes of ischemia induced by a blood pressure cuff around the upper leg. Execution of this complex measurement proved challenging which led to limited data quality; therefore, it is not reported.

DATA HANDLING MVRC variables were generated using QTracP (Institute of Neurology, London, UK), details described previously.²

From the recovery cycles recordings, latency from test stimulus to peak muscle action potential is measured. The effect of conditioning stimuli on the latency after the test pulse are estimated as the percentage change compared to an unconditioned test pulse.^{8,11} As published previously,¹¹ the following endpoints were generated for recovery cycles with one, two and five conditioning stimuli. Muscle relative refractory period (MRRP): interpolated ISI at which the latency of the unconditioned response, and latency of the response after one conditioning stimulus, are the same. Early supernormality (ESN): peak percentual latency change induced by one conditioning stimulus at ISIs <15 ms. Early supernormality is also calculated for five conditioning pulses: 5ESN. Time to peak ESN (ESN@) is the ISI corresponding to ESN. SN20 is the supernormality at ISI 20 ms. Late

supernormality (LSN) is defined as the mean percentage latency change due to one conditioning stimulus, at ISIs between 50 and 150 ms. XLSN: the difference in LSN between two and one conditioning stimuli, and 5XLSN: the difference in LSN between five and one conditioning stimuli. Residual supernormality (RSN) is the percentage latency change between ISIs 900 and 1000 ms, and 5XRSN is the difference in RSN between five and one conditioning stimuli.

For frequency ramp, latency change is calculated as the percentage of unconditioned action potentials recorded before the ramp.¹¹ Latency changes after stimulus trains with pulse frequencies of 15 Hz (Lat[15Hz]) and 30 Hz (Lat[30Hz]) were calculated, as well as percentage change in amplitudes of the action potentials after 15 Hz (Peak[15Hz]) and 30 Hz (Peak[30Hz]) trains. The minimal latency (expressed as percentage of the unconditioned pre-ramp potential) measured during the ramp is LatMin, the corresponding frequency when latency is minimal is FreqLatMin. Latency and amplitude changes are calculated for the first and last potential in each train, and these are indicated as 'First' and 'last'. Percentage change in amplitude between 30 and 15 Hz (Peak[30-15Hz]) is calculated, as well as percentage latency and peak change 30 seconds after the ramp (Lat[30Hz30s] and Peak[30Hz30s], respectively).

Before generation of the endpoints, raw data was visually inspected by blinded study staff, and interpolation of single datapoints was performed in case of single outliers with an abnormal muscle response. Additionally, a blinded data review was performed to remove measurements with technical abnormalities from analysis.

STATISTICAL ANALYSIS Statistical analysis was performed in SAS version 9.4 (SAS Institute, Inc., Cary, NC, USA). Visual evaluation of normal distribution was performed during analysis, and no variables needed log-transformation to correct for log-normal distribution. Repeatedly measured MVRC data are analysed with a mixed effects model with fixed factors: treatment, period, time and treatment by time, random factors: subject, subject by treatment and subject by time, and the average pre-value as covariate. The contrast calculated within the model is placebo versus mexiletine. To indicate inter- and intrasubject variability of MVRC, coefficients of variation (CV%) were calculated from placebo measurements (within-day variability) and derived from the raw data as well as model covariate variables. Statistical significance was defined at the 5% level.

We used previously published variability data of MVRC in healthy subjects¹⁸ to estimate the required sample size. Because no pharmacodynamic effects on MVRC had been reported previously in healthy subjects, expected effect sizes for this study were based on those observed with ischemia.² A sample size of twelve subjects in a cross-over design would be able to detect a difference in MRRP of 0.37 ms, and difference in ESN of 1.16%, with a power of 0.8.

RESULTS

A total of 15 subjects were enrolled, of which 14 subjects completed the study. This includes three replacement subjects enrolled due to insufficient quality of MVRC measurements in three of the first 12 subjects. Demographics are summarized in Supplementary Table 1.

A total of 85 measurements were performed in 15 subjects. One subject only underwent two measurements and was subsequently excluded. One measurement in another subject was not obtained for technical reasons. Additionally, the following measurements were excluded from analysis in a blinded data review (see chapter Data handling): for eleven measurements the recovery cycles were (partially or fully) excluded, for eight measurements frequency ramp was (partially or fully) excluded. Individual and mean plasma concentrations of mexiletine are shown in Supplementary Figure 1, mean concentrations per protocol time are in Supplementary Figure 2. Adverse events reported in the study were mild to moderate in intensity, and transient.

TEST-RETEST RELIABILITY Test-retest reliability, estimated in CV%, of all MVRC variables is shown in Supplementary Table 3. Raw baseline MVRC endpoints and estimated means of measurements 3- and 5-hours post-dose, are shown in Supplementary Table 4.

EFFECTS OF MEXILETINE ON RECOVERY CYCLES Effects of mexiletine on recovery cycles are listed in Table 1. Mexiletine significantly decreased early supernormality after five conditioning stimuli (5ESN) compared to placebo (Figure 1). Moreover, difference in late supernormality after five versus one conditioning stimuli (5XLSN) was significantly decreased (Figure 2).

To visualize these treatment effects, average post-dose recovery cycles recordings with five conditioning stimuli are shown in Figure 3, for mexiletine and placebo. Average post-dose recovery cycles recordings with one conditioning stimulus and two conditioning stimuli are shown in Supplementary Figure 2 and Supplementary Figure 3, respectively.

FIGURE 1 Effects of mexiletine versus placebo on early supernormality after five conditioning stimuli (5ESN), shown as the estimated mean change from baseline (CFB) at three- and five-hours post-dose. Error bars indicate the 95% confidence interval of the estimated mean.

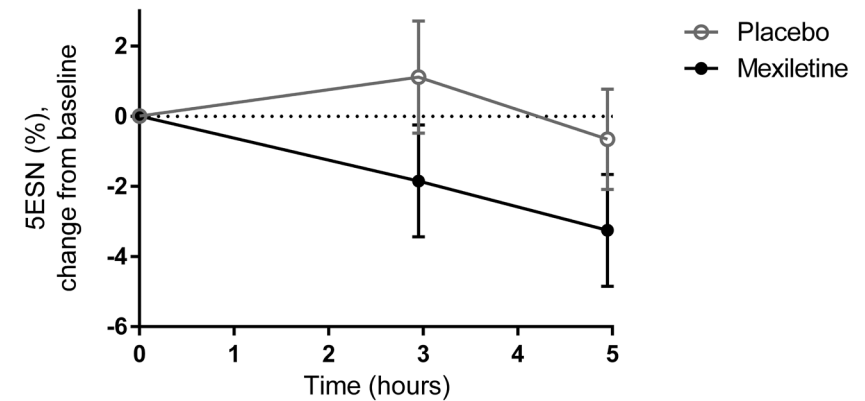


FIGURE 2 Effects of mexiletine versus placebo on the difference in late supernormality of five versus one conditioning stimuli (5XLSN), shown as the estimated mean change from baseline (CFB) at three- and five-hours post-dose. Error bars indicate the 95% confidence interval of the estimated mean.

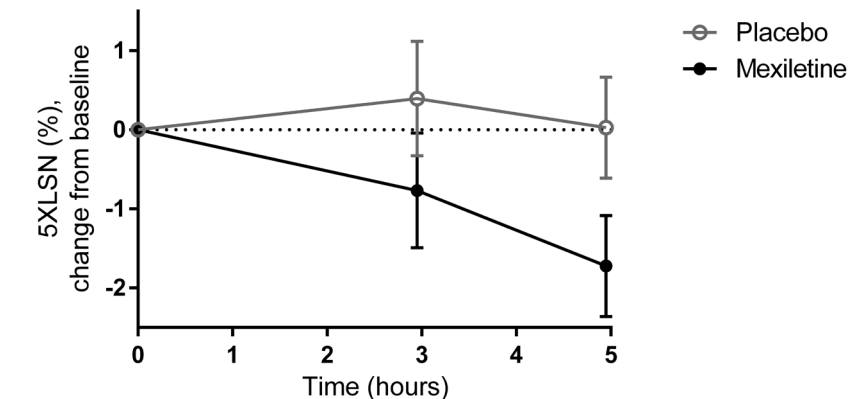


TABLE 1 Effects of mexiletine versus placebo on MVRC endpoints, shown as the estimated mean of the treatment period (post-dose) and the estimated difference of mexiletine versus placebo, reported with 95% confidence interval and p-value.

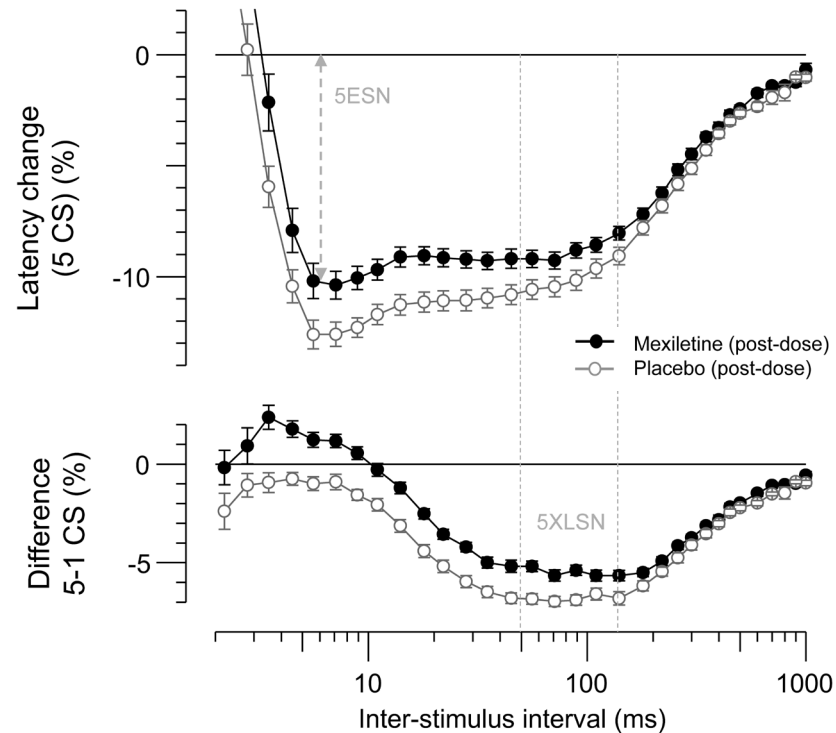
	Treatment	Estimated mean treatment period	Estimated difference	95% confidence interval	P value	
RECOVERY CYCLES WITH 1, 2 AND 5 CONDITIONING STIMULI	MRRP (ms)	Placebo	3.03			
		Mexiletine	3.09	0.058	(-0.250, 0.365)	0.702
	ESN (%)	Placebo	12.40			
		Mexiletine	11.55	-0.854	(-2.760, 1.051)	0.328
	ESN@ (ms)	Placebo	6.27			
		Mexiletine	6.62	0.34	(-0.48, 1.17)	0.401
	5ESN (%)	Placebo	13.41			
		Mexiletine	10.64	-2.78	(-4.157, -1.396)	<0.001*
	SN20 (%)	Placebo	6.42			
		Mexiletine	5.92	-0.497	(-1.33, 0.340)	0.230
	LSN (%)	Placebo	3.19			
		Mexiletine	3.26	0.075	(-0.527, 0.676)	0.797
	2XLSN (%)	Placebo	2.47			
		Mexiletine	2.08	-0.39	(-0.811, 0.032)	0.068
	5XLSN (%)	Placebo	6.95			
		Mexiletine	5.49	-1.46	(-2.258, -0.653)	0.001*
	RSN (%)	Placebo	0.166			
		Mexiletine	0.165	-0.001	(-0.331, 0.330)	0.997
	5XRSN (%)	Placebo	0.888			
		Mexiletine	0.717	-0.171	(-0.573, 0.231)	0.388

(Continuation Table 1)

	Treatment	Estimated mean treatment period	Estimated difference	95% confidence interval	P value	
FREQUENCY RAMP	Lat[15Hz] _{first} (%)	Placebo	96.3			
		Mexiletine	96.5	0.20	(-0.69, 1.10)	0.650
	Lat[15Hz] _{last} (%)	Placebo	86.6			
		Mexiletine	89.3	2.77	(0.99, 4.55)	0.004*
	Lat[30Hz] _{first} (%)	Placebo	97.2			
		Mexiletine	98.2	0.98	(-0.75, 2.71)	0.252
	Lat[30Hz] _{last} (%)	Placebo	87.4			
		Mexiletine	95.0	7.58	(3.80, 11.4)	<0.001*
	Lat[30Hz+30s] (%)	Placebo	101.6			
		Mexiletine	100.7	-0.90	(-2.30, 0.49)	0.190
	Peak[15Hz] _{first} (%)	Placebo	110.5			
		Mexiletine	109.5	-1.02	(-9.24, 7.19)	0.801
	Peak[15Hz] _{last} (%)	Placebo	107.5			
		Mexiletine	110.4	2.84	(-12.45, 18.14)	0.692
	Peak[30Hz] _{first} (%)	Placebo	112.8			
		Mexiletine	112.6	-0.13	(-13.48, 13.21)	0.983
	Peak[30Hz] _{last} (%)	Placebo	88.3			
		Mexiletine	89.5	1.20	(-19.45, 21.84)	0.903
	Peak[30-15Hz] (%)	Placebo	1.80			
		Mexiletine	4.49	2.69	(-3.49, 8.86)	0.376
Peak[30Hz+30s] (%)	Placebo	98.1				
	Mexiletine	97.8	-0.23	(-7.28, 6.82)	0.948	
LatMin _{first} (%)	Placebo	95.4				
	Mexiletine	95.9	0.45	(-0.80, 1.70)	0.435	
LatMin _{last} (%)	Placebo	85.01				
	Mexiletine	88.76	3.75	(1.55, 5.95)	0.002*	
FreqLatMin _{first} (Hz)	Placebo	20.12				
	Mexiletine	18.54	-1.57	(-5.48, 2.33)	0.412	
FreqLatMin _{last} (Hz)	Placebo	21.61				
	Mexiletine	17.79	-3.82	(-6.09, -1.54)	0.002*	

Significant results are highlighted with *. ESN, early supernormality; ESN@, time to peak early supernormality; LSN, late supernormality; MRRP, Muscle relative refractory period; MVRC, muscle velocity recovery cycle; RSN, Residual supernormality; SN20, supernormality at interstimulus interval 20 ms.

FIGURE 3 Mean post-dose recordings of recovery cycles with five conditioning stimuli, for mexiletine (black, filled) and placebo (grey, empty). Error bars show the standard error. The upper graph shows the percentual latency change after five conditioning stimuli at different interstimulus intervals. The lower graph shows the additional change in latency of five versus one conditioning stimuli. Variables with significant effects (mexiletine versus placebo) are visualized by indicating the name of the variable. Variable visualization is reproduced from¹¹. Note this graph is meant to visualize treatment effects, but does not fully reflect the statistical analysis, because the statistical model includes baseline as a covariate which is not reflected in the graph.



EFFECTS OF MEXILETINE ON FREQUENCY RAMP Effects of mexiletine versus placebo on frequency ramp are listed in Table 1. Mexiletine significantly increased the percentual latency after the last pulse of a 15 Hz train ($Lat[15Hz]_{last}$) and a 30 Hz train ($Lat[30Hz]_{last}$), as shown in Figure 4 and 5, respectively. Moreover, mexiletine increased the minimal latency during the ramp ($LatMin_{last}$) and decreased the frequency at which the latency was minimal ($FreqLatMin_{last}$) (Supplementary Figure 4 and Supplementary Figure 5, respectively).

Average post-dose frequency ramp recordings (Figure 6) visualize these effects, showing that the latency decrease due to the 15 Hz and 30 Hz trains is reduced by mexiletine.

FIGURE 4 Effects of mexiletine versus placebo on the latency change after a 15 Hz train of stimuli ($Lat[15Hz]_{last}$), shown as the estimated mean change from baseline (CFB) at three and five hours post-dose. Error bars indicate the 95% confidence interval of the estimated mean.

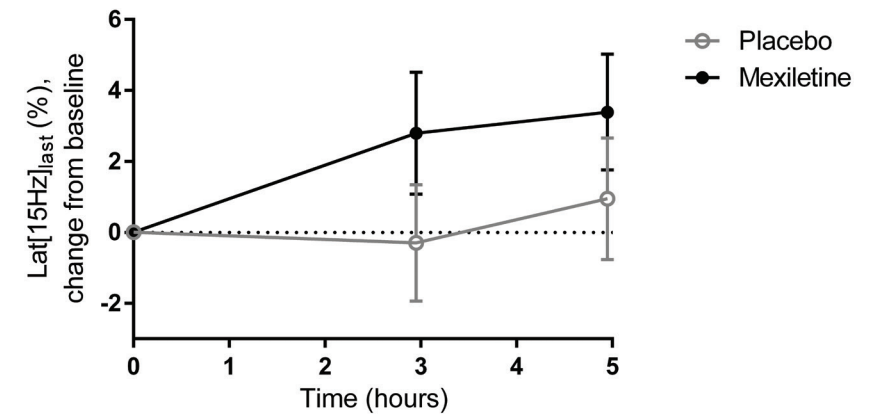


FIGURE 5 Effects of mexiletine versus placebo on the latency change at the end of a 30 Hz train of stimuli ($Lat[30Hz]_{last}$), shown as the estimated mean change from baseline (CFB) at three and five hours post-dose. Error bars indicate the 95% confidence interval of the estimated mean.

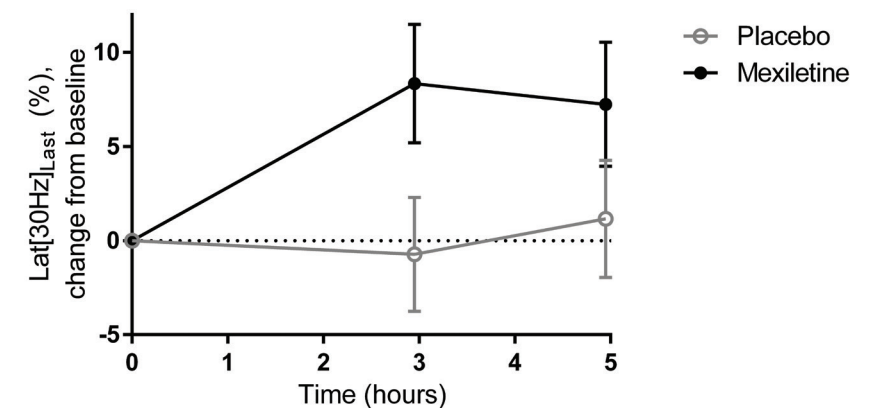
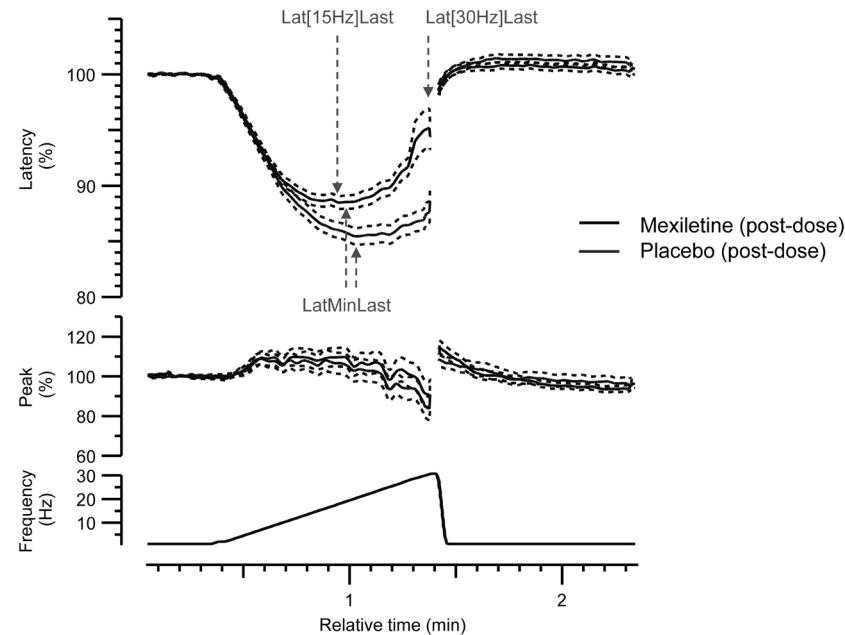


FIGURE 6 Mean post-dose recordings of frequency ramp, for mexiletine (black) and placebo (grey). Dotted lines show the standard error. The upper graph shows the percentual latency (compared to unconditioned latency) by a train of pulses (stimulation rate shown in the lowest graph). The middle graph shows the percentual amplitude change (compared to unconditioned amplitude values). Both graphs show the last-in-train values. Variable with significant effects (mexiletine versus placebo) is visualized by indicating the name of the variable. Variable visualization is reproduced from¹¹. Note this graph is meant to visualize treatment effects, but does not fully reflect the statistical analysis, the statistical model includes baseline as a covariate which is not reflected in the graph.



DISCUSSION

The aim of this study was to investigate the use of MVRC as a tool to demonstrate pharmacodynamic effects on muscle excitability. As a proof-of-concept we compared effects of mexiletine to placebo in healthy subjects and were able to demonstrate significant effects of mexiletine on several MVRC variables. The recovery cycles variables 5ESN and 5XLSN were decreased by mexiletine, indicating that mexiletine decreases supernormality of the muscle action potential after five conditioning stimuli, at long and short ISIs. Moreover, we detected a significant increase of $\text{Lat}[15\text{Hz}]_{\text{last}}$, $\text{Lat}[30\text{Hz}]_{\text{last}}$, $\text{LatMin}_{\text{last}}$ and $\text{FreqLatMin}_{\text{last}}$ by

mexiletine using the frequency ramp paradigm. In this paradigm, a train of conditioning stimuli physiologically results in an increase in latency at the end of the train – we show that mexiletine suppresses this latency increase after a 15 Hz and 30 Hz stimulus train.

These results indicate that MVRC endpoints are sensitive to detect effects of pharmacological interventions on muscle excitability. The effects on 5ESN and 5XLSN, and $\text{Lat}[15\text{Hz}]_{\text{last}}$, $\text{Lat}[30\text{Hz}]_{\text{last}}$, $\text{LatMin}_{\text{last}}$ and $\text{FreqLatMin}_{\text{last}}$, can be explained by the mechanism of action of mexiletine. Mexiletine reduces muscle cell excitability through a use-dependent block of $\text{Na}_V1.4$, with higher affinity for Na_V channels in the open and inactivated state.^{13–15} This pharmacological property may explain why mexiletine significantly reduces early and late supernormality after five conditioning pulses, as an increased number of $\text{Na}_V1.4$ channels will be in the open or inactivated state after previous activations shortly before the test pulse. Additionally, our finding that ESN is only affected by mexiletine after five conditioning stimuli, and not after one or two conditioning stimuli, may be explained by the use-dependence of the Na_V blockade, as fewer conditioning stimuli would result in a relatively lower availability of inactivated Na_V channels that can be bound by mexiletine. When observing effects of mexiletine on post-dose recovery cycles recordings of one (Supplementary Figure 2) and two conditioning stimuli (Supplementary Figure 3), there is no effect on recovery cycles with one conditioning stimulus, and a small (non-significant) effect on supernormality after two conditioning stimuli, in the same direction as the effect seen with five conditioning stimuli (Figure 3). This appears to indicate that the effect of mexiletine indeed increases with an increasing number of conditioning stimuli. The effects on frequency ramp – significant decrease in supernormality due to stimulus trains at high frequencies ($\text{Lat}[15\text{Hz}]_{\text{last}}$ and $\text{Lat}[30\text{Hz}]_{\text{last}}$) – also corresponds to effects expected from a use-dependent Na_V block: effects of mexiletine are larger after repetitive stimulation. Additionally, the difference between mexiletine and placebo is much larger after 30 Hz trains than 15 Hz trains, suggesting an increasing effect at higher stimulation frequencies.

To our knowledge, this is the first study to evaluate effects of Na_V blockers on muscle excitability using MVRC in placebo-controlled manner. An interesting report in this context however, evaluated effects of a gain-of-function mutation in $\text{Na}_V1.4$ channels on MVRC in patients with sodium channel myotonia.⁹ This mutation results in slowed Na_V inactivation,⁹ which should theoretically exhibit somewhat opposite

effects to mexiletine as $\text{Na}_V1.4$ blocker. Indeed, 5ESN and 5XLSN (amongst others) were significantly increased, and $\text{Lat}[15\text{Hz}]_{\text{last}}$ and $\text{Lat}[30\text{Hz}]_{\text{last}}$ significantly decreased in sodium channel myotonia, strengthening our results and confirming the mechanism involved in influencing MVRC.

Another relevant paper in this context describes muscle excitability in myotonia congenita patients. Patients with myotonia congenita carry a mutation in ClC-1 , resulting in an increase in muscle excitability. The authors compared MVRC of myotonia congenita patients off-treatment, to patients using Na_V blockers (mainly mexiletine).¹¹ Tan *et al.* showed that the presence of myotonia congenita (in patients who are not on treatment) results in an increase in ESN , 5ESN , LSN and 5XLSN compared to healthy subjects. The authors showed that patients on-treatment with Na_V blockers have a significant decrease in all these variables (a change in the direction of normal controls). This suggests a (partial) reversing of the effects of myotonia congenita by Na_V blockers. Although the results cannot directly be compared to our study because Tan *et al.* did not measure the effects within a patient on- and off-drug, but between patients using or not using Na_V blockers chronically, their findings do corroborate the decrease of 5ESN and 5XLSN due to mexiletine that we found. Moreover, although no significant difference in $\text{Lat}[15\text{Hz}]_{\text{last}}$ was found between myotonia congenita and healthy subjects, patients using Na_V blockers did have a significant increase in $\text{Lat}[15\text{Hz}]_{\text{last}}$, in line with our results. $\text{FreqLatMin}_{\text{last}}$ is significantly decreased in patients using Na_V blockers when compared to patients without these drugs, in line with our findings for mexiletine.

MVRC AS A BIOMARKER IN DRUG DEVELOPMENT Our study shows that MVRC endpoints are suitable to detect drug effects on muscle excitability, even in a small number of healthy subjects, with a limited number of post-dose measurements. The sample size used here is a typical sample size used in phase I studies. Additionally, the MVRC measurement was safe and well-tolerated in this study. The duration of one measurement allows for pre-dose and multiple post-dose measurements: the stimulation protocol used in this study takes approximately 7 minutes. In addition, the intra-subject variability derived from the model is acceptable, reflected by CV%s below 20% for 17 of 25 variables, which supports the use of MVRC as a biomarker in a cross-over study design. As these test-retest reliability results are based on the data in

the placebo treatment, this indicates that the endpoints were rather stable under placebo, i.e. there was no apparent placebo response. These properties are a prerequisite for a valuable biomarker in early phase clinical trials. Whether effects of compounds developed for various NMDs can be detected using MVRC will have to be confirmed in future studies. However, we propose the use of MVRC as a biomarker for target engagement of drugs developed to influence muscle excitability, such as novel (subtype-specific) Na_V blockers,^{19,20} or existing sodium- or potassium channel modulating therapies proposed as new treatments for myotonia.²¹⁻²³ This biomarker may therefore be used for proof of target engagement but may also facilitate an informed choice of the dose level in the translation from Phase I studies in healthy subjects to Phase 2 and 3 studies in patient populations. Furthermore, MVRC may also be used in the translational phase between preclinical and clinical studies because the measurement can also be performed in animal studies.^{24,25}

For further development of MVRC as pharmacodynamic biomarker, it would be of interest to explore concentration effect relationships on MVRC. The current study is not set up to reliably evaluate this, because the spread in plasma concentrations is insufficient: we only performed two post-dose PD measurements, both at high plasma concentrations.

LIMITATIONS Due to potential effects of oedema or bleeding around the needle electrodes on consecutive measurements, the insertion location of the needle varied slightly (approximately 0.5 cm) between measurements on the same day. This may influence the conduction distance slightly between measurements performed on the same day. However, intra-subject variability was low, suggesting that this was not a major problem. Moreover, a previous variability study did not report a significant effect of conduction distance on the MVRC endpoints calculated as percentage latency change.¹⁸

A potential limitation of MVRC is that it can be challenging to find suitable muscle responses to perform the MVRC measurement. This can lead to technically aberrant measurements that have to be removed from analysis, although this occurred rarely in our dataset (see section Data handling).

The analyses presented here were not corrected for multiple testing, due to the exploratory nature of the study.

CONCLUSION The aim of this study was to evaluate MVRC as a biomarker for pharmacodynamic effects on muscle excitability. We demonstrated significant effects of the use-dependent Na_v channel blocker mexiletine on MVRC in healthy subjects. The results indicate a reduction of muscle excitability by mexiletine, in line with its suggested mechanism of action. Whether MVRC can detect pharmacodynamic effects of other (novel) treatments for NMDs remains to be determined in future work. However, this study encourages the use of MVRC as a tool to demonstrate pharmacodynamic effects of drugs targeting muscle excitability in early phase clinical drug development.

SUPPLEMENTARY MATERIAL

SUPPLEMENTARY TABLE 1 Demographics of the study population.

	N	15
Age (years)	Mean (SD)	24 (5)
	Median	22
	Range	19-41
Height (cm)	Mean (SD)	179 (8)
	Median	179
Weight (kg)	Mean (SD)	74 (12)
	Median	75
BMI (kg/m ²)	Mean (SD)	23 (2)
	Median	22

BMI = body mass index; SD = standard deviation.

SUPPLEMENTARY TABLE 2 Mean, standard deviation (SD), and median plasma concentrations of mexiletine at each protocol time.

Time after dosing	Mean concentration (mg/L)	SD	Median concentration (mg/L)
2h 39m	1.34	0.27	1.27
4h 39m	1.16	0.27	1.16

SUPPLEMENTARY TABLE 3 Coefficients of variation (cv%) of MVRC endpoints. Intrasubject cv% is calculated within-day (placebo occasion), from the raw data as well as the estimated values from the model (corrected for baseline). Intersubject cv% is calculated from estimated values from the model.

		Raw Intrasubject cv%, within-day	Model Intrasubject cv%, within-day	Model Intersubject cv%	
RECOVERY CYCLES WITH 1, 2 AND 5 CONDITIONING STIMULI	MRRP	13.80%	13.80%	13.80%	
	ESN	18.90%	16.80%	20.40%	
	ESN@	15.30%	15.60%	15.60%	
	5ESN	18.80%	18.80%	21.90%	
	SN20	18.0%	16.0%	16.0%	
	LSN	28.60%	25.60%	25.60%	
	2XLSN	25.10%	22.90%	22.90%	
	5XLSN	16.40%	15.50%	15.50%	
	RSN	429.10%	277.30%	287.90%	
	5XRSN	57.10%	79.40%	79.40%	
	FREQUENCY RAMP	Lat[15Hz] _{first}	1.20%	1.50%	1.50%
		Lat[15Hz] _{last}	2.70%	3.00%	3.00%
Peak[15Hz] _{last}		23.20%	20.60%	21.10%	
Peak[15Hz] _{first}		12.40%	12.10%	12.30%	
Lat[30Hz] _{first}		1.70%	1.70%	1.70%	
Lat[30Hz] _{last}		6.0%	4.4%	4.4%	
Peak[30Hz] _{first}		12.90%	15.10%	15.10%	
Peak[30Hz] _{last}		31.90%	27.30%	27.30%	
Peak[30-15Hz]		507.20%	385.90%	385.90%	
Lat[30Hz+30s]		1.50%	1.00%	1.00%	
Peak[30Hz+30s]		13.50%	11.80%	11.80%	
LatMin _{first}		1.8%	1.6%	1.7%	
LatMin _{last}		3.4%	3.6%	3.6%	
FreqLatMin _{first}		25.3%	28.6%	28.6%	
FreqLatMin _{last}		14.7%	17.8%	18.7%	

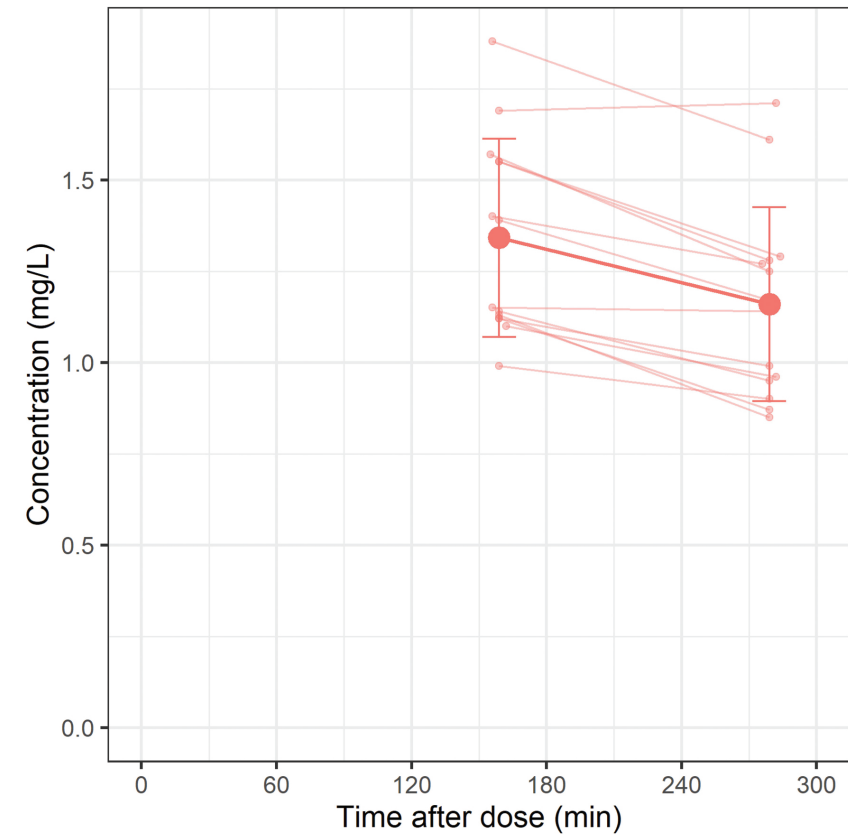
SUPPLEMENTARY TABLE 4 Raw mean baseline (pre-dose) values of MVRC endpoints, and estimated means of post-dose measurements at three- and five-hours post-dose, are listed.

		Treatment	Raw mean baseline	Estimated mean 3h post-dose	Estimated mean 5h post-dose
RECOVERY CYCLES WITH 1, 2, AND 5 CS	MRRP (ms)	Placebo	3.03	2.84	3.23
		Mexiletine	3.42	2.99	3.19
	ESN (%)	Placebo	13.1	13.1	11.7
		Mexiletine	12.9	12.1	11.0
	ESN@ (ms)	Placebo	6.57	5.98	6.57
		Mexiletine	7.57	6.52	6.72
	5ESN (%)	Placebo	13.3	14.3	12.5
		Mexiletine	12.8	11.3	9.9
	SN20 (%)	Placebo	6.60	6.77	6.07
		Mexiletine	6.52	6.39	5.46
	LSN (%)	Placebo	3.49	3.55	2.83
		Mexiletine	3.32	3.55	2.98
2XLSN (%)	Placebo	2.28	2.49	2.44	
	Mexiletine	2.37	2.29	1.86	
5XLSN (%)	Placebo	6.58	7.13	6.77	
	Mexiletine	6.93	5.97	5.02	
RSN (%)	Placebo	0.01	0.12	0.22	
	Mexiletine	0.31	0.19	0.14	
5XRSN (%)	Placebo	1.11	0.98	0.80	
	Mexiletine	1.26	0.87	0.56	

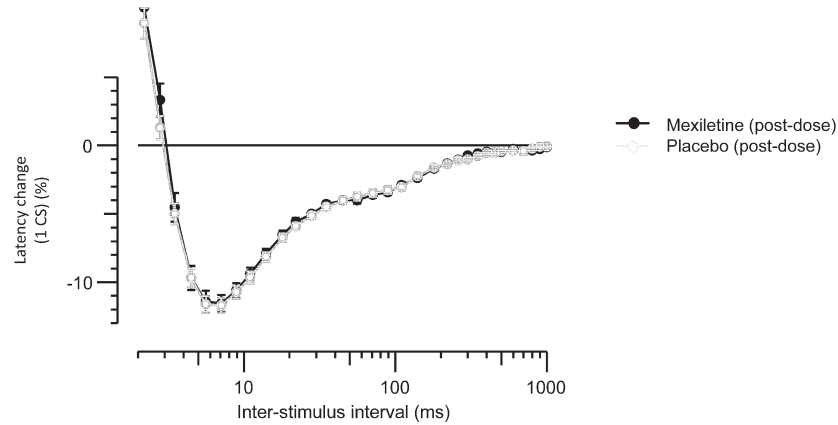
(Continuation Supplementary Table 4)

	Treatment	Raw mean baseline	Estimated mean 3h post-dose	Estimated mean 5h post-dose	
FREQUENCY RAMP	Lat[15Hz] _{first} (%)	Placebo	95.6	96.2	96.4
		Mexiletine	95.9	96.3	96.7
	Lat[15Hz] _{last} (%)	Placebo	86.2	85.9	87.2
		Mexiletine	86.2	89.0	89.6
	Lat[30Hz] _{first} (%)	Placebo	95.8	96.8	97.5
		Mexiletine	97.0	98.2	98.2
	Lat[30Hz] _{last} (%)	Placebo	88.3	86.5	88.4
		Mexiletine	87.4	95.6	94.5
	Lat[30Hz+30s] (%)	Placebo	102	101	101
		Mexiletine	102	102	100
	Peak[15Hz] _{first} (%)	Placebo	113	113	111
		Mexiletine	114	108	108
	Peak[15Hz] _{last} (%)	Placebo	119	113	102
		Mexiletine	114	119	102
	Peak[30Hz] _{first} (%)	Placebo	116	116	115
		Mexiletine	121	109	111
	Peak[30Hz] _{last} (%)	Placebo	95.6	92.6	84.1
		Mexiletine	102.6	93.0	86.0
	Peak[30-15Hz] (%)	Placebo	2.73	2.13	1.48
		Mexiletine	5.76	4.98	4.00
Peak[30Hz+30s] (%)	Placebo	98.3	101	97.6	
	Mexiletine	100	95.0	98.1	
LatMin _{first} (%)	Placebo	94.4	95.4	95.5	
	Mexiletine	94.8	95.6	96.2	
LatMin _{last} (%)	Placebo	84.9	84.3	85.7	
	Mexiletine	84.7	88.7	88.9	
FreqLatMin _{first} (Hz)	Placebo	20.6	18.6	21.7	
	Mexiletine	21.9	18.4	18.7	
FreqLatMin _{last} (Hz)	Placebo	20.8	21.2	22.1	
	Mexiletine	20.7	17.7	17.9	

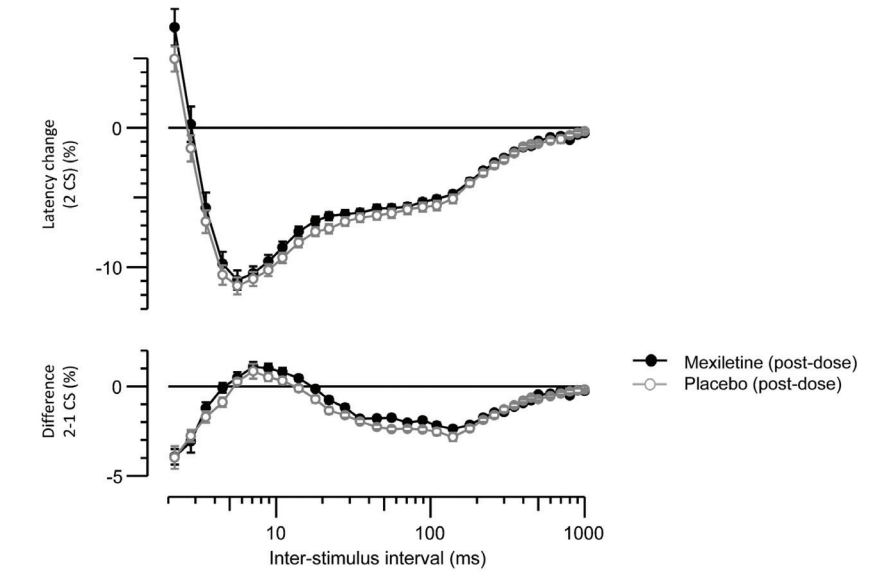
SUPPLEMENTARY FIGURE 1 Individual and mean \pm SD plasma concentration of mexiletine, before the start of the post-dose MVRC measurements (2 hours and 39 minutes post-dose, and 4 hours and 39 minutes post-dose).



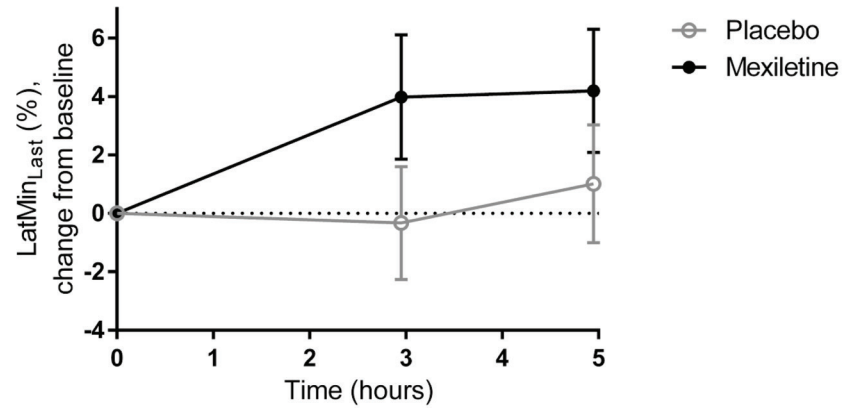
SUPPLEMENTARY FIGURE 2 Mean post-dose recordings of recovery cycles with one conditioning stimulus, for mexiletine (black, filled) and placebo (grey, empty). Error bars show the standard error. The graph shows the percentual latency change after one conditioning stimuli at different interstimulus intervals. Note this graph is meant to visualize treatment effects, but does not fully reflect the statistical analysis, because the statistical model includes baseline as a covariate which is not reflected in the graph.



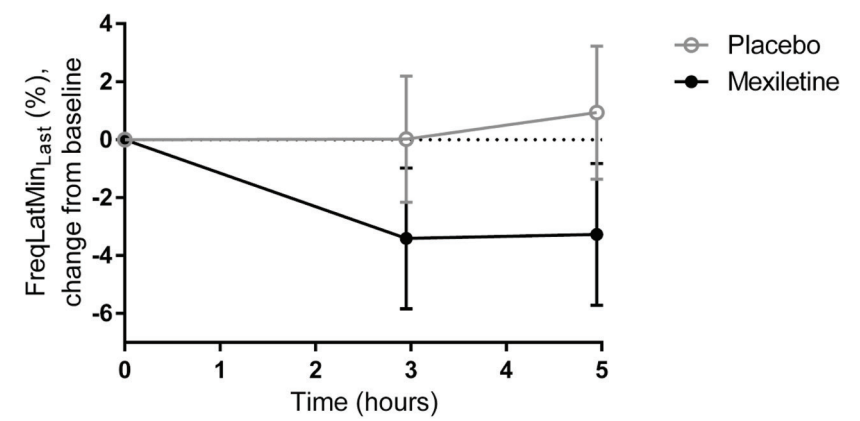
SUPPLEMENTARY FIGURE 3 Mean post-dose recordings of recovery cycles with two conditioning stimuli, for mexiletine (black, filled) and placebo (grey, empty). Error bars show the standard error. The upper graph shows the percentual latency change after two conditioning stimuli at different interstimulus intervals. The lower graph shows the additional change in latency of two versus one conditioning stimuli. Note this graph is meant to visualize treatment effects, but does not fully reflect the statistical analysis, because the statistical model includes baseline as a covariate which is not reflected in the graph.



SUPPLEMENTARY FIGURE 4 Effects of mexiletine versus placebo on the minimal latency (last in train) recorded during the ramp ($\text{LatMin}_{\text{Last}}$), shown as the estimated mean change from baseline (CFB) at three- and five-hours post-dose. Error bars indicate the 95% confidence interval of the estimated mean.



SUPPLEMENTARY FIGURE 5 Effects of mexiletine versus placebo on the frequency at which the minimal latency (last in train) was recorded during the ramp ($\text{FreqLatMin}_{\text{Last}}$), shown as the estimated mean change from baseline (CFB) at three- and five-hours post-dose. Error bars indicate the 95% confidence interval of the estimated mean.



REFERENCES

- 1 Scotton C, Passarelli C, Neri M, Ferlini A. Biomarkers in rare neuromuscular diseases. *Exp Cell Res*. 2014;325(1). doi:10.1016/j.yexcr.2013.12.020
- 2 Z'Graggen WJ, Bostock H. Velocity recovery cycles of human muscle action potentials and their sensitivity to ischemia. *Muscle Nerve*. 2009;39(5). doi:10.1002/mus.21192
- 3 Boland-Freitas R, Lee J, Howells J, et al. Sarcolemmal excitability in the myotonic dystrophies. *Muscle Nerve*. 2018;57(4). doi:10.1002/mus.25962
- 4 Lee JH, Boland-Freitas R, Liang C, Ng K. Sarcolemmal depolarization in sporadic inclusion body myositis assessed with muscle velocity recovery cycles. *Clinical Neurophysiology*. 2019;130(12):2272-2281. doi:10.1016/j.clinph.2019.08.019
- 5 Veronica Tan S, Suetterlin K, Männikkö R, Matthews E, Hanna MG, Bostock H. In vivo assessment of interictal sarcolemmal membrane properties in hypokalaemic and hyperkalaemic periodic paralysis. *Clinical Neurophysiology*. 2020;131(4). doi:10.1016/j.clinph.2019.12.414
- 6 Tan SV, Z'Graggen WJ, Boërio D, et al. Membrane dysfunction in Andersen-Tawil syndrome assessed by velocity recovery cycles. *Muscle Nerve*. 2012;46(2). doi:10.1002/mus.23293
- 7 Tan SV, Z'Graggen WJ, Boërio D, Turner C, Hanna MG, Bostock H. In vivo assessment of muscle membrane properties in myotonic dystrophy. *Muscle Nerve*. 2016;54(2). doi:10.1002/mus.25025
- 8 Z'Graggen WJ, Brander L, Tuchscherer D, Scheidegger O, Takala J, Bostock H. Muscle membrane dysfunction in critical illness myopathy assessed by velocity recovery cycles. *Clinical Neurophysiology*. 2011;122(4). doi:10.1016/j.clinph.2010.09.024
- 9 Tan SV, Z'Graggen WJ, Hanna MG, Bostock H. In vivo assessment of muscle membrane properties in the sodium channel myotonias. *Muscle Nerve*. 2018;57(4). doi:10.1002/mus.25956
- 10 Tankisi A, Pedersen TH, Bostock H, et al. Early detection of evolving critical illness myopathy with muscle velocity recovery cycles. *Clinical Neurophysiology*. 2021;132(6). doi:10.1016/j.clinph.2021.01.017
- 11 Tan SV, Z'Graggen WJ, Boërio D, et al. Chloride channels in myotonia congenita assessed by velocity recovery cycles. *Muscle Nerve*. 2014;49(6):845-857. doi:10.1002/mus.24069
- 12 Z'Graggen WJ, Aregger F, Farese S, et al. Velocity recovery cycles of human muscle action potentials in chronic renal failure. *Clinical Neurophysiology*. 2010;121(6). doi:10.1016/j.clinph.2010.01.024
- 13 Wang GK, Russell C, Wang SY. Mexiletine block of wild-type and inactivation-deficient human skeletal muscle hNav1.4 Na⁺ channels. *J Physiol*. 2004;554(3):621-633. doi:https://doi.org/10.1113/jphysiol.2003.054973
- 14 Logigian EL, Martens WB, Moxley RT 4th, et al. Mexiletine is an effective antimyotonia treatment in myotonic dystrophy type 1. *Neurology*. 2010;74(18):1441-1448. doi:10.1212/WNL.0b013e3181dca13a
- 15 Lehmann-Horn F, Jurkat-Rott K. Voltage-gated ion channels and hereditary disease. *Physiol Rev*. 1999;79(4):1317-1372. doi:10.1152/physrev.1999.79.4.1317
- 16 Pringle T, Fox J, McNeill JA, et al. Dose independent pharmacokinetics of mexiletine in healthy volunteers. *Br J Clin Pharmacol*. 1986;21(3):319-321. doi:10.1111/j.1365-2125.1986.tb05196.x
- 17 Witt A, Bostock H, Z'Graggen WJ, et al. Muscle velocity recovery cycles to examine muscle membrane properties. *Journal of Visualized Experiments*. 2020;2020(156). doi:10.3791/60788
- 18 Z'Graggen WJ, Troller R, Ackermann KA, Humm AM, Bostock H. Velocity recovery cycles of human muscle action potentials: Repeatability and variability. *Clinical Neurophysiology*. 2011;122(11). doi:10.1016/j.clinph.2011.04.010
- 19 De Bellis M, De Luca A, Desaphy JF, et al. Combined Modifications of Mexiletine Pharmacophores for New Lead Blockers of Nav1.4 Channels. *Biophys J*. 2013;104(2):344-354. doi:https://doi.org/10.1016/j.bpj.2012.11.3830
- 20 de Bellis M, Carbonara R, Roussel J, et al. Increased sodium channel use-dependent inhibition by a new potent analogue of tocainide greatly enhances in vivo antimyotonic activity. *Neuropharmacology*. 2017;113(Pt A):206-216. doi:10.1016/j.neuropharm.2016.10.013
- 21 Ravaglia S, Maggi L, Zito A, et al. Buprenorphine may be effective for treatment of paramyotonia congenita. *Muscle Nerve*. 2021;64(1):95-99. doi:10.1002/mus.27249
- 22 Desaphy JF, Carbonara R, Costanza T, Conte Camerino D. Preclinical evaluation of marketed sodium channel blockers in a rat model of myotonia discloses promising antimyotonic drugs. *Exp Neurol*. 2014;255(100):96-102. doi:10.1016/j.expneurol.2014.02.023
- 23 Dupont C, Denman KS, Hawash AA, Voss AA, Rich MM. Treatment of myotonia congenita with retigabine in mice. *Exp Neurol*. 2019;315:52-59. doi:10.1016/j.expneurol.2019.02.002
- 24 Boërio D, Corrêa TD, Jakob SM, Ackermann KA, Bostock H, Z'Graggen WJ. Muscle membrane properties in A pig sepsis model: Effect of norepinephrine. *Muscle Nerve*. 2018;57(5). doi:10.1002/mus.26013
- 25 Suetterlin KJ, Tan SV, Mannikko R, et al. Ageing contributes to phenotype transition in a mouse model of periodic paralysis. *JCSM Rapid Commun*. 2021;4(2):245-259. doi:https://doi.org/10.1002/rco2.41

The background of the slide is a light blue color with a pattern of small, dark blue, irregularly shaped particles scattered across it. Several dried, pressed leaves are visible, showing their intricate vein structures. The leaves are a light tan or beige color, contrasting with the blue background. One large leaf is prominently displayed in the center-right, while others are partially visible in the top-left and bottom-left corners.

CHAPTER 6

SAFETY, PHARMACOKINETICS, AND PHARMACODYNAMICS OF A CLC-1 INHIBITOR – A FIRST-IN-CLASS COMPOUND THAT ENHANCES MUSCLE EXCITABILITY: A PHASE I, SINGLE- AND MULTIPLE-ASCENDING DOSE STUDY

**THIS CHAPTER (PAGES 132 TO 161) IS SUBJECT TO AN
EMBARGO AND IS THEREFORE NOT INCLUDED IN THIS FILE**

Titia O. Ruijs^{1,2}, Catherine M.K.E. de Cuba^{1,2}, Jules A.A.C. Heuberger¹, John Hutchison³, Jane Bold³,
Thomas S. Grønnebak³, Klaus G Jensen³, Eva Chin³, Jorge A. Quiroz³, Peter Flagstad³, Marieke L. de Kam¹,
Michiel J. van Esdonk¹, Erica Klaassen¹, Robert J. Doll¹, Ingrid W. Koopmans^{1,2}, Annika A. de Goede¹,
Thomas H. Pedersen³, Geert Jan Groeneveld^{1,2}

1. Centre for Human Drug Research, Leiden, NL
2. Leiden University Medical Centre, Leiden, NL
3. NMD Pharma A/S, Aarhus N, DK



CHAPTER 7

FIRST IN CLASS CLC-I INHIBITOR IMPROVES SKELETAL MUSCLE FUNCTION IN ANIMAL MODELS AND PATIENTS WITH MYASTHENIA GRAVIS

Submitted to Science Translational Medicine

Martin Skov^{1*}, Titia Q. Ruijs^{2,3*}, Thomas S. Grønnebak¹, Marianne Skals¹, Anders Riisager¹,
Jeppe Blichfeldt Winther¹, Kamilla Løhde Tordrup Dybdahl¹, Anders Findsen¹,
Jeanette Jeppesen Morgen¹, Nete Huus¹, Martin Broch-Lips¹, Ole Bækgaard Nielsen^{1,2},
Catherine M.K.E. de Cuba^{2,3}, Jules A.A.C. Heuberger², Marieke L. de Kam²,
Martijn Tannemaat³, Jan Verschuuren³, Lars J. S. Knutsen¹, Nicholas M. Kelly¹,
Klaus Gjervig Jensen¹, William David Arnold⁵, Arthur H. Burghes^{6,7}, Claus Olesen^{1,4},
Jane Bold¹, Thomas K. Petersen¹, Jorge A. Quiroz¹, John Hutchison¹, Eva R. Chin¹,
Geert Jan Groeneveld^{2,3}, Thomas H. Pedersen^{1,4}. *Shared first author

1. NMD Pharma A/s, Aarhus N, DK

2. Centre for Human Drug Research, Leiden, NL

3. Leiden University Medical Centre, Leiden, NL

4. Aarhus University, Department of Biomedicine, Aarhus C, DK

5. NextGen Precision Health, University of Missouri, Columbia, USA

6. Department of Biological Chemistry and Pharmacology, The Ohio State
University Wexner Medical Center, Columbus, USA

7. Department of Neurology, Neuromuscular Division, The Ohio State
University Wexner Medical Center, Columbus, USA

ABSTRACT

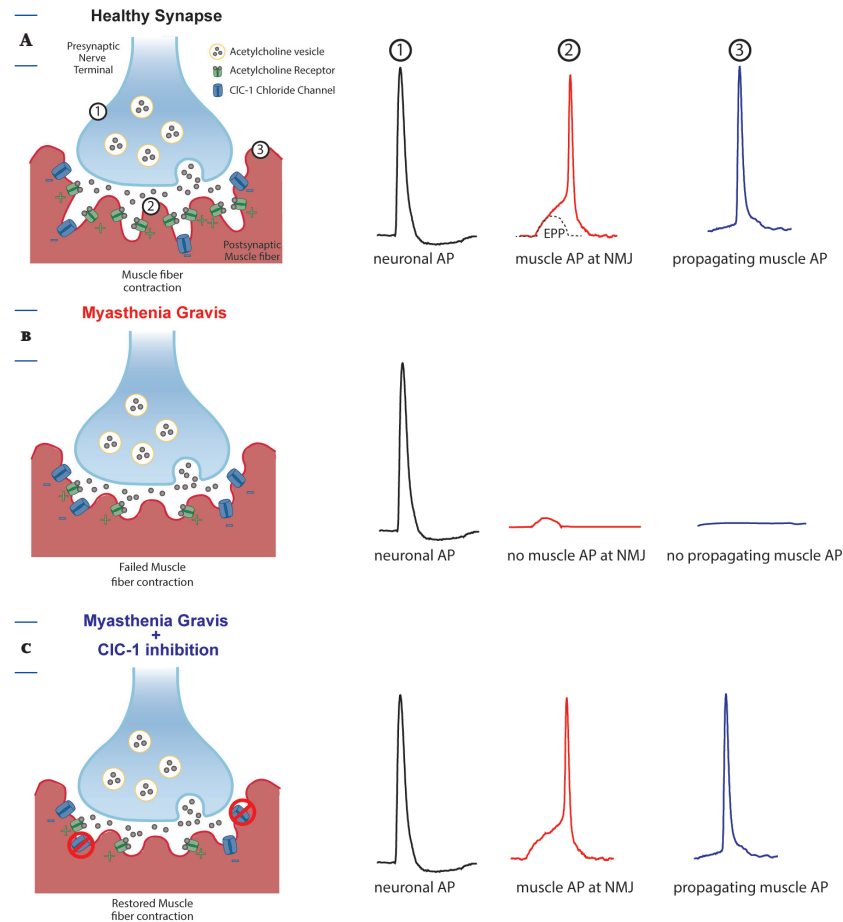
Myasthenia gravis (MG) is a neuromuscular disease that results in compromised transmission of electrical signals from motor neurons to skeletal muscle fibers. As a result, MG patients have reduced skeletal muscle function and present with symptoms of severe muscle weakness and fatigue. ClC-1 is a skeletal muscle specific chloride (Cl⁻) ion channel that plays important roles for regulating neuromuscular transmission and muscle fiber excitability during intense exercise. Here we show for the first time that partial inhibition of ClC-1 with a novel, selective, and orally bioavailable ClC-1-inhibiting small molecule (NMD670) can restore muscle function in rat models of MG and in MG patients. Thus, in severely affected MG rats, ClC-1 inhibition enhanced neuromuscular transmission, restored muscle function, and improved mobility following both single and prolonged administrations of NMD670. On this basis, NMD670 was progressed through nonclinical safety pharmacology and toxicology studies leading to approval for testing in clinical studies. After successfully completing Phase I single ascending dose in healthy volunteers, NMD670 was tested in MG patients in a randomized, placebo-controlled, single-dose, three-way cross-over clinical trial. The clinical study evaluated safety, pharmacokinetics, and pharmacodynamics of NMD670 in 12 MG patients with mild symptoms. NMD670 had a favorable safety profile and led to clinically relevant improvements in the Quantitative myasthenia gravis (QMG) total score. This study provides the first indications of ClC-1 inhibition as a novel and highly translational therapeutic approach to improve symptoms in MG and, potentially, other diseases with compromised neuromuscular transmission.

INTRODUCTION

Contractions of skeletal muscle enable activities such as walking, breathing, and eating. Such complex and essential behavior requires well-functioning control and coordination of the muscle contractions by the nervous system. The neuromuscular junction (NMJ) is the specialized synapse where propagating action potentials (APs) are transmitted from motor neurons to muscle fibers. In healthy muscles, generation of muscle fiber APs at the NMJ is highly reliable, even during intense muscle activity. Contrastingly, in some neuromuscular diseases excitation failures at the NMJ cause severe muscle weakness that can become life-threatening. Myasthenia gravis (MG) is one of the most common diseases that compromises AP generation at the NMJ resulting in muscle weakness and excessive fatigability.¹ In most cases, MG is caused by an autoimmune response directed against post-synaptic components of NMJ, e.g., acetylcholine receptor (AChR) (Figure 1). It is a serious and sometimes life-threatening disease that requires chronic treatment in most patients. Drugs used in the treatment of MG can be categorized into treatments that directly enhance neuromuscular transmission (e.g. pyridostigmine, an acetylcholinesterase inhibitor), and immunomodulatory treatments that focus on the autoimmune response (e.g. steroids, non-steroidal immunosuppressants, complement cascade inhibitors, and FCN antagonists). There is no curative treatment, and most patients are treated with a combination of drugs from both categories.² While there has been some important progress in development of new immunomodulatory MG treatments,³⁻⁷ there are still limited treatment options to directly restore muscle function by enhancing neuromuscular transmission.^{8,9}

ClC-1 channel is a skeletal muscle specific member of the family of nine ClC proteins known in man. The physiological role of ClC-1 is to dampen muscle fiber excitability by stabilizing the resting membrane potential. Regulation of ClC-1 during intense physical activity via cellular signals that arise in the active muscle fibers has been shown to be a key determinant for controlling muscle function.¹⁰ Thus, during intense muscle activity, ClC-1 function is partially inhibited via activity-induced protein kinase C phosphorylation with ensuing enhancement of neuromuscular transmission.¹⁰ A role of ClC-1 for neuromuscular transmission has been further corroborated by a study showing that pharmacological inhibition of ClC-1 can restore nerve-stimulated force in isolated

FIGURE 1 Illustration of how low EPP amplitudes results in excitation failures in MG and the working hypothesis for how CLC-1 inhibition enhances neuromuscular transmission restoring of AP excitations.



(A) Neuromuscular transmission in a healthy synapse. Inwardly directed current flow through activated ACHR causes a local depolarization of the muscle fiber membrane potential at the NMJ that is known as the endplate potential (EPP). Provided the EPP reaches a sufficient amplitude, the depolarization results in activation of voltage gated sodium channels with ensuing excitation of a propagating AP in the muscle fiber. Numbers refer to electrical events at NMJ shown conceptually in the right panel: 1) the neuronal AP in black, 2) the muscle fiber AP when excited at NMJ in red with the EPP indicated by the dotted line, and 3) the propagating AP in the muscle fiber membrane in blue. (B) Illustration of the alterations at NMJ in MG including reduced ACHR numbers and shallow post-synaptic folds. The neuronal AP is unaffected, but the muscle fiber AP is not excited at NMJ due to the diminished EPP. (C) Partial inhibition of CLC-1 channels enhances neuromuscular transmission by enlarging the EPP allowing restoration of AP excitation in the muscle fiber at NMJ in MG.

nerve-muscle preparations from rat during sub-maximal exposure to ACH receptor antagonists.¹¹ Prompted by these indications of a key role of CLC-1 for NMJ function, the present study explored the hypothesis that CLC-1 inhibition may enhance neuromuscular transmission and restore muscle function in diseases characterized by NMJ transmission failure eventually leading to improvement in symptoms of weakness and fatigue.

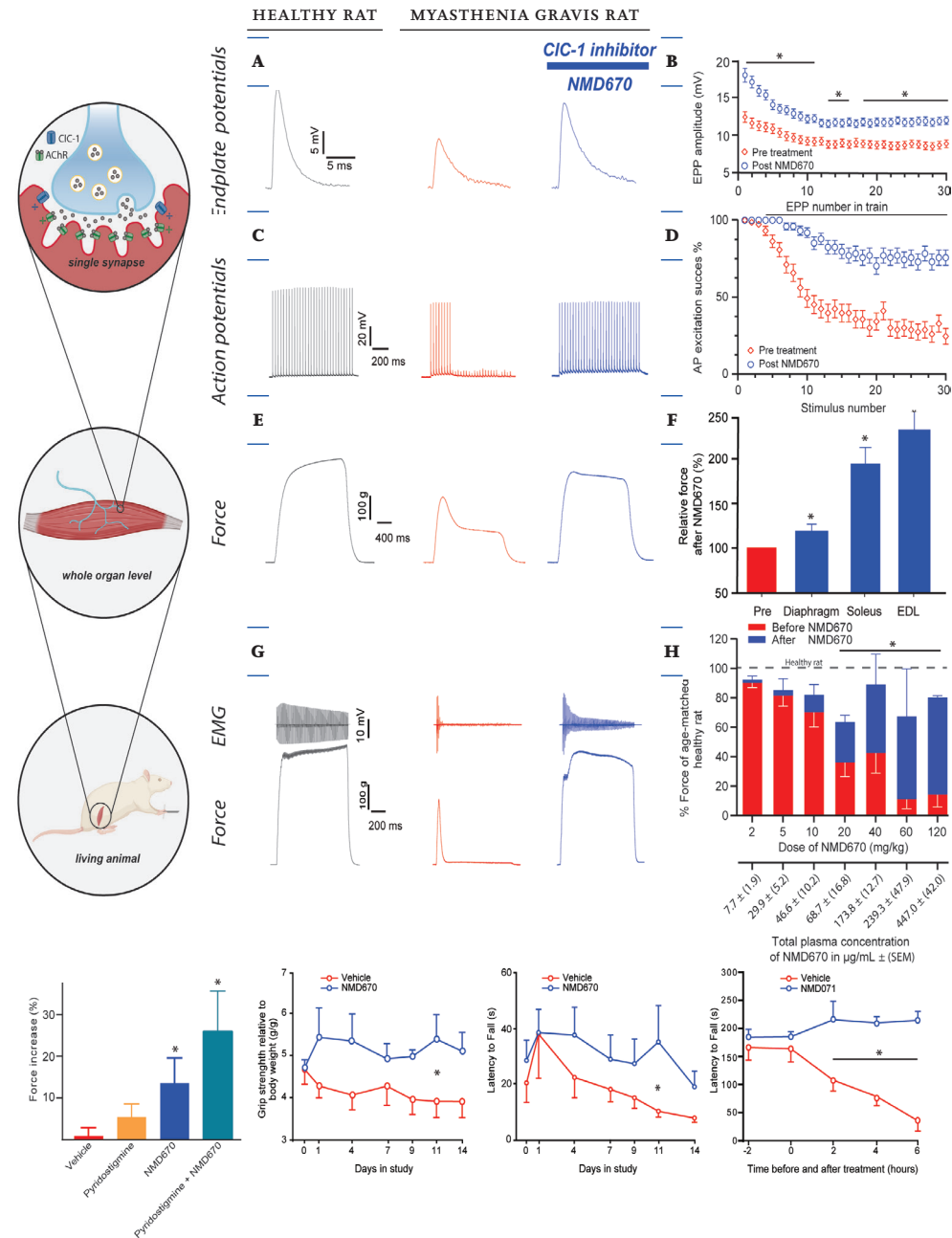
Here we report a comprehensive series of pre-clinical and clinical studies that were conducted to test the hypothesis that pharmacological inhibition of CLC-1 with NMD670, a novel first-in-class CLC-1 inhibitor, can enhance neuromuscular transmission and restore muscle function in MG patients (Figure 1C). First, using severely affected MG rats, NMD670 was observed to enhance neuromuscular transmission and restore muscle function when tested at all levels of biological organization from the single synapse to prolonged dosing. Second, these pre-clinical findings predicted and translated to clinical observations in patients with MG. Thus, single dose administrations of NMD670 showed clinically meaningful and statistically significant improvement of muscle function in MG patients while having a favorable safety profile. The findings provide the first evidence that CLC-1 inhibition can be developed as a new treatment approach in MG and potentially other diseases with NMJ transmission deficits.

RESULTS

To test the hypothesis that CLC-1 inhibition can enhance NMJ transmission, restore muscle function, and improve symptoms in MG, two small molecule CLC-1 inhibitors were first identified (NMD670 and NMD071) and shown to be selective and orally bioavailable. The effect of CLC-1 inhibition was then evaluated in MG rat models at all functional levels from the single synapse to prolonged dosing in whole animals. Finally, it was explored whether treatment effects with CLC-1 inhibition in MG rats could translate into clinically meaningful proof-of-mechanism observations in patients with symptomatic MG.

A screen testing the ability of compounds to inhibit the CLC-1 channel in muscle fibers from healthy rats was used, employing a previously described electrophysiological technique with three intracellular micro-electrodes.¹² Briefly, CLC-1 function was evaluated from measurements of the resting membrane conductance in individual muscle fibers and a reduction in the membrane conductance reflects CLC-1 inhibition.

FIGURE 2 CIC-1 inhibition increases neuromuscular transmission and restores muscle force and motor performance in rat models of MG.



(Continuation Figure 2)

Panels (A, C, E, and G) show representative traces of electrophysiological signals or force from healthy rats in grey, untreated MG rats in red, and MG rats after addition/dosing of the CIC-1 inhibiting agent NMD670 in blue. (A) Shows EPP recording obtained at the single synapse level with intracellular electrode in response to stimulation of the motor nerve. Shown is the first EPP in a train of 30 EPPs elicited at 12 Hz in a healthy muscle fiber and in muscle fibers from MG rats before and after NMD670. (B) Average EPP amplitudes in 68 MG muscle fibers without (red) and 82 MG muscle fibers with presence of NMD670 (blue) during protocol in (A). (C) Action potentials recorded from single muscle fibers with intracellular electrodes inserted at NMJ during 30 Hz nerve-stimulation in muscle fibers from healthy epitrochlearis muscle fibers and from MG muscle fibers before and after adding NMD670. (D) Average AP excitation success (%) of attempted stimulations at 30 Hz stimulation in MG muscle fibers before and after addition of NMD670 (n = 74 epitrochlearis MG muscle fibers in both groups). (E) Force from isolated soleus muscle from healthy and from MG animals during nerve-stimulation at 60 Hz, before and after addition of NMD670. (F) Average force relative to pre-NMD670 in isolated nerve-stimulated diaphragm (n = 11), soleus (n = 14) and EDL (n = 14) muscles from MG animals. (G) Force (lower panel) and CMAP (upper panel) in triceps surae muscle from an age-matched healthy rat and a MG rat with MG score 2. Force and CMAP elicited by stimulation of the sciatic nerve at 80 Hz for 1 second, before (red traces) and 20 minutes after per oral administration of 40 mg/kg NMD670 (blue traces). (H) Average muscle force from MG animals (as exemplified in G) before (red) and after (blue) receiving NMD670 per oral (from 2 to 120 mg/kg), relative to muscle force from healthy age-matched rats plotted against observed total plasma concentration of NMD670 (µM). n values were (4, 3, 6, 5, 5, 3 and 2), for (2, 5, 10, 20, 40, 60 and 120 mg/kg), respectively. (I) Percent increase in grip strength force in MG rats 45 mins after treatment, compared to before treatment, with either vehicle (n = 35), 0.375 mg/kg Pyridostigmine (n = 10), 20 mg/kg NMD670 (n = 17), or a combination of 0.375 mg/kg Pyridostigmine and 20 mg/kg NMD670 (n = 5). (J) Shows grip strength relative to bodyweight, and (K) rotarod performance, during 14-day chronic dosing in MG rats receiving vehicle (red lines/symbols) or NMD670 (blue lines/symbols). (L) Shows rotarod performance in rats injected with mAb 35 antibodies (passive MG model) subsequently treated with vehicle (red, n = 6) or 30 mg/kg NMD670 (blue, n = 4). For B, D, F, H, I, J, K and L values are shown as mean ± SEM. For statistics see (see Supplementary Table 1).

NMD071 was an early hit with moderate CIC-1 potency (Supplementary Figure 1A) and good bioavailability in rat that was suitable for early in vivo studies. Iterative design and structure-activity analysis resulted in NMD670 having improved CIC-1 potency, good bioavailability and half-life in rat and dog and an acceptable off-target profile. NMD670 was tested in muscle fibers from rats with experimental autoimmune MG and neither CIC-1 function nor the ability of NMD670 to inhibit CIC-1 were altered in muscle fibers from the MG rats (Supplementary Figures 1B and 2). Inhibition of CIC-1 was also found to increase the excitability of muscle fibers, as evident from a reduction in the injected current required to trigger a muscle fiber AP (i.e. reduced rheobase current) (Supplementary Figure 3).

To determine the effect of CIC-1 inhibition at the single synapse level, two series of experiments were conducted using isolated nerve-muscle preparations from severely affected MG rats. In both series, the motor nerve was stimulated electrically, and intracellular electrodes were inserted in muscle fibers to record the membrane potential at NMJ. First, the effect of CIC-1 inhibition on EPP amplitude was determined. To

record EPP amplitude without eliciting an interrupting muscle fiber AP, the experiments were conducted in the presence μ -conotoxin to selectively and fully block the skeletal muscle specific voltage gated Na^+ channels. EPP amplitudes were markedly reduced in muscle fibers from MG rats as compared to EPP amplitudes in fibers from healthy rat muscles (Figure 2A). This is similar to findings in muscle fibers from MG patients¹³ and low EPP amplitude is considered a main contributor to the NMJ excitation failures that underlie muscle weakness and fatigability in MG.¹⁴ With CLC-1 inhibition by NMD670, the EPP amplitudes increased by more than 35% in the MG muscle fibers (Figure 2B). Second, and still at the single synapse level, it was explored whether CLC-1 inhibition could restore NMJ excitations in the fibers from MG rats. Here we recorded APs during short trains of nerve-stimulation before and after CLC-1 inhibition. Before CLC-1 inhibition, excitation failures were frequently observed in the fibers from MG rats (Figure 2C red trace), clearly contrasting observations in fibers from healthy rats where excitation failures were not observed (Figure 2C grey trace). As shown by the representative traces (Figure 2C) and average data (Figure 2D), the probability of successful AP excitations was improved in the MG fibers when subsequently exposed to NMD670. Taken together, the increased EPP amplitude and restored NMJ excitation in MG rat muscle fibers upon exposure to NMD670 provide pre-clinical evidence at the single synapse level that CLC-1 inhibition enhances neuromuscular transmission in an animal model of MG.

To next determine whether enhanced neuromuscular transmission with CLC-1 inhibition could restore muscle function, isolated nerve-muscle preparations from healthy rats and from MG rats were mounted in tissue baths where force production in response to nerve-stimulation could be recorded. In contrast to well-maintained force production in muscles from age-matched healthy rats, muscles from MG rats were unable to sustain force during short periods of nerve-stimulation (Figure 2E). Compromised muscle function was prominent in hindlimb muscles from MG rats and was also observed in diaphragm muscles. In all MG muscles tested, CLC-1-inhibition by NMD670 restored force production (Figure 2F) to levels that were close to observations in muscles from healthy animals. NMD670 had no or minimal effect in muscles from healthy animals where NMJ deficits are not present.

The effect of CLC-1 inhibition on muscle force was also assessed *in vivo* in highly symptomatic MG rats using an experimental setup described in detail in *Supplementary Methods*. Briefly, rats were anesthetized, and

concurrent recordings of electromyography (EMG) and force were obtained from the triceps surae muscle during stimulation of the sciatic nerve. Measurements were made before and after oral administration of NMD670, and blood samples were obtained to measure plasma concentrations of NMD670. This enabled pharmacokinetic/pharmacodynamic (PK/PD) relationship to be determined between restoration of muscle force and plasma concentration of the CLC-1 inhibitor. As expected from the observations in isolated nerve-muscle preparations, both EMG signals and nerve-stimulated muscle force were greatly depressed (Figure 2G red trace) in MG rats as compared to healthy rats (Figure 2G black trace). Administration of NMD670 to the MG rats, however, caused rapid and dose-dependent restoration of both EMG amplitude and force (Figure 2G blue traces, and 2H).

Whether the enhanced neuromuscular transmission and restored nerve-stimulated muscle force with CLC-1 inhibition would translate to improved muscle strength during voluntary movement in MG rats was next evaluated. Initially, the effect of a single administration of NMD670 on grip strength was determined in severely affected MG rats. The experiments were conducted in a blinded manner and pyridostigmine was included as a positive control and for comparison to NMD670. MG rats were randomized to receive vehicle, pyridostigmine, NMD670, or NMD670 combined with pyridostigmine. As shown in Figure 2I, grip strength increased by $15 \pm 5\%$ after NMD670 administration and $5 \pm 4\%$ with pyridostigmine. NMD670 and pyridostigmine act via different mechanisms and grip strength increased by $24 \pm 12\%$ when NMD670 and pyridostigmine were combined. Vehicle treatment did not affect grip strength ($1 \pm 2\%$). Taken together, these data show that single administration of a CLC-1 inhibitor was able to restore skeletal muscle function in MG rats.

Given the chronic nature of MG,¹⁵ a novel therapy to enhance neuromuscular transmission has to remain efficacious during chronic use. Thus, the effect of prolonged administration of NMD670 was explored in the MG rats. Specifically, effects of twice daily dosing of NMD670 or vehicle for 2 weeks were evaluated on bodyweight, grip strength, and running (rotarod) in two groups of MG rats expressing stable and severe signs of the disease. The study was blinded, and all rats had confirmed presence of antibodies against the AChR (*Supplementary Figure 4*). Blood sampling was conducted during the 14 days of study, and muscle biopsies were taken at study termination to confirm correct dosing and the presence of NMD670 in the target tissue (*Supplementary Figure 5*). As shown in

Figure 2J, NMD670-treated MG rats experienced increased grip strength and higher endurance on rotarod during the entire treatment period (Figure 2K) as compared to before treatment and when compared to the vehicle-treated MG rats. For ethical reasons, termination of animals was required if their body weight declined below 80% of the maximum body weight observed prior to disease induction. Animals treated with NMD670 showed attenuated loss of body weight during the study (Supplementary Figure 6) and therefore showed better survival. Thus, 6 of the 8 NMD670-treated rats completed the study whilst only 3 out of 8 vehicle-treated rats completed the study due to the bodyweight criteria. This study indicates that prolonged CLC-1 inhibition is well tolerated and consistently restored muscle function and overall health status of MG rats during the prolonged dosing.

It was important to ensure that the treatment benefits with NMD670 in MG rats were not due to the specific CLC-1 inhibitor or the specific MG rat model, but, more generally, reflected the novel treatment approach of CLC-1 inhibition to improve myasthenic symptoms. For this reason, a final series of pre-clinical experiments was performed with a different CLC-1 inhibitor molecule (NMD071) in a passive immunization rat MG model (Figure 2L). In passive immunization MG models, the disease onset is rapid, and the disease progresses rapidly to severe symptoms. This makes it difficult to treat animals for a prolonged period or even to reach a stable disease presentation. In the present experiments, disease progression and treatment effects were monitored using running performance on rotarod.¹⁶ In symptomatic rats showing reasonably stable and depressed performance within a two-hour interval, a single dose of either vehicle or 30 mg/kg of NMD071 was administered in a blinded manner. As evident from Figure 2L, and in contrast to vehicle-treated rats, endurance stabilized or recovered in NMD071-treated MG rats.

In summary, the pre-clinical experiments demonstrated that CLC-1 inhibition can enhance neuromuscular transmission, restore muscle function, and alleviate MG signs in animal models of MG. These findings prompted the subsequent exploration into whether these pre-clinical findings would translate into clinically meaningful benefits in patients suffering from MG.

To this end, NMD670 was taken through a battery of nonclinical safety pharmacology and toxicology studies including two 28-day ICH-GLP

toxicology studies in rat and mini-pig (unpublished data). This non-clinical development program showed that NMD670 has a favorable safety profile, and the molecule was approved for clinical testing. The safety, tolerability, PK, and PD of NMD670 were subsequently assessed in a Phase I randomized, placebo-controlled, double-blind, single, and multiple ascending dose study in healthy male and female subjects (data in preparation). Based on a favorable safety profile of NMD670, a study in 12 MG patients was initiated under the same protocol.

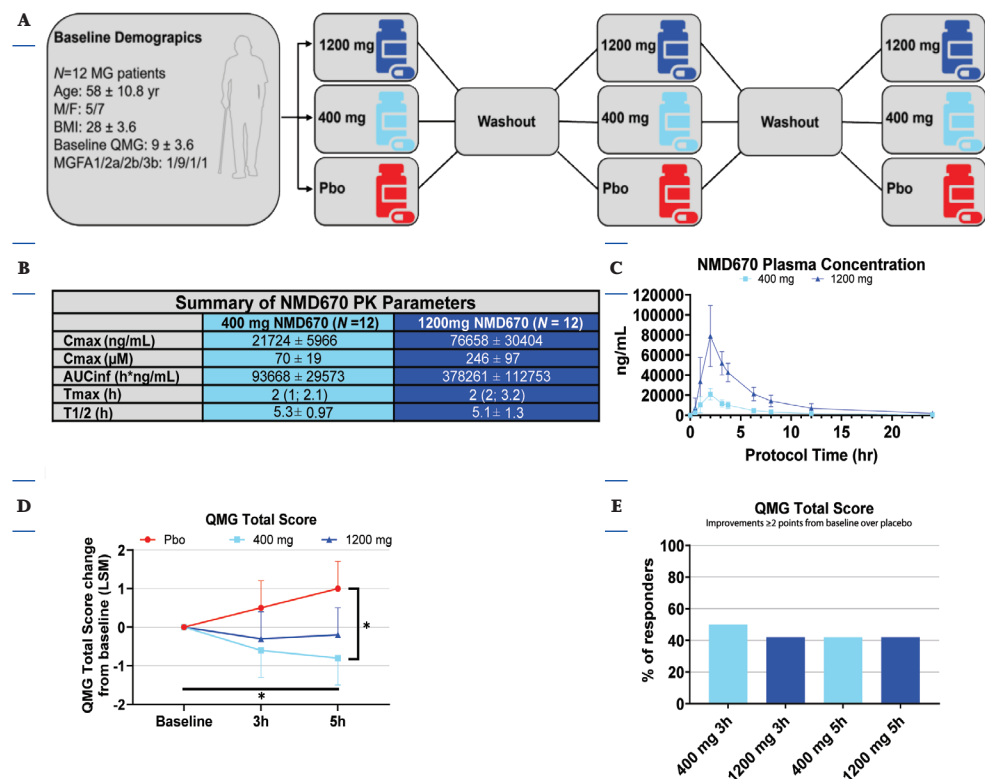
The study was a randomized, double-blind, placebo-controlled, three-way cross-over comparison of two single oral doses of NMD670 and placebo in male and female patients with symptomatic MG. At three separate visits, patients received either placebo, NMD670 at 400mg, or NMD670 at 1200mg (Figure 3A).

A total of 12 patients were enrolled and all subjects completed the study (Supplementary Figure 7). Patients had a mean age of 58 years (range: 36 to 78), 5 were male and 7 were female. Patients had a mean Quantitative myasthenia gravis (QMG) score of 9.0 points (SD: 3.6) and 75% of patients had an MGFA Clinical Classification class II, both indicative of mild weakness. Other baseline demographics are listed in (Figure 3A).

Patients treated with pyridostigmine (N=8 of 12) withheld dosing for at least 14 hours before each visit. Other treatments were allowed if maintained at stable doses during the study: 9 patients were on prednisolone, 5 on azathioprine, and 1 had previously received immunoglobulin.

NMD670 was safe and well tolerated, and the incidence of patients with treatment emergent adverse events (TEAEs) during the study were similar between NMD670 and placebo (Table 1 and 2). All TEAEs were mild in intensity except for one moderate event of gastroenteritis reported for NMD670 at 400 mg that was considered unrelated to treatment (Table 2). The most common TEAEs (i.e. TEAEs reported by more than one patient) were fatigue, headache, gastroenteritis, diplopia, back pain, and dizziness. There were no relationships between treatments and the incidences of TEAEs following administration of a single dose of NMD670 or placebo. Myotonia, a hyperexcitability of skeletal muscle and delayed muscle relaxation due to CLC-1 inhibition or genetic loss of CLC-1 function C,¹⁷ was not observed in patients following the administration of NMD670. Clinical safety laboratory parameters did not reveal clinically meaningful changes during the study.

FIGURE 3 Baseline demographics, PK and PD effects of single tablet administration of NMD670 in patients with Myasthenia gravis.



Panel A shows patient baseline demographics and study design. Panels (b,c) show descriptive PK summary statistics (b) and 24-h PK profiles (c). Panel (d) shows the a priori analyses of QMG total score. Panel (e) shows the post hoc responder analyses of the QMG total score. For (b), data are mean ± SEM except for time of maximal exposure (T_{max}), which is presented as medians with range. For (c), data are presented as mean ± SD. For (d), data are least square means ± SEM. For (e), data are percent of subjects responding to treatment. n = 12.

TABLE 1 Summary of Treatment Emergent Adverse Events (AE) by treatment.

	400mg NMD670 (N = 12)		1200mg NMD670 (N = 12)		Placebo (N = 12)	
	Events N	Subjects N (%)	Events N	Subjects N (%)	Events N	Subjects N (%)
Any AE	15	8 (66.7)	16	7 (58.3)	13	7 (58.3)
Any SAE	-	-	-	-	-	-
Any AE Leading to Dropout	-	-	-	-	-	-
Any AE Leading to Death	-	-	-	-	-	-
Any AE Possibly or Probably Related to Treatment	12	9 (75)	6	3 (25)	7	5 (41.6)
Any AEs of Severe Intensity	-	-	-	-	-	-
Any AEs of Moderate Intensity	1*	1 (8.3)*	-	-	-	-
Any AEs of Mild Intensity	14	8 (66.7)	16	7 (58.3)	13	7 (58.3)

SAE = serious adverse event. *AE of gastroenteritis considered unrelated to treatment

TABLE 2 Summary of Treatment Emergent Adverse Events by Treatment, System Organ Class, and Preferred Term

System Organ Class/ Preferred Term	400mg NMD670 (N = 12)		1200mg NMD670 (N = 12)		Placebo (N = 12)	
	Events N	Subjects N (%)	Events N	Subjects N (%)	Events N	Subjects N (%)
EYE DISORDERS	1	1 (8.3)	2	2 (16.7)	1	1 (8.3)
Diplopia	-	-	1	1 (8.3)	1	1 (8.3)
Eye irritation	-	-	1	1 (8.3)	-	-
Photophobia	1	1 (8.3)	-	-	-	-
GASTROINTESTINAL DISORDERS	-	-	2	1 (8.3)	-	-
Abdominal pain	-	-	1	1 (8.3)	-	-
Diarrhoea	-	-	1	1 (8.3)	-	-
GENERAL DISORDERS AND ADMINISTRATION SITE CONDITIONS	3	3 (25.0)	5	4 (33.3)	4	3 (25.0)
Chest discomfort	-	-	1	1 (8.3)	-	-
Fatigue	3	3 (25.0)	4	4 (33.3)	3	2 (16.7)
Influenza like illness	-	-	-	-	1	1 (8.3)
INFECTIONS AND INFESTATIONS	1	1 (8.3)	3	3 (25.0)	1	1 (8.3)
Bacteriuria	-	-	1	1 (8.3)	-	-
Corona virus infection	-	-	1	1 (8.3)	-	-
Gastroenteritis	1	1 (8.3)	1	1 (8.3)	1	1 (8.3)
MUSCULOSKELETAL AND CONNECTIVE TISSUE DISORDERS	2	2 (16.7)	-	-	3	2 (16.7)
Back pain	1	1 (8.3)	-	-	1	1 (8.3)
Muscle spasms	-	-	-	-	1	1 (8.3)
Musculoskeletal pain	1	1 (8.3)	-	-	-	-
Musculoskeletal stiffness	-	-	-	-	1	1 (8.3)
NERVOUS SYSTEM DISORDERS	8	6 (50.0)	3	2 (16.7)	3	2 (16.7)
Dizziness	1	1 (8.3)	1	1 (8.3)	-	-
Headache	7	6 (50.0)	-	-	2	2 (16.7)
Hypoaesthesia	-	-	1	1 (8.3)	-	-
Presyncope	-	-	-	-	1	1 (8.3)
Somnolence	-	-	1	1 (8.3)	-	-
RENAL AND URINARY DISORDERS	-	-	1	1 (8.3)	-	-
Pollakiuria	-	-	1	1 (8.3)	-	-
VASCULAR DISORDERS	-	-	-	-	1	1 (8.3)
Flushing	-	-	-	-	1	1 (8.3)

Pharmacokinetic (PK) profiles and descriptive summaries for NMD670 at 400 mg and 1200 mg are provided in Figure 3B, C. Briefly, there was a clear dose dependent exposure, the time to maximum plasma concentration was observed at approximately 2 hours, and the half-life was approximately 5 hours for both NMD670 400 mg and 1200 mg. This is very similar to observations in healthy volunteers.

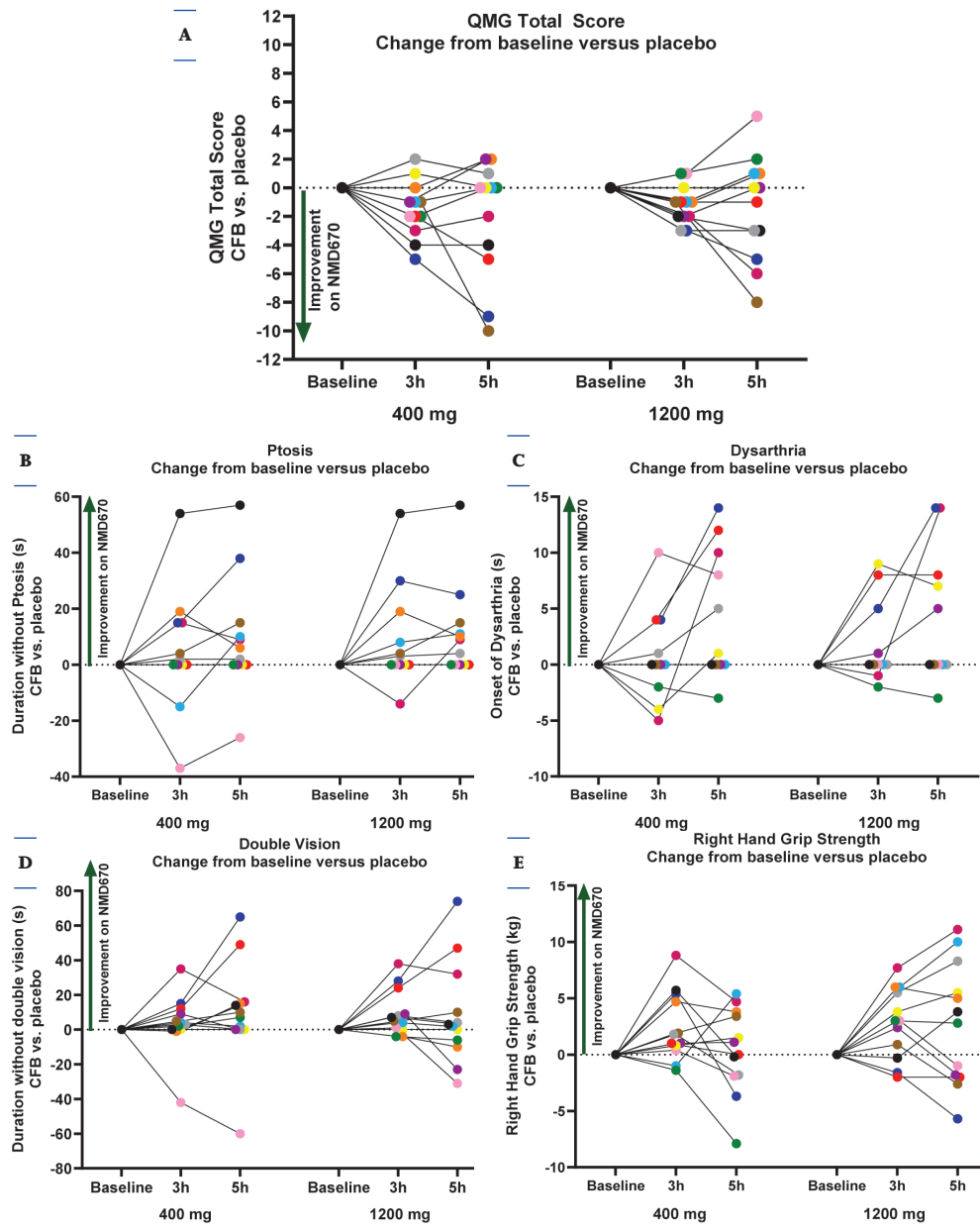
At all three visits to the clinic when dosing of placebo or NMD670 was scheduled, efficacy outcome measurements were performed in the morning prior to dosing and at approximately 3- and 5-hours post dose. Importantly, due to the cross-over design of the study, subjects acted as their own control. This enabled a direct comparison of read-outs within patients from days when dosed with NMD670 to observations on the day when dosed with placebo. Because of the exploratory nature of these endpoints, p values were not adjusted for multiple comparisons.

An improvement in the QMG total score in favor of the drug vs. placebo was detected at both dose levels and it was largest after NMD670 at 400 mg; the least mean square (LMS) change from baseline on NMD670 at 400mg versus placebo was of -1.5 points (95% CI = -2.8, -0.1; p = 0.03), for the overall treatment arm, and specifically it was -1.2 points at 3 hours (95% CI = -2.7, 0.3; p = 0.12), and -1.7 points at 5 hours (95% CI = -3.3, -0.2; p = 0.02) (Figure 3D). The LMS change from baseline on NMD670 at 1200 mg versus placebo was of -1.0 point (95% CI = -2.3, -0.3; p = 0.14) for the overall treatment arm and, of -0.9 points at 3 hours (95% CI = -2.4, 0.6; p=0.25), and of -1.1 points at 5 hours (95% CI = -2.6, 0.4; p = 0.14) (Figure 3D).

A post hoc responder analysis was conducted to characterize the clinical relevance of the QMG total score improvements, previously defined as an improvement equal to or larger than 2 points in patients with mild to moderate disease (baseline QMG total score up to 9 and up to 16 points, respectively).¹⁸ Importantly, 42% to 50% of the patients were responders to NMD670 (change from baseline compared to placebo) across dose levels and time points (Figure 3E and 4A). On further investigating the individual functional tests comprising the QMG total score, improvements were observed in most patients in continuous measurement including hand grip strength, dysarthria, ptosis, and double vision (Figure 4B-E).

As a separate indicator of NMJ function and effect of NMD670 in the patients, repetitive nerve stimulation (RNS) at 5Hz was included as a PD outcome to evaluate the effect of NMD670 on CMAP decrement, an indicator of neuromuscular junction transmission dysfunction.¹⁹⁻²¹

FIGURE 4 Individual treatment responses for QMG Total Score and Ptosis, Double Vision and Right-Hand Grip Strength.



(Continuation Figure 4)

Panel A shows individual changes from baseline over placebo for NMD670 at 400 mg and 1200 mg treatment arms on QMG total score. Panels B-E show individual changes from baseline over placebo for NMD670 400 mg and 1200 mg treatment arms on ptosis, dysarthria, double vision, and right-hand grip strength (continuous data). $n = 12$ except for dysarthria where $n = 11$ as pre-dose data was missing on one subject at the placebo visit. Several subjects did not develop symptoms of ptosis ($n=2$), dysarthria ($n=3$), and double vision ($n=1$) at any timepoint at any visit. In these patients there was therefore no potential for improvement with NMD670 on these parameters.

No significant treatment effects were found on RNS at the group level, across parameters (Supplemental figure 8). However, it should be noted that effects could only be expected in patients who had CMAP decrement in the morning of the clinic visits before either drug or placebo was administered, and that the number of patients with decrement in RNS was low. Therefore, a post hoc responder analysis was conducted to better characterize the RNS observations (Supplemental Figure 8) including only patients who had pre-treatment CMAP decrement as defined by more than 5% reduction in CMAP amplitude from the first to the fifth stimulus.^{22,23} The subsets of patients who presented with decrement in the morning were 3 on the day of placebo treatment, 6 on the day of 400 mg NMD670 administration, and 3 on the day of 1200 mg NMD670 administration. Responders, defined as patients who displayed reversal of decrement to less than 5% post-dose, were only observed in the NMD670 groups. Thus, after placebo administration 0% of the patients recovered compared to 83% of patients recovering or normalizing their decrement after administration of NMD670 at 400 mg, and 33% recovered after administration of NMD670 at 1200 mg.

DISCUSSION

Transmission failure at the NMJ is a well-established contributor to muscle weakness and fatigability in MG.¹⁵ Here we show for the first time that NMD670, a novel first-in-class ClC-1 inhibitor can enhance neuromuscular transmission, restore muscle function in animal models of MG, and alleviate symptoms in patients with MG.

Pre-clinical investigation in isolated nerve-muscle preparations from severely affected MG rats showed that ClC-1 inhibition enhances NMJ transmission by increasing EPP amplitude leading to increased probability of AP generation upon nerve-stimulation. Enhanced neuromuscular transmission after ClC-1 inhibition was associated with restored muscle

function as determined both in isolated muscles and in living animals. In the latter, restored muscle function with NMD670 was furthermore closely correlated to improvement in CMAP decrement showing that the restored force resulted from enhanced NMJ transmission. Restored muscle function with CLC-1 inhibition led to functional benefits in the MG rats. Thus, in a blinded pre-clinical study with repeated dosing of NMD670, there was a clear restoration of grip strength and reduced loss of body weight in NMD670-treated MG rats compared to MG rats treated with vehicle. NMD670-treated rats also showed improved running endurance when tested on rotarod.

The beneficial effects of NMD670 in MG rats translated to positive proof-of-mechanism in patients, and NMD670 was found to be safe and well tolerated during early evaluations. Despite relatively mild symptomatology of the enrolled patients, which may have imposed a ceiling effect for improvement, findings on the QMG total score showed improvement after single administrations of 400 mg or 1200 mg versus placebo. Importantly, on the QMG total score, patients experienced a clinically relevant improvement of 2 points or more compared to their placebo treatment in 42% to 50% across dose-levels and timepoints. These results indicate that mean improvements are not due to individual outliers and are of magnitudes that are clinically relevant for patients suffering from mild to moderate MG. On investigating individual functional tests that comprise the QMG total score, continuous measurements including hand grip strength, dysarthria, ptosis, and double vision, showed improvement in patients on NMD670 compared to placebo, despite their mild symptomatology at baseline. This reflects improvements in different muscle groups including distal, bulbar, and ocular regions showing that the mechanism of CLC-1 inhibition restores muscle function across skeletal muscles, both central and distal.

The effects of NMD670 on QMG were similar for the two doses, and it was not possible to observe a dose-response relationship, probably due to the small number of patients enrolled and their mild disease severity. Future clinical studies with a larger sample size, with repeat-dose administration and additional dose levels of NMD670 in MG patients with more prominent disease severity will determine the relationship between administered dose and QMG improvements.

As only a small subset of patients presented with CMAP decrement at baseline, a post-hoc responder analysis was conducted revealing higher

rates of responders with NMD670 versus placebo. However, it is important to acknowledge that the presence of decrement was variable within participants and that a regression to the mean phenomenon cannot be ruled out in the 400 mg group, as a higher percentage of patients presented the abnormality at baseline on that treatment day.

This study shows for the first time that CLC-1 inhibition offers a way to restore muscle function in MG patients by directly enhancing neuromuscular transmission. Given that CLC-1 inhibition does not interfere either with the autoimmune response or with ACh release or metabolism, it is plausible that drugs from this novel family will be additive to other therapies available for MG patients and to MG treatments in development.³⁻⁷ In support of this notion, we report here that NMD670 led to more pronounced increases in muscle force in MG rats compared to pyridostigmine but also that there was an (at least) additive effect when they were combined. In the clinical study, patients were taken off pyridostigmine prior to receiving NMD670 although most of the enrolled patients were on some form of immunomodulatory treatment that was not discontinued during testing. The positive effects of NMD670, on top of the immunomodulatory treatment, thus further supports that CLC-1 inhibition is additive to other types of MG therapies. In a recent study, patients with MG reported that the nature of the fluctuating and often unpredictable symptom severity necessitates better treatment options that allow patients to quickly return to symptom stability.²⁴ From the current work, CLC-1 inhibition appears to have a fast onset of action and good oral bioavailability, adding further value to this new treatment approach. The data presented here supports that CLC-1 inhibitors could be potentially used as monotherapy in some patients and also be additive to existing treatments.

Our study in patients with MG has several potential limitations, including: 1) the small sample size which requires further confirmation of the results in larger studies; 2) the single administration of the investigational drug; 3) the exploratory nature and statistical investigation the PD endpoints, 4) the mild severity of the disease in enrolled patients that may have limited the magnitude of the true treatment effect. However, the translational effort and positive proof of mechanism in patients warrants further investigation in additional controlled studies in patients with MG, including repeated doses at different levels in patients with moderate or severe disease to enable the full expression of the treatment effect.

Taken together, the observed PD effects of NMD670 in MG patients suggest a strong translation from pre-clinical to clinical studies, and provides the first ever proof of mechanism that CLC-1 inhibition can enhance neuromuscular transmission and improve muscle function in patients suffering from MG. As neuromuscular transmission failure has been reported in other neuromuscular diseases than MG, the present study supports further investigations of the potential benefit of CLC-1 inhibitors in other diseases with compromised neuromuscular transmission.²⁵

METHODS

INDUCTION AND HANDLING OF RATS WITH ACTIVE EXPERIMENTAL AUTOIMMUNE MG All handling, use, and housing of animals complied with European and Danish Animal Welfare regulations, including euthanasia. Active experimental autoimmune MG rats were produced as described elsewhere²⁶ and in the *Supplementary Methods* using an immunogenic antigen derived from human AChR that was supplied by the Hellenic Pasteur institute. All activities pertaining to handling, disease induction, disease scoring,²⁷ and testing of novel compounds in animals were covered by license numbers 2018-15-0201-01408 and 2018-15-0201-01420.

EXPERIMENTS INVOLVING ISOLATED NERVE-MUSCLE PREPARATIONS FROM HEALTHY AND MG RATS Isolated nerve-muscle preparations were used for measurements of electrophysiological properties at the cellular level and for measurements of force. For these experiments, animals were euthanized, and muscles were dissected out with 1 to 3 cm of intact nerve. The isolated nerve-muscle preparations were transferred to organ baths for experiments (see below) and were allowed to recover for at least 30 minutes prior to experiments. The organ baths were perfused with Normal Krebs-Ringer (NKR) solution, containing (in mM); 122 NaCl, 25 NaHCO₃, 2.8 KCl, 1.2 KH₂PO₄, 1.2 MgSO₄, 1.27 CaCl₂, and 5 D-glucose. The NKR solution was continuously gassed with a mixture of 95% oxygen and 5% CO₂ to maintain pH of approx. 7.4 when at 30-31 °C. In some experiments, methyl-sulphate salts were used to replace Cl⁻ in the solution (Cl⁻-free solutions). All chemicals used were of analytical grade.

MEMBRANE CONDUCTANCE AND RHEOBASE IN MUSCLE FIBERS OF ISOLATED NERVE-MUSCLE PREPARATIONS Capacity of compounds to inhibit CLC-1 was evaluated in native tissue by measuring their effect on the resting membrane conductance (G_m) in single muscle fibers of freshly dissected intact muscles from adult rats. G_m is an electrical measure of the flow of ions across the surface membrane through the ion channels that are open at the resting membrane potential. CLC-1 is responsible for around 80% of G_m in both rat and man, and it is the only known surface membrane Cl⁻ channel in skeletal muscle.²⁸ Any changes in G_m with a compound can therefore be taken to reflect alterations of CLC-1 function. Nevertheless, an effect of a compound on CLC-1, was further confirmed by comparing recordings of G_m between experiments with and without Cl⁻ in the experimental solution.

Experimentally, soleus or diaphragm muscles from healthy rats and MG rats with scores 0, 1 or 2 were used. G_m and rheobase was measured using electrophysiological technique that involves insertion of 3 intracellular microelectrodes into individual muscle fiber as explained in detail elsewhere.¹² See *Supplementary Methods* for details.

RECORDINGS OF ENDPLATE POTENTIALS AND ACTION POTENTIALS IN RESPONSE TO NERVE-STIMULATION Endplate potentials (EPPs) were recorded with intracellular electrodes in isolated nerve-muscle preparations from healthy and MG rats (score 0-2). Muscle preparations used in the experiments were diaphragm or levator longus auris (LAL). Nerve-stimulations were delivered by an external constant current stimulator (DS3 Isolated Constant Current Stimulator; Digitimer, U.S.) controlled by the recording software (Signal version 6.4, Cambridge Electronics Design Ltd, Cambridge, UK). Stimulation of the nerve was achieved by applying a small electric field across the isolated nerve with sufficiently low voltage to exclusively activate the nerve and not the muscle fibers directly. Positioning of the nerve-stimulating electrodes was achieved by a micromanipulator. The stimulation protocol for evoking EPPs consisted of 2 different trains of trigger pulses, first at 12 Hz for 30 pulses, and then a second train at 30 Hz for 30 pulses. There was 10 s of rest between the two trains. This resulted in recordings of 2 EPP trains per fiber from which EPP amplitudes were analyzed. For each muscle, a set of control measurements was first obtained from

approx. 20 fibers before compound addition, and then from approx. 20 fibers starting 20-30 mins after incubation at 20 μ M NMD670. See Supplementary Methods for details.

FORCE MEASUREMENT IN ISOLATED INTACT NERVE-MUSCLE PREPARATIONS Force production in response to nerve-stimulation was evaluated in soleus, extensor digitorum longus (EDL), and diaphragm muscles from healthy rats and from MG rats. After dissection, all muscles were mounted on force transducers (FORT 250, WPI instruments DE) in organ baths, each containing 20 mL NKR. The data acquisition program (Signal version 6.4, Micro 1401, Cambridge Electronics Design Ltd, Cambridge, UK) was used to control stimulation, delivered by an isolated stimulator (Isostim 01D NPI electronics, DE). After equilibration in the organ baths, muscles were stretched to their optimal length and stimulated at a range of frequencies for 1-2 s using field stimulation. The field stimulation was used to stimulate the muscles both directly and via the nerve at 12 V. Separation between direct stimulation of muscle fibers and indirectly via nerve-stimulation was accomplished by using different durations of stimulation pulses (0.02 ms for nerve, 0.2 ms for direct muscle fiber stimulation). During the experiment, the muscles were stimulated every 10 min at 60 Hz for 1 second, either directly or via the nerve. Once a steady force production had been observed, which typically was after 6 contractions, different concentrations of CLC-1 inhibitor were added directly to the organ bath of individual muscles, and force was allowed to recover to a new elevated level. The increase in force after adding the compound was measured and compared to force before adding compound.

FORCE AND EMG IN SEDATED MG RATS An experimental setup was designed to enable co-temporal measurements of electromyographic recordings of compound muscle action potentials (CMAP) and force from triceps surae muscle in sedated and mechanically ventilated MG rats in response to stimulation of the sciatic nerve. Anesthesia was introduced with a 1:1 mix of Fentanyl (Hypnorm) and Midazolam (Dormicum 5mg/mL) (Hameln Pharma Plus GmbH, DE) at a subcutaneous dose of 1 mL/kg. The rats were then intubated and mechanically ventilated to ensure adequate pulmonary gas exchange (Hallowell MicroVent 1 Rodent Anesthe-

sia Ventilator, Dre Veterinary, KY, USA), and anesthesia was maintained by mixing isoflurane (2-3%) into the ventilation gas. A tube was inserted through the esophagus to the ventricle to allow PO dosing. The jugular vein was cannulated for blood sampling. The animals' core body temperature was continuously monitored and maintained at 37 °C by a heating pad upon which the animal was positioned. To measure force produced by triceps surae in the sedated animals, the Achilles tendon was carefully cut and connected to a force transducer with a short string (FORT 1000, World Precision Instruments, FL, USA). Two stimulation electrodes (Monopolar EMG Needle Electrode 25mm x 27 g, Chalgren, London, UK) were inserted to stimulate the sciatic nerve to elicit nerve-stimulated contractile responses of the triceps surae. EMG electrodes (subdermal needle electrodes, Cadwell Kennewick, WA, USA) were placed subcutaneously with the active recording electrode placed distal to the knee joint over the proximal portion of the triceps surae muscle and the reference electrode was placed over the metatarsal region of the foot. The acquisition program (Signal version 6.4, Cambridge Electronics Design Ltd, Micro 1401, Cambridge, UK) was used to control stimulation, delivered by an isolated stimulator (Isostim 01D NPI electronics, DE).

COMBINED PYRIDOSTIGMINE AND CLC-1 INHIBITOR ADMINISTRATION TO MG RATS In rats with severe MG symptoms, the effects of CLC-1 inhibitor and pyridostigmine bromide (Mestinon®) alone or in combination were assessed on grip strength. Within 2-4 days after reaching disease score of 2, MG rats were allocated to treatment groups such that grip strength relative to bodyweight ratio was comparable between groups. The study was blinded to both the experimenter and during subsequent data analysis. Animals were subjected to grip strength test before compound administration, as described above and then dosed per oral with either 0.375 mg/kg pyridostigmine bromide (Mestinon®) (CAS-no 101-26-8), 20 mg/kg NMD670 or a combination of both pyridostigmine and NMD670. Grip strength was tested 45 minutes post dosing. The average bodyweight across the groups before dosing was 190 \pm 9 grams, and the average grip strength before dosing was 1165 \pm 102 grams. The change in grip strengths after dosing was calculated for individual animals relative to the grip strength obtained prior to administration of compound.

IN VIVO 14-DAY DOSING OF NMD670 IN MG RATS Sixteen (16) rats with an MG score of 2 were allocated to the study and stratified to one of two treatment groups (vehicle vs. NMD670, 8 rats per group). Stratification was based on running performance (rotarod) and grip strength performance to obtain similar average starting points for the two groups. Grip strength and running performance were measured prior to treatment (day 0) and on days 1, 4, 7, 9, 11 and 14 during treatment (see details in *Supplementary Methods*). The treatment was administered by oral gavage. Dosing was twice daily with 20 mg/kg NMD670 (40 mg/kg BID) or vehicle (sterile water) for 14 days unless subjected to premature termination due to reaching humane end-points. The dose solutions for the treatment groups were blinded. Thus, experimenters were blinded, and full analysis of data and statistics were concluded before unblinding the data. Plasma samples were obtained on days 0, 1 and 14, with muscle samples obtained on day 14 or at termination.

ACETYLCHOLINE RECEPTOR ANTIBODY IN BLOOD SAMPLES, BIO-ANALYSIS, AND LC-MS/MS To determine ACh receptor antibody titer in blood samples from MG rats a method using displacement of ¹²⁵I- α -bungarotoxin was used as described elsewhere²⁷ and in *Supplementary Methods*. Concentrations of NMD670 were determined in both plasma and muscles from MG rats. For experiments involving anaesthetized rats, the blood samples were drawn using jugular vein catheter while for experiments with rats that were not anesthetized the blood samples were drawn by sublingual bleeding. Plasma samples were collected in K₃EDTA coated 0.5 mL tubes (Sarstedt, DE). Muscle samples were obtained by surgically removing approx. 250 mg muscle tissue from the triceps surae, after the animal had been sacrificed, then immediately SNAP-frozen in liquid nitrogen. Detailed bioanalysis is described in *Supplementary Methods*.

PASSIVE TRANSFER MYASTHENIA GRAVIS MODEL WITH MAB35 Production and handling of passive immunization MG rat model was covered by license number 2014-15-0201-0382. Cages were maintained in ventilated racks under temperature (20 to 22 °C) and humidity (\pm 55%) control, under a 12-h light/12-h dark cycle with food and water provided ad libitum. Four-week-old Wistar rats were injected intraperitoneal with

mAb35 antibodies to induce MG-like signs (0.5 mg/kg of bodyweight, GeneTex International, Hsinchu, TW).¹⁶ Animals were monitored for signs of muscle weakness and fatigue in the time after injection and subjected to rotarod test 17 hours after injection of mAb35 antibodies. If animals displayed reduced albeit consistent performances on rotarod on two consecutive occasions (2 hours apart) they were included into the study and received intraperitoneal injections of either vehicle (n = 6) or 30 mg/kg NMD071 (n = 4) (20 mg/mL dose solution). After administration, the rats were again subjected to test on rotarod every 2 hours for 6 hours. Details on how the rotarod tests were performed are provided in *Supplementary Methods*. Animals were euthanized at the end of the protocol or earlier if they displayed overt signs of discomfort, lack of mobility, labored ventilation, or sign of cyanosis.

DATA ACQUISITION AND STATISTICAL ANALYSIS For pre-clinical studies, data was sampled using interfaces from Cambridge Electronic Design and Signal 6.4 software (CED, Cambridge, UK) or Cadwell Sierra Summit EMG unit (Cadwell laboratories, Kennewick, WA, USA). Data was analyzed statistically using GraphPad Prism version 9 (GraphPad Software, San Diego CA, USA) applying one-way or two-way ANOVA with Tukey's multiple comparison test or students t-test, paired or unpaired were appropriate. A p-value < 0.05 was considered statistically significant. Values are mean \pm SEM and n represents number of animals/muscles or muscle fibers used depending on the specific experiment. All statistics are detailed in *Supplementary Table 1* with reference to the figure it relates to.

METHODS – CLINICAL

STUDY DESIGN The study was a randomised, double-blind, placebo-controlled, three-way cross-over comparison of two single oral doses of NMD670 and placebo in men and women with stable symptomatic MG. The primary purpose was to evaluate safety and tolerability of NMD670 in MG patients. Assessment of pharmacokinetic (PK) parameters was included as secondary outcome and investigation of pharmacodynamic (PD) effects was included as exploratory outcome.

The study was conducted at Centre for Human Drug Research (CHDR), Leiden, The Netherlands and in accordance with International

Conference of Harmonization Good Clinical Practice and the Declaration of Helsinki. Before study initiation, approval was obtained from Ethics Committee Stichting 'Beoordeling Ethiek Biomedisch Onderzoek', The Netherlands, and before any study procedures, each patient provided written informed consent. The study was registered in the Dutch Trial Registry (NTR) under number: NL8692.

At three separate visits, patients received either a single dose of NMD670 400 mg or 1200 mg, or placebo. The treatment order was randomized (see Supplementary Figure 7). For each subject, the total study duration was up to 66 days and included five visits: screening, three treatment visits (each consisting of 3 days with a washout period of at least 7 days between visits) and a follow-up visit. On the three treatment visits, subjects were admitted to the study unit on Day -1 for baseline eligibility checks. On Day 0, subjects were dosed in the morning. Baseline and post-dose PK and PD measurements were performed at standardized time points. Subjects stayed overnight at CHDR and were discharged in the following day on Day 1, approximately 24 hours post-dose. On each treatment occasion, patients taking pyridostigmine were asked to refrain from their regular dose from 14 hours before dosing placebo or NMD670 and until after the final PD assessment. The follow-up visit was performed 7 to 10 days after last dose.

PARTICIPANTS Eligible patients included males and females above 18 years of age and with a body mass index (BMI) between 18 and 34 kg/m², inclusive at screening, and a minimum weight of 50 kg. Patients were required to have a diagnosis of myasthenia gravis, MGFA class I, II, III or IVa, based on characteristic muscle weakness and a positive AChR or muscle-specific tyrosine kinase (MUSK) antibody test. Subjects with MGFA 0 using pyridostigmine were also allowed to participate, if muscle weakness was present when refraining from pyridostigmine (as assessed by a medical doctor based on an interview of the patient at screening). Patients using steroids should be using a stable dose of steroids for at least 1 month before dosing, and the dose of steroids should be expected to remain stable for the duration of the study. A detailed list of inclusion and exclusion criteria are available in Supplementary Materials.

OUTCOME MEASURES Safety and tolerability were assessed by adverse event (AE) monitoring, assessment of concomitant medication and

medical history, safety laboratory tests (blood chemistry, hematology, urinalyses, drugs of abuse, alcohol test, pregnancy test), vital signs, ECG, physical, and neurological examinations. In addition, muscle relaxation was tested (90-5% and 90-50% release times) using handgrip dynamometer (RS G200, Biometrics, Newport, UK) and wireless data transmitter (DataLite Pioneer – wso, Biometrics) with the aim to detect subclinical myotonia.²⁹

Plasma concentrations of NMD670 were analyzed (treated 1:1 (v/v) with water: Orthophosphoric Acid (100:2), using EDTA as an anticoagulant) by a validated method using liquid chromatography tandem mass spectrometry (LC-MS/MS) at Labcorp Early Development Laboratories Ltd, Harrogate, UK. All plasma samples were analyzed within the validated storage period. The validated range for NMD670 was 50-50000 ng/mL in plasma.

Pharmacodynamic effects were assessed by QMG and RNS. The QMG score for Disease Severity is a 13-item validated clinical outcome measure of sentinel muscle groups developed by the myasthenia gravis Foundation of America and is recommended for all prospective clinical trials in MG.³⁰⁻³² The items measure the following symptoms and signs: ptosis, diplopia, double vision, swallowing, speech (onset of dysarthria), percent predicted forced vital capacity, grip strength (2 items), arm muscle endurance (2 items), leg muscle endurance (2 items), and head lifting endurance. All items are scored on a scale of 0 to 3, and total scores range from 0 to 39; higher scores indicate greater disease severity. A 2-point change is considered clinically relevant in patients with mild to moderate severity (QMG total score <16).¹⁸ The absolute scores of the individual data were also available for analysis of continuous measurements.

Repetitive nerve stimulation was performed in accordance with previously published techniques.¹⁹⁻²¹ Briefly, CMAPs were recorded from nasalis muscle during RNS with a train of 10 supramaximal electrical stimuli at 5 Hz using a Medelec Synergy 11.0. The optimal stimulation site on the skin was identified using submaximal stimuli, after which the limit of supramaximal intensity was established. Decrement was defined as the percentage change in CMAP amplitude from stimulation 1-5.

DATA ACQUISITION AND STATISTICAL ANALYSIS The per protocol analyses were preceded by a blinded data review. All data were summarized using descriptive statistics.

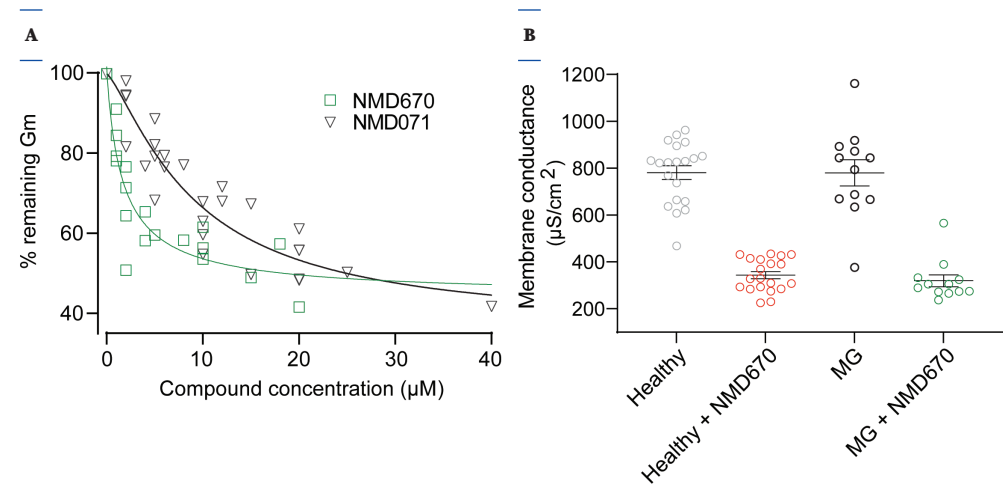
The number and frequency of treatment emergent adverse events (TEAEs) were summarized by MEDRA system organ class, preferred term, treatment, drug relatedness and severity for the safety population (participants that received at least 1 dose). A TEAE was defined as an adverse event observed after starting treatment, or up to 5 days (120 hours) after treatment. If a subject experienced an event both prior to and after starting administration of a treatment, the event was considered a TEAE (of the treatment) only if it worsened in severity (i.e., it was reported with a new start date) after starting administration of the specific treatment, and prior to the start of another treatment, if any.

Non-compartmental analysis of PK was performed using R (V4.0.3, R Core Team, Vienna, Austria) and the PKNCA package (v0.9.4).

Pharmacodynamic outcomes were analyzed with a repeated measures linear mixed effects model with treatment, time, treatment by time and visit as fixed factors and subject as random factor and time within subject by visit as repeated factor, and the baseline (pretreatment value) as covariate. As this was an exploratory study with no sample size calculation, no correction for multiple comparisons were performed. Post hoc responder analyses were performed to better characterize the PD data. For QMG total score, responders were defined as subjects showing improvement of 2 points or more with NMD670 versus placebo.

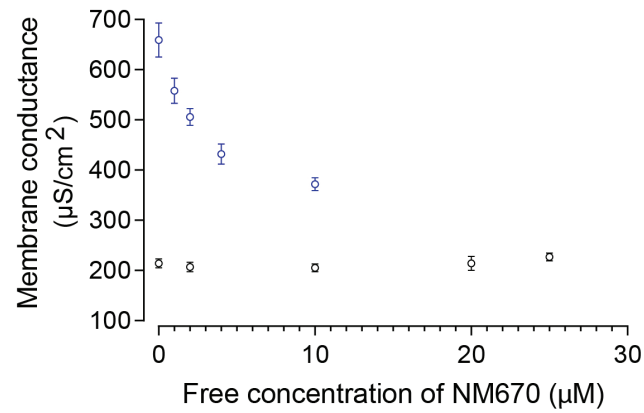
SUPPLEMENTARY MATERIAL

SUPPLEMENTARY FIGURE 1 Effect of NMD071 and NMD670 on CLC-1 function in soleus muscles from healthy rats and from MG rats.



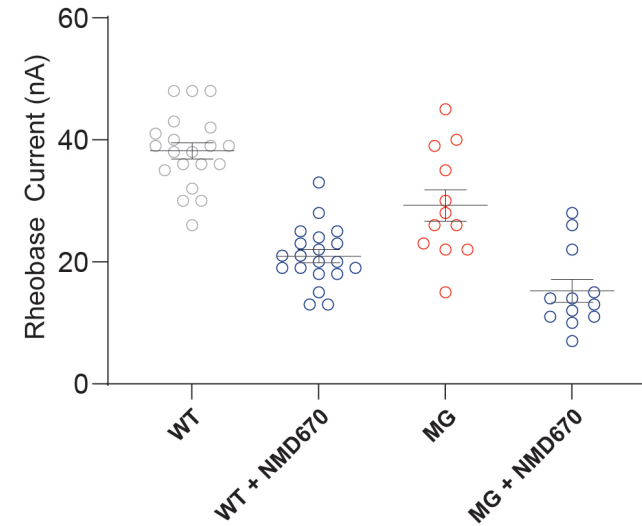
(A) The membrane conductance (Gm) measured in soleus muscle fibers from healthy rats before and, subsequently, at increasing concentrations of NMD670 (green, $n = 5$), or NMD071 (black $n = 7$). Gm was measured at several concentrations (usually 4) in each muscle. Data included in the plot is from all muscles for each compound. A four parameter Hill function with variable slope was fitted to extract an apparent affinity at 50% of the total observed reduction of Gm determined to be 1.71 μM for NMD670 and 9.18 μM for NMD071. (B) Membrane conductance in in soleus muscle fibers from healthy rats ($n = 20$) and from MG rats ($n = 12$) as the average Gm measured before (grey/black circles) and after addition of 20 μM NMD670 (red circles for healthy and green for MG). Black overlay bars show averages \pm SEM of groups. Addition of NMD670 significantly reduced both parameters in fibers from both healthy rats and from MG rats ($p < 0.05$).

SUPPLEMENTARY FIGURE 2 Effect of NMD670 on membrane conductance (Gm) with and without Cl⁻ in solution.



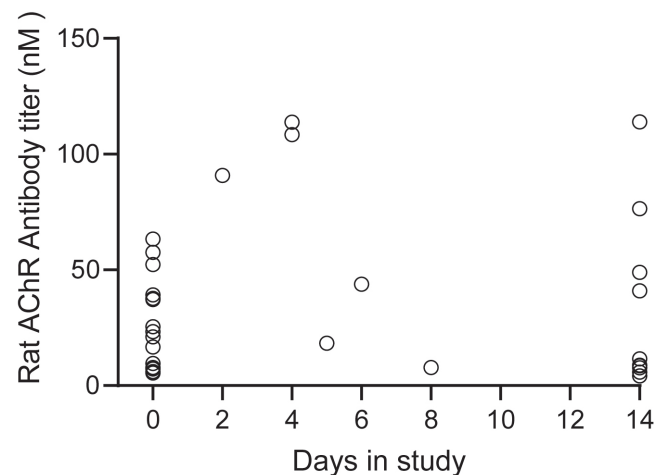
Average Gm ($\mu\text{S}/\text{cm}^2$) in fibers from isolated soleus muscle from healthy rats in the absence and presence of different concentrations of NMD670, under physiological conditions (blue circles) at 127 mM Cl⁻ in the bathing solution, and in the absence of Cl⁻ in the bathing solution (black circles). In the presence of Cl⁻ in the bathing solution, Gm was reduced with increasing concentration of NMD670 (0 to 10 μM), while in the absence of Cl⁻ there was no change in Gm at any concentration of NMD670. To avoid spontaneous contractions and thus movement of the muscle fibers in the absence of Cl⁻ in the bathing solution, 20 nM of the sodium channel inhibitor Tetrodotoxin (TTX) was added to the bathing solution.

SUPPLEMENTARY FIGURE 3 Effect of CLC-1 inhibition on skeletal muscle fiber excitability as evaluated from rheobase current in skeletal muscle fibers from healthy rats and from MG rats.



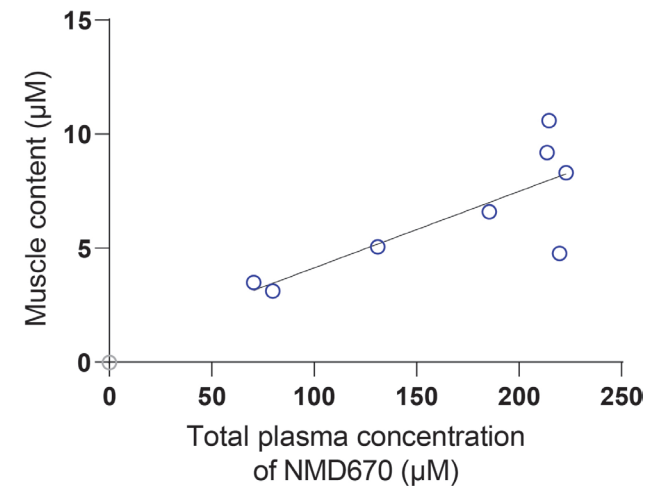
Rheobase current (nA) in soleus muscle fibers from healthy rats ($n = 20$) and from MG rats ($n = 12$) shown as the average rheobase current measured before (grey/red circles) and after addition of 20 μM NMD670 (blue circles). Black overlay bars show averages \pm SEM of groups. Addition of NMD670 significantly reduced rheobase current in muscle fibers from both groups of rats, see Supplementary Table 1 for details.

SUPPLEMENTARY FIGURE 4 Acetylcholine receptor antibody titer from immunized rats.



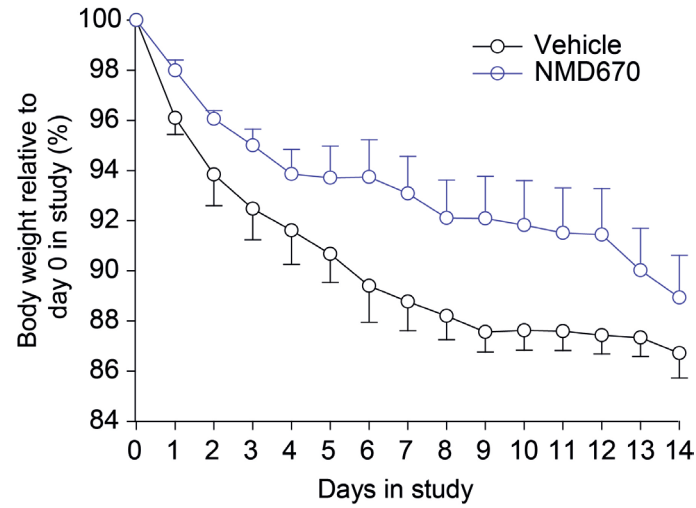
Antibody titer from the immunized rats (MG rats) included in a 14-day chronic dosing receiving vehicle or NMD670. The titer levels were determined from blood samples at day 0, and at the final day in study (some animals were euthanized before day 14 due to reaching humane endpoints). The global average for all animals at all timepoints was 35.2 ± 5.98 nM, ($n = 16$). The ACh-receptor antibody titer was not statistically significantly different between animals receiving NMD670 or vehicle, on day 0 or 14 (see Supplementary Table 1).

SUPPLEMENTARY FIGURE 5 Plasma concentration of NMD670 vs. muscle tissue concentration of NMD670 after 14 days of chronic dosing in actively immunized MG rats.



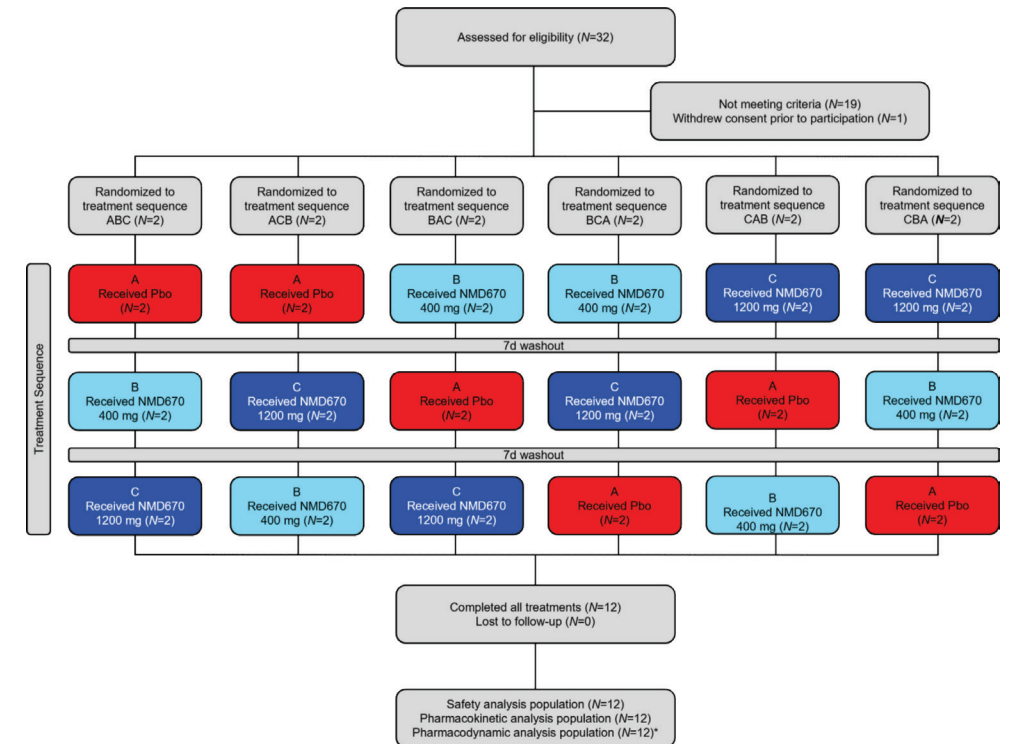
The total plasma and muscle concentration of NMD670 (in μM) from MG rats dosed chronically for 14 days at 40 mg/kg b.i.d (blue circles, $n = 8$) and vehicle-dosed animals (grey circles at origin, $n = 8$), measured by blood sample 1 hour after the final dose on day 14. The individual muscle concentrations of NMD670 have been plotted against the matching plasma concentrations of NMD670.

SUPPLEMENTARY FIGURE 6 Bodyweight of severely affected MG rats during 14-day chronic dosing study.

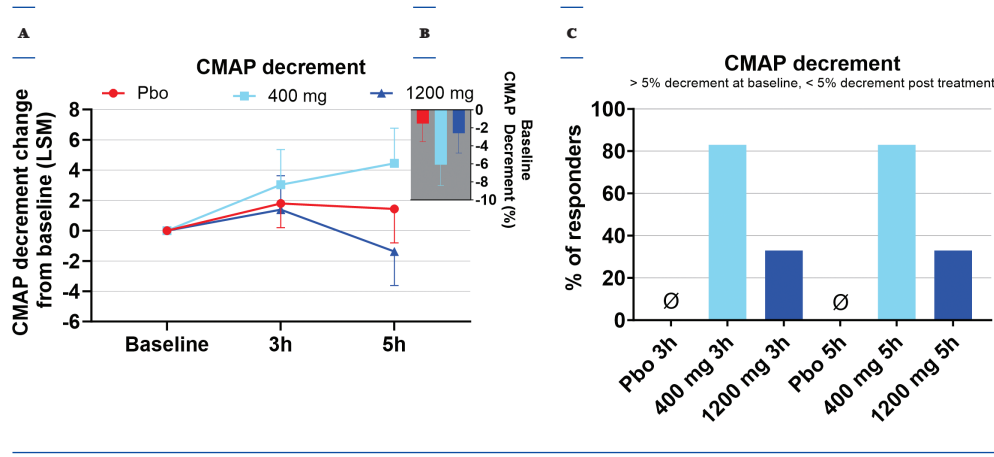


Bodyweight relative to the individual bodyweight at day 0 of study during 14-day chronic dosing in MG rats receiving vehicle (black lines/symbols) or 40 mg/kg b.i.d NMD670 (blue lines/symbols). Groups not significantly different at any timepoint (see Supplementary Table 1).

SUPPLEMENTARY FIGURE 7 A) placebo, B) NMD670 400mg, C) NMD670 1200mg. Two values were excluded from RNS analysis prior to database lock and unblinding of the data due to data quality issues; One was a baseline value in the NMD670 400mg treatment arm, the other was a post treatment value at 3hour time point in the Pbo treatment arm. Both post treatment values were missing from 1 subject in the 1200mg treatment arm as measurements were erroneously not performed.



SUPPLEMENTARY FIGURE 8 Panel A) shows the a priori analyses of CMAP decrement from stimulation I-5 using repetitive nerve stimulation at 5 Hz. Panel B) shows baseline CMAP decrement. Panel C) shows the post hoc responder analyses of the CMAP decrement. For A), data are least square means \pm SEM. For B), data are mean \pm SEM. For C), data are percent of subjects responding to treatment. n = 12 except for baseline in NMD670 400mg and at 3hr in placebo treatment arms and at 3h and 5h in NMD670 1200mg treatment arm where n=11 (see also Supplementary Figure 7)



SUPPLEMENTARY TABLE I A summary of the statistics, with reference to the figure it relates to.

Figure and number of animals or muscles/muscle fibers used	Statistical Analysis	Post hoc tests	Mean \pm SEM
2B EPP amplitude MG control (n = 68) MG + NMD670 (n = 82)	Two-way ANOVA; EPP amplitude in mV EPP number: F (29, 4440) = 11.54, p < 0.001 Group: F (1, 4440) = 493.8 p < 0.0001 EPP number x Group: F (29, 4440) = 0.8715 p = 0.6638	For all timepoints (EPP number 1 to 30, except number 12 and 17: MG vs. MG + NMD670 P < 0.05 At EPP 12 p = 0.0949 At EPP 17 p = 0.0665	Data available upon request
2D AP generation success MG (n = 74) MG + NMD670 (n = 74)	Two-way ANOVA; AP Success (0 or 1) AP number: F (29, 4205) = 10.93, p < 0.001 Group: F (1, 145) = 54.77, p < 0.001 EPP number x Group: F (145, 4205) = 30.80 p < 0.001	For AP number 1 to 6 MG vs. MG + NMD670: N.S. For AP number 7 to 30 MG vs. MG + NMD670: P < 0.01	Data available upon request
2E Increase in muscle force in ex vivo soleus muscle from MG rats. Soleus (n = 14) EDL (n = 14) Diaphragm (n = 11)	Students T-test (paired) Effect of Treatment, before vs. after. Before = 100.	Soleus P = 0.0001 EDL P = 0.0001 Diaphragm P = 0.0038	Soleus after 199 \pm 17.09 EDL 235.1 \pm 25.03 Diaphragm 120.2 \pm 5.04
2H Average force in Triceps surae muscle in situ from MG rats, before and after CLC-1 inhibition with NMD670. n values were (4, 3, 6, 5, 5, 3 and 2), for (2, 5, 10, 20, 40, 60 and 120 mg/kg), respectively	Two-way ANOVA; % force of healthy rat Dose (mg/kg): F (6, 42) = 18.56, p < 0.001 Group(pre/post): F (1, 42) = 78.28, p < 0.001 Dose x Group: F (6, 42) = 7.337 p < 0.001	Post hoc tests, Difference between pre and post treatment in the group, for each tested dose (in mg/kg) 2 P > 0.9999 5 P = 0.9999 10 P = 0.5066 20 P = 0.0061 40 P < 0.0001 60 P < 0.0001 120 P < 0.0001	Dose (mg/kg) pre post 2 90.1 \pm 2.9 92.2 \pm 3.1 5 81.5 \pm 7.2 85.15 \pm 7.9 10 70.3 \pm 10.1 82.2 \pm 6.8 20 36.4 \pm 9.7 63.6 \pm 4.6 40 42.6 \pm 13.6 89.0 \pm 20.7 60 11.1 \pm 6.4 67.4 \pm 32.3 120 14.3 \pm 8.4 80.2 \pm 1.3
2I Change in grip strength (force), after administration of test article.	One-way ANOVA Force as % increase in grips strength Treatment (between groups), F (3, 65) = 5.591 p = 0.0018.	Post hoc tests, Difference between treatment groups, Group 1 = vehicle (n = 35), group 2 = 0.375 mg/kg Pyridostigmine (n = 10), group 3 20 mg/kg NMD670 (n = 17), group 4 0.375 mg/kg Pyridostigmine and 20 mg/kg NMD670 (n = 5) Group 1 vs. group 2 P = 0.7634 Group 1 vs. group 3 P = 0.0154 Group 1 vs. group 4 P = 0.01 Group 2 vs. group 3 P = 0.4338 Group 2 vs. group 4 P = 0.1669 Group 3 vs. group 4 P = 0.5962	Change in Force Group 1 0.6 \pm 1.7 % Group 2 5.3 \pm 3.8 % Group 3 14.5 \pm 5.1 % Group 4 24.2 \pm 11.8 %

Figure and number of animals or muscles/muscle fibers used	Statistical Analysis	Post hoc tests	Mean ± SEM
2J Grip Strength (average) relative to individual bodyweight in 14-day study (MG rats). Last observation was carried forward in both groups.	Two-way RM ANOVA; Average Grip strength relative to Body Weight Time: F (6, 84) = 0.52, p=0.7920 Group (treatment): F (1, 14) = 8.28, p=0.0122 Time x Group (treat): F (6, 84) = 1.70 p = 0.1304	Difference between treatment groups, Group 1 = vehicle (n = 8) and group 2 = NMD670 (n = 8), at time: Day # p-value 0 P > 0.9999 1 P = 0.1225 4 P = 0.0629 7 P = 0.7266 9 P = 0.2100 11 P = 0.0206 14 P = 0.1010	Day # Gi G2 0 4.7 ± 0.29 4.8 ± 0.17 1 4.3 ± 0.24 5.5 ± 0.46 4 4.1 ± 0.29 5.4 ± 0.38 7 4.3 ± 0.38 4.9 ± 0.26 9 3.9 ± 0.30 5.0 ± 0.27 11 3.9 ± 0.33 5.4 ± 0.41 14 3.9 ± 0.33 5.1 ± 0.47 Day # Healthy Rat 0 7.4 ± 0.25 1 7.4 ± 0.23 4 7.3 ± 0.23 7 7.1 ± 0.25 9 7.2 ± 0.25 11 7.1 ± 0.25 14 6.9 ± 0.21
2K Rotarod performance, Latency to fall in 14-day study (MG rats). Last observation was carried forward in both groups.	Two-way RM ANOVA; Average Grip strength relative to Body Weight Time: F (6, 42) = 6.124, p = 0.0001 Group (treatment): F (1, 7) = 1.156, p=0.3179 Time x Group (treat): F (6, 42) = 0.7728 p = 0.5957	Difference between treatment groups, Group 1 = vehicle (n = 8) and group 2 = NMD670 (n = 8), at time: Day # p-value 0 P = 0.9478 1 P > 0.9999 4 P = 0.4613 7 P = 0.7852 9 P = 0.6753 11 P = 0.0353 14 P = 0.8122	Day # Gi G2 0 20.9 ± 6.3 28.5 ± 7.3 1 37.9 ± 15.2 38.4 ± 8.7 4 22.8 ± 7.6 37.8 ± 10.1 7 18.0 ± 5.9 29.1 ± 8.8 9 15.0 ± 6.0 27.5 ± 9.1 11 10.3 ± 3.6 35.5 ± 12.6 14 8.2 ± 2.6 19.0 ± 5.7
2L Rotarod performance in Passive transfer Mab35 MG animals over time.	Two-way RM ANOVA. Time: F (5, 50) = 30.77, p<0.0001 Group (treatment): F (1, 10) = 20.35, p=0.0009 Time x Group: F (5, 50) = 10.22 p<0.0001	Difference between treatment groups, Group 1 = vehicle (n = 8) and group 2 = NMD670 (n = 4), at time: Time # p-value -4 P > 0.9999 -2 P = 0.9263 0 P = 0.6628 2 P = 0.0002 4 P < 0.0001 6 P < 0.0001	Day # Gi G2 -4 300 ± 0 300 ± 0 -2 157.9 ± 21.5 184.3 ± 14.0 0 145.8 ± 23.9 185.2 ± 8.7 2 87.13 ± 19.8 215.3 ± 32.9 4 60.5 ± 16.9 210.0 ± 11.3 6 39.8 ± 14.6 214.5 ± 15.6

Figure and number of animals or muscles/muscle fibers used	Statistical Analysis	Post hoc tests	Mean ± SEM
SUPPL. FIGURE 1B Membrane conductance from muscle fibers from MG rats.	One-way ANOVA Membrane conductance ($\mu\text{S}/\text{cm}^2$), average from muscles. Treatment (between groups), F (5, 60) = 69.47 p < 0.0001.	Post hoc tests, Difference between treatment groups, Group 1 = HEALTHY (n = 20), group 2 = HEALTHY + NMD670 (n = 20), group 3 = MG (n = 12), group 4 = MG + NMD670 (n = 12). Group 1 vs. group 2 P < 0.0001 Group 1 vs. group 3 P = 0.9999 Group 1 vs. group 4 P < 0.0001 Group 2 vs. group 3 P < 0.0001 Group 2 vs. group 4 P = 0.9533 Group 3 vs. group 4 P < 0.0001	Group 1: 780.8 ± 29.56 Group 2: 343.0 ± 15.54 Group 3: 779.7 ± 55.87 Group 4: 319.3 ± 25.03
SUPPL. FIGURE 2 Rheobase current from muscle fibers from MG rats.	One-way ANOVA Rheobase current (nA), average from muscles. Treatment (between groups), F (5, 60) = 40.29 p < 0.0001.	Post hoc tests, Difference between treatment groups, Group 1 = HEALTHY (n = 20), group 2 = HEALTHY + NMD670 (n = 20), group 3 = MG (n = 12), group 4 = MG + NMD670 (n = 12). Group 1 vs. group 2 P < 0.0001 Group 1 vs. group 3 P = 0.0017 Group 1 vs. group 4 P < 0.0001 Group 2 vs. group 3 P < 0.0041 Group 2 vs. group 4 P = 0.0809 Group 3 vs. group 4 P < 0.0001	Group 1: 38.2 ± 1.343 Group 2: 20.95 ± 1.08 Group 3: 29.25 ± 2.56 Group 4: 15.35 ± 1.90
SUPPL. FIGURE 4 Acetylcholine receptor antibody titer from immunized rats, in 14 day chronic dosing study.	Multiple T-tests, antibody titer count.	Day 0 P = 0.2212 Day 14 P = 0.5033	Vehicle: 32.29 ± 8.29 NMD670: 19.89 ± 4.78 NMD670: 44.77 ± 24.99 NMD670: 24.63 ± 11.76
SUPPL. FIGURE 6 Body Weight, set to 100% for each individual at day 0 in 14-day study (MG rats). Last observation was carried forward in both groups.	Two-way ANOVA; Body Weight Time: F (14, 196) = 25.88, p<0.0001 Group (treatment): F (1, 14) = 0.8664, p=0.3677 Time x Group (treat): F (14, 196) = 0.5894 p = 0.8716	Treatment groups N.S. (group 1 = vehicle (n = 8), group 2 = NMD670 (n = 8)) at any timepoint.	Day # Gi G2 0 100 ± 0 100 ± 0 1 96.3 ± 0.6 97.9 ± 0.4 2 94.4 ± 1.2 96.2 ± 0.4 3 93.3 ± 1.3 95.0 ± 0.7 4 92.8 ± 1.7 93.9 ± 1.0 5 92.1 ± 1.7 93.7 ± 1.3 6 90.8 ± 1.8 93.8 ± 1.5 7 90.3 ± 1.8 93.1 ± 1.5 8 89.8 ± 1.8 92.1 ± 1.5 9 89.4 ± 1.9 92.1 ± 1.7 10 89.5 ± 2.0 91.8 ± 1.8 11 89.5 ± 2.0 91.5 ± 1.8 12 89.2 ± 1.9 91.4 ± 1.8 13 89.3 ± 2.1 90.0 ± 1.7 14 88.8 ± 2.3 88.9 ± 1.7

REFERENCES

- 1 Patrick J, Lindstrom J. Autoimmune response to acetylcholine receptor. *Science*. 1973;180(4088):871-872. doi:10.1126/science.180.4088.871
- 2 Twork S, Wiesmeth S, Klewer J, Pöhlau D, Kugler J. Quality of life and life circumstances in German myasthenia gravis patients. *Health and quality of life outcomes*. 2010;8:129. doi:10.1186/1477-7525-8-129
- 3 Howard JF, Bresch S, Genge A, et al. Safety and efficacy of zilucoplan in patients with generalised myasthenia gravis (RAISE): a randomised, double-blind, placebo-controlled, phase 3 study. *The Lancet Neurology*. 2023;22(5):395-406. doi:10.1016/S1474-4422(23)00080-7
- 4 Bril V, Druzdź A, Grosskreutz J, et al. Safety and efficacy of rozanolixizumab in patients with generalised myasthenia gravis (MycarinG): a randomised, double-blind, placebo-controlled, adaptive phase 3 study. *The Lancet Neurology*. 2023;22(5):383-394. doi:10.1016/S1474-4422(23)00077-7
- 5 Vu T, Meisel A, Mantegazza R, et al. Terminal Complement Inhibitor Ravulizumab in Generalized Myasthenia Gravis. *NEJM Evidence*. 2022;1(5):1-12. doi:10.1056/EVIDO2100066
- 6 Howard JF, Bril V, Vu T, et al. Safety, efficacy, and tolerability of efgartigimod in patients with generalised myasthenia gravis (ADAPT): a multicentre, randomised, placebo-controlled, phase 3 trial. *The Lancet Neurology*. 2021;20(7):526-536. doi:10.1016/S1474-4422(21)00159-9
- 7 Howard JF, Utsugisawa K, Benatar M, et al. Safety and efficacy of eculizumab in anti-acetylcholine receptor antibody-positive refractory generalised myasthenia gravis (REGAIN): a phase 3, randomised, double-blind, placebo-controlled, multicentre study. *The Lancet Neurology*. 2017;16(12):976-986. doi:10.1016/S1474-4422(17)30369-1
- 8 Gilhus NE, Verschuuren JJ. Myasthenia gravis: subgroup classification and therapeutic strategies. *The Lancet Neurology*. 2015;14(10):1023-1036. doi:10.1016/S1474-4422(15)00145-3
- 9 Remijn-Nelissen L, Verschuuren JJGM, Tannemaat MR. The effectiveness and side effects of pyridostigmine in the treatment of myasthenia gravis: a cross-sectional study. *Neuromuscular disorders : NMD*. 2022;32(10):790-799. doi:10.1016/j.nmd.2022.09.002
- 10 Riisager A, de Paoli FV, Yu WP, Pedersen TH, Chen TY, Nielsen OB. Protein kinase C-dependent regulation of ClC-1 channels in active human muscle and its effect on fast and slow gating. *The Journal of physiology*. 2016;594(12):3391-3406. doi:10.1113/jp271556
- 11 Pedersen TH, Macdonald WA, Broch-Lips M, Halldorsdottir O, Bækgaard Nielsen O. Chloride channel inhibition improves neuromuscular function under conditions mimicking neuromuscular disorders. *Acta Physiologica*. 2021;(May):1-14. doi:10.1111/apha.13690
- 12 Riisager A, Duehmke R, Nielsen OB, Huang CL, Pedersen TH. Determination of cable parameters in skeletal muscle fibres during repetitive firing of action potentials. *The Journal of physiology*. 2014;592(20):4417-4429. doi:10.1113/jphysiol.2014.280529
- 13 Elmqvist D, Quastel DM. A quantitative study of end-plate potentials in isolated human muscle. *The Journal of Physiology*. 1965;178(3):505-529. doi:10.1113/jphysiol.1965.sp007639
- 14 Elmqvist D, Hofmann WW, Kugelberg J, Quastel DMJ. An electrophysiological investigation of neuro-muscular transmission in myasthenia gravis. *The Journal of Physiology*. 1964;174(3):417-434. doi:10.1113/jphysiol.1964.sp007495
- 15 Gilhus NE, Tzartos S, Evoli A, Palace J, Burns TM, Verschuuren JJGM. Myasthenia gravis. *Nature Reviews Disease Primers*. 2019;5(1):1-19. doi:10.1038/s41572-019-0079-y
- 16 Tzartos S, Hochschwender S, Vasquez P, Lindstrom J. Passive transfer of experimental autoimmune myasthenia gravis by monoclonal antibodies to the main immunogenic region of the acetylcholine receptor. *Journal of Neuroimmunology*. 1987;15(2):185-194. doi:10.1016/0165-5728(87)90092-0
- 17 Koch MC, Steinmeyer K, Lorenz C, et al. The skeletal muscle chloride channel in dominant and recessive human myotonia. *Science (New York, NY)*. 1992;257(5071):797-800.
- 18 Katzberg HD, Barnett C, Merckes ISJ, Bril V. Minimal clinically important difference in myasthenia gravis: outcomes from a randomized trial. *Muscle & nerve*. 2014;49(5):661-665. doi:10.1002/MUS.23988
- 19 Niks EH, Badrising UA, Verschuuren JJ, Van Dijk JG. Decremental response of the nasalis and hypothenar muscles in myasthenia gravis. *Muscle & nerve*. 2003;28(2):236-238. doi:10.1002/MUS.10411
- 20 Ruys-Van Oeyen AEWM, Van Dijk JG. Repetitive nerve stimulation of the nasalis muscle: technique and normal values. *Muscle & nerve*. 2002;26(2):279-282. doi:10.1002/MUS.10201
- 21 Schumm F, Brinkmann A, Fateh-Moghadam A. Antibody-controlled cytostatic treatment of malignant thymoma with accompanying myasthenia gravis. *Deutsche Medizinische Wochenschrift*. 1984;109(33):1244-1246. doi:10.1055/s-2008-1069357
- 22 Killian JM, Wilfong AA, Burnett L, Appel SH, Boland D. Decremental motor responses to repetitive nerve stimulation in ALS. *Muscle & Nerve*. 1994;17(7):747-754. doi:10.1002/mus.880170708
- 23 Amandusson Å, Elf K, Grindlund ME, Punga AR. Diagnostic Utility of Repetitive Nerve Stimulation in a Large Cohort of Patients with Myasthenia Gravis. *Journal of Clinical Neurophysiology*. 2017;34(5):400-407. doi:10.1097/WNP.0000000000000398
- 24 Jackson K, Parthan A, Lauher-Charest M, Broderick L, Law N, Barnett C. Understanding the Symptom Burden and Impact of Myasthenia Gravis from the Patient's Perspective: A Qualitative Study. *Neurology and Therapy*. 2022;12(1):107-128. doi:10.1007/s40120-022-00408-x
- 25 Arnold WD, Severyn S, Zhao S, et al. Persistent neuromuscular junction transmission defects in adults with spinal muscular atrophy treated with nusinersen. *BMJ Neurology Open*. 2021;3(2):e000164. doi:10.1136/bmjno-2021-000164
- 26 Losen M, Martinez-Martinez P, Molenaar PC, et al. Standardization of the experimental autoimmune myasthenia gravis (EAMG) model by immunization of rats with Torpedo californica acetylcholine receptors-Recommendations for methods and experimental designs. *Experimental Neurology*. 2015;270:18-28. doi:10.1016/j.expneurol.2015.03.010
- 27 Lazaridis K, Baltatzidi V, Trakas N, Koutroumpi E, Karandreas N, Tzartos SJ. Characterization of a reproducible rat EAMG model induced with various human acetylcholine receptor domains. *Journal of Neuroimmunology*. 2017;303:13-21. doi:10.1016/J.JNEUROIM.2016.12.011
- 28 Pedersen TH, Riisager A, de Paoli FV, Chen TY, Nielsen OB. Role of physiological ClC-1 Cl- ion channel regulation for the excitability and function of working skeletal muscle. *The Journal of general physiology*. 2016;147(4):291-308. doi:10.1085/jgp.201611582
- 29 Statland JM, Bundy BN, Wang Y, et al. A quantitative measure of handgrip myotonia in non-dystrophic myotonia. *Muscle and Nerve*. 2012;46(4):482-489. doi:10.1002/mus.23402
- 30 Barohn RJ, Mcintire D, Herbelin L, Wolfe GI, Nations S, Bryan WW. Reliability Testing of the Quantitative Myasthenia Gravis Score. *Annals of the New York Academy of Sciences*. 1998;841(1 MYASTHENIA GR):769-772. doi:10.1111/j.1749-6632.1998.tb11015.x
- 31 Jaretzki A, Barohn RJ, Ernststoff RM, et al. Myasthenia gravis: recommendations for clinical research standards. Task Force of the Medical Scientific Advisory Board of the Myasthenia Gravis Foundation of America. *Neurology*. 2000;55(1):16-23. doi:10.1212/WNL.55.1.16
- 32 Bedlack R.S, Simel D.L, Bosworth H sdb. myasthenia gravis score : Assessment of responsiveness and. *Neurology*. 2005;64:1968-1970.
- 33 del Castillo J, Katz B. Quantal components of the end-plate potential. *The Journal of Physiology*. 1954;124(3):560-573. doi:10.1113/jphysiol.1954.sp005129



CHAPTER 7

FIRST IN CLASS CLC-I INHIBITOR IMPROVES SKELETAL MUSCLE FUNCTION IN ANIMAL MODELS AND PATIENTS WITH MYASTHENIA GRAVIS

**THIS CHAPTER (PAGES 164 TO 203) IS SUBJECT TO AN
EMBARGO AND IS THEREFORE NOT INCLUDED IN THIS FILE**

Martin Skov^{1*}, Titia Q. Ruijs^{2,3*}, Thomas S. Grønnebak¹, Marianne Skals¹, Anders Riisager¹,
Jeppe Blichfeldt Winther¹, Kamilla Løhde Tordrup Dybdahl¹, Anders Findsen¹,
Jeanette Jeppesen Morgen¹, Nete Huus¹, Martin Broch-Lips¹, Ole Bækgaard Nielsen^{1,2},
Catherine M.K.E. de Cuba^{2,3}, Jules A.A.C. Heuberger², Marieke L. de Kam²,
Martijn Tannemaat³, Jan Verschuuren³, Lars J. S. Knutsen¹, Nicholas M. Kelly¹,
Klaus Gjervig Jensen¹, William David Arnold⁵, Arthur H. Burghes^{6,7}, Claus Olesen^{1,4},
Jane Bold¹, Thomas K. Petersen¹, Jorge A. Quiroz¹, John Hutchison¹, Eva R. Chin¹,
Geert Jan Groeneveld^{2,3}, Thomas H. Pedersen^{1,4}. *Shared first author

1. NMD Pharma A/S, Aarhus N, DK
2. Centre for Human Drug Research, Leiden, NL
3. Leiden University Medical Centre, Leiden, NL
4. Aarhus University, Department of Biomedicine, Aarhus C, DK
5. NextGen Precision Health, University of Missouri, Columbia, USA
6. Department of Biological Chemistry and Pharmacology, The Ohio State University Wexner Medical Center, Columbus, USA
7. Department of Neurology, Neuromuscular Division, The Ohio State University Wexner Medical Center, Columbus, USA

The background of the page is a light blue color, heavily textured with numerous small, dark blue ink splatters and larger, irregular blue blotches. Scattered across this background are several dried, pressed leaves. The leaves are mostly light brown or tan in color, showing a clear, intricate network of veins. Some leaves are fully visible, while others are partially obscured or overlapping. The overall aesthetic is artistic and somewhat ethereal.

CHAPTER 8

DISCUSSION AND CONCLUSIONS

Abnormalities in cell excitability can be found in multiple neurological and neuromuscular disorders, such as epilepsy;¹ amyotrophic lateral sclerosis (ALS);²⁻⁶ and myotonia congenita.⁷ Excitability is driven by voltage- and neurotransmitter-gated ion channels.^{8,9} Pharmacological modulation of these ion channels is therefore promising as treatment for excitability-related diseases.⁸ In early phase drug development, the use of biomarkers for pharmacodynamic effects in healthy subjects and first-in-patient studies is pivotal.¹⁰ In this thesis I describe the potential of three measures of excitability to detect pharmacodynamic effects of ion channel modulators: transcranial magnetic stimulation (TMS) combined with electromyography (EMG) and electroencephalography (EEG), nerve excitability threshold tracking (NETT), and muscle velocity recovery cycles (MVRC). We used TMS-EMG/EEG to evaluate effects on cortical excitability; NETT to assess peripheral nerve excitability; and MVRC to explore muscle cell excitability. Firstly, we tested these measurements in proof-of-concept studies using registered drugs known to influence excitability. These studies were used to explore if the measurements are sensitive to drug-induced changes in excitability, and the test-retest variability and feasibility to apply them in the context of a clinical study in healthy subjects were evaluated. After validation of the methods, we used the measurements in early phase clinical drug studies with novel drug candidates. In the following discussion the implications of our findings for use of these methods as biomarkers in future drug development programs will be discussed: an evaluation of their general value as pharmacodynamic biomarkers for ion channel modulators; their feasibility for use in early phase drug studies; and finally, ideas for future research.

TRANSCRANIAL MAGNETIC STIMULATION

The development of a non-invasive biomarker for pharmacodynamic effects on cortical excitability is useful for clinical application and for drug development, especially in the context of epilepsy, where cortical hyperexcitability is an important disease factor.¹ The prospect of novel pharmacological treatments aimed to target cortical excitability, led us to implement TMS-EMG/EEG in a clinical study setting to validate it as pharmacodynamic biomarker. Firstly, we focused on the pharmacodynamic effects of registered antiepileptic drugs –levetiracetam and valproic acid– and benzodiazepine lorazepam, on TMS-EMG/EEG in healthy subjects, as

described in **CHAPTER 2**. We evaluated effects on single pulse (sp) and paired pulse (pp) TMS-EMG/EEG in a double-blind, placebo-controlled, four-way crossover study. Levetiracetam, valproic acid, and lorazepam decreased the motor-evoked potential (MEP) amplitude compared to placebo. Moreover, levetiracetam significantly increased TMS-evoked potential (TEP) component N45, and decreased N100.¹¹ The decrease in MEP amplitude – observed for all three study drugs – corresponds to inhibition of cortico-spinal excitability. We therefore concluded that TMS measures can detect general changes in excitability induced by these antiepileptic drugs, and that TMS biomarkers could be helpful in early phase drug development.

After the proof-of-concept study described above, we implemented TMS in an early phase drug study, to evaluate effects of TAK-653, a α -amino-3-hydroxy-5-methyl-4-isoxazolepropionic acid receptor (AMPA) -positive allosteric modulator, on TMS-EEG (**CHAPTER 3**). TAK-653 is a drug candidate under development for major depressive disorder. We found that 6 mg TAK-653 affected the TEP amplitude 60-70 ms after the TMS pulse. Although further research is needed to confirm these results, our findings indicate that TMS-EEG is sensitive to AMPAR modulation.

We conclude from these studies that TMS-EMG/EEG is feasible in small studies in the early phase of clinical drug development. The measurement is non-invasive and can be repeated multiple times before and after drug administration. However, the measurement also has limitations. It is challenging to perform reproducible TMS measurements, resulting in a relatively high variability in TMS outcome measures, particularly between individuals. This limitation may make it difficult to detect more subtle drug effects. The measurement is therefore most suitable for use in a cross-over design, rather than parallel (single- or multiple-ascending dose) studies. Furthermore, TMS-EMG endpoints provide an indirect measure of excitability and reflect general changes in cortico-spinal excitation or inhibition.¹² TMS-EMG could therefore be a valuable tool to demonstrate drug effects on general excitability, but this makes TMS-EMG less suitable to distinguish between different pharmacological mechanisms of action, or to highlight certain channel activity. TMS-EEG provides a more direct insight into the cortical response¹³ and may therefore be more useful for this purpose, however the physiology of the TEP response is still largely unknown. A third limitation is the lack of consensus within the TMS community when it comes to stimulation

methods (e.g. interstimulus intervals of interest) and analysis methods (e.g. artifact removal methods).¹⁴ This heterogeneity makes it difficult to compare results from different research groups.

In our opinion these limitations do not disqualify the use of TMS-EMG/EEG as pharmacodynamic biomarkers for proof-of-mechanism studies. Although the variability is relatively high, significant treatment effects on cortical excitability were detected at therapeutic dose levels for all tested compounds. Moreover, with further research and further measurement standardization, evaluation of TEPs may even prove to be useful for differentiating specific pharmacological mechanisms of action.

NERVE EXCITABILITY THRESHOLD TRACKING

We had two driving factors for the introduction of NETT as pharmacodynamic biomarker. Firstly, there is a considerable interest from the pharmaceutical industry in the development of non-addictive and safe analgesics, among which (selective subtype-specific) voltage-gated sodium channel (Na_v) blockers.¹⁵ Secondly, potassium channel activators, like retigabine, are of interest to lower increased nerve excitability in amyotrophic lateral sclerosis,¹⁶ and effects of retigabine have been demonstrated using NETT.¹⁷ Therefore, we decided to study whether pharmacological inhibition of Na_v conductance can be detected in healthy volunteers using NETT (**CHAPTER 4**). This was assessed in a randomized, double-blind, three-way crossover study, comparing effects of two registered Na_v channel blockers – mexiletine, and lacosamide – to placebo. Motor and sensory nerve excitability measurements were evaluated at multiple pre- and post-dose time points. We found that mexiletine and lacosamide significantly decrease motor and sensory nerve excitability, corresponding to their mechanism of action.¹⁸

Our results show that NETT can detect (subtle) drug-induced changes in motor and sensory nerve excitability, with significant dose-effect relationships, even in a small group of healthy subjects. Furthermore, the inter- and intra-subject variability of the NETT endpoints is low- an important characteristic of a valuable pharmacodynamic biomarker. We conclude that NETT can be a useful tool in the clinical development of novel Na_v channel modulators, and potentially other modulators of (peripheral nerve-specific) ion channels. A general limitation of NETT (as well as TMS, and MVRC) is that it requires specialized equipment

and trained staff. However, the low variability in our study indicates that the measurement can be performed repeatably and in standardized manner. Furthermore, a possible limitation of NETT in the context of pain research, is that it measures excitability at the stimulation site¹⁹ (in this case the median nerve- a large, myelinated nerve), not the target site (unmyelinated nociceptive nerves).

Further research, with other modulating drugs, could help to create a channel-specific nerve excitability profile in healthy human subjects. If a distinct fingerprint of affected NETT variables could be linked to a specific channel, this could facilitate confirmation of target engagement in early phase drug studies with novel pharmaceuticals. For example, if nerve excitability profiles of Na_v subtype 1.6, 1.7, and 1.8 blockers are compared, findings may help determine target engagement and/or off-target effects. Moreover, further information may be gained by combining these findings with computational nerve modelling.²⁰

MUSCLE VELOCITY RECOVERY CYCLES

The need for a pharmacodynamic biomarker for drugs targeting muscle excitability arose when we were planning to perform a Phase I study with an inhibitor of muscle-specific chloride channel ClC-1 . The drug candidate (NMD670) was a first-in-class compound, designed to increase muscle excitability and subsequently improve muscle function in neuromuscular diseases such as myasthenia gravis (MG). MVRC, a measurement that estimates muscle cell excitability, had been shown to be sensitive to abnormalities in ClC-1 function in patients with myotonia congenita,⁷ which is caused by a congenital loss-of-function mutation of ClC-1 .²¹ Therefore, we decided to perform a proof-of-concept study to explore the potential of MVRC as pharmacodynamic biomarker for drugs targeting muscle excitability (**CHAPTER 5**). We compared effects of a registered drug known to influence muscle excitability by inhibition of Na_v channels (mexiletine)²²⁻²⁴ to placebo in a randomized, double-blind, two-way crossover study in healthy subjects. MVRC recordings were evaluated at baseline and at multiple post-dose time points. We found that MVRC could detect a decrease in muscle membrane excitability by mexiletine.²⁵ Our results indicate that MVRC is sensitive to pharmacodynamic effects, and we concluded that MVRC could potentially be a useful tool for our planned first-in-human study with ClC-1 inhibitor NMD670.

In **CHAPTER 6** we described the first administration of NMD670 to healthy human subjects. Safety, pharmacokinetics, and pharmacodynamics of NMD670 were assessed in male and female subjects in a randomized, double-blind, placebo-controlled, single- and multiple-ascending dose study. Pharmacodynamic effects were evaluated using MVRC. We found that NMD670 increased muscle excitability, as expected from the pharmacological mechanism of action. This was reflected in increased MVRC parameters of early supernormality, and clinical symptoms of myotonia at the highest dose levels. The effects on MVRC parameters were similar to findings in myotonia congenita,⁷ and therefore indicate proof-of-mechanism of ClC-1 inhibitor NMD670. These findings further emphasize that MVRC can detect pharmacological changes in muscle excitability in healthy subjects.

After evaluation of the safety of NMD670 in healthy subjects, we tested pharmacodynamic effects of NMD670 in patients with MG as proof-of-mechanism, with multiple pharmacodynamic measurements, including MVRC.

In **CHAPTER 7** we describe the findings of preclinical studies with NMD670, and the clinical pharmacodynamic effects of NMD670 in patients with MG. In the patient study, pharmacodynamic effects were evaluated by clinical evaluation of myasthenic symptoms using the Quantitative myasthenia gravis (QMG) score, and also neurophysiological tests, among which MVRC. In patients with MG, we found significant improvements on the clinical QMG score after NMD670, indicating that ClC-1 inhibition may indeed have positive effects on muscle function in these patients. The effects of NMD670 on MVRC in MG patients are not described in this thesis and will be published in a separate manuscript on this study focusing on MVRC only. To summarize our findings, MVRC endpoints were affected in the same direction as in the healthy volunteer study, an effect that reached statistical significance for one parameter after NMD670 1200 mg compared to placebo in patients with MG (unpublished data). These findings were dose dependent, in line with the findings in healthy participants, and corresponding to an increase in muscle cell excitability (unpublished data). Therefore, these data confirm the suggested ClC-1 target engagement of NMD670 in patients with myasthenia gravis. Moreover, our findings show that MVRC can detect pharmacodynamic effects of ClC-1 inhibition in both health and disease, further encouraging the use of this biomarker for assessment of pharmacological effects on muscle excitability.

In conclusion, our findings support the use of MVRC as pharmacodynamic biomarker in early phase drug development. The measurement is able to detect effects of different types of drugs on muscle cell excitability, in both healthy subjects and patients with MG. Our findings support pharmacological target engagement of both mexiletine (Na_v blocker) and NMD670 (ClC-1 inhibitor). Furthermore, MVRC variables have a relatively low inter- and intra-subject variability, the measurement can be performed quickly, and it can be repeatedly measured. Although the measurement is more invasive than TMS and NETT, because it uses recording and stimulation needles inserted in the muscle, this measurement is well-tolerated. What might limit MVRC's feasibility is its relative complexity to perform, and to interpret – although we have shown this is not a limitation at our centre.

IDEAS FOR FUTURE STUDIES

The use of TMS-EEG, NETT, and MVRC as pharmacodynamic biomarkers is still in its infancy. In our opinion, the next step in the validation of these biomarkers would be to investigate their sensitivity to a range of different ion channel modulators. Firstly, because this would extend the use of these biomarkers to a larger variety of pharmacological targets and disease indications. Secondly, it would be important to compare the excitability profiles of these different ion channel modulators, to see if the distinct excitability variables can be used to differentiate pharmacological effects on a channel level. In other words, the proposed studies should inform if certain variables provide a high specificity for modulation of corresponding channels, as opposed to a more general indication of increased and decreased excitability. Ideally, this would lead to a channel-specific fingerprint of variables, which can be used for proof of target engagement.

It would be interesting to investigate whether findings on TMS-EMG/EEG, NETT, and MVRC in healthy subjects are translatable to clinical treatment effects in patients. One way towards answering this question, would be to evaluate whether differences in excitability can be detected in the target patient population when compared to normal controls, and whether these variables change in the direction of normal after treatment administration. For example, differences in TMS-EMG/EEG variables can be detected between (drug-naïve) epilepsy patients and

healthy subjects.¹ It would be useful to investigate whether treatment with (novel) anti-epileptic drugs could change this enhanced excitability in patients with epilepsy. We are currently performing such a study in our unit. Additionally, although outside the scope of drug development, it would be extremely helpful if a biomarker, such as TMS-EMG/EEG, could reliably predict seizure control after subscription of anti-epileptic drugs in the clinic. This would require long-term follow-up studies to investigate whether significant (acute) effects on TMS-EMG/EEG correlate with seizure control.

In the case of myasthenia gravis, on the other hand, there is theoretically no clear abnormality in muscle membrane potential, because the pathophysiology of myasthenia gravis is based on the loss of acetylcholine receptors in postsynaptic membrane of the neuromuscular junction, leading to disturbed neuromuscular transmission.²⁶ Therefore, we may not be able to use pathophysiological changes of myasthenia gravis on MVRC outcomes, to evaluate treatment effects of drugs targeting muscle excitability. It should thus be noted that the use of MVRC in our study with NMD670 was based on the mechanism of action of the drug, not on the pathophysiology of myasthenia gravis. With MVRC, we were able to detect significant effects of NMD670 on muscle excitability in healthy subjects, and in patients with myasthenia gravis. The finding of increased muscle excitability provides us an indication of target engagement and proof-of-mechanism in healthy subjects, but it does not indicate that there was a clinical improvement of muscle function in patients with myasthenia gravis. The combination of MVRC and clinical evaluations (such as QMG score) in patients is therefore recommended. In our study described in **CHAPTER 6** and **8**, the MVRC results for NMD670 strengthen our positive findings on the clinical QMG score, because it indicates that increased muscle excitability may indeed be responsible for an improvement of muscle function in patients with myasthenia gravis.

The same may be considered when investigating novel analgesics using NETT. There are conflicting findings in literature on the presence of abnormalities in NETT variables in chronic pain,^{27,28} possibly because NETT does not examine the excitability of nociceptive nerve fibers, but of a large, myelinated nerve.²⁸ In our study with mexiletine and lacosamide (**CHAPTER 4**), we found significant excitability lowering effects of Na_v channel blockers on NETT in healthy subjects, which shows target engagement at the median nerve. In the same study, we have also performed

evoked pain tests. Mexiletine increased cold pressor pain tolerance and lowered cold pain perception; lacosamide showed no analgesic effects on these tests (unpublished data). Considering the abundant effects of lacosamide on NETT, it can be questioned whether a significant effect on peripheral nerve excitability as measured with NETT, corresponds with analgesic effects. However, it should be noted that investigation of NETT may still be useful to investigate pharmacological target engagement on channels that populate both myelinated axons and unmyelinated nociceptive nerve fibres, because the confirmation of target engagement can be pivotal in the early phase of drug development (in healthy subjects).

Lastly, it may be useful to investigate the potential of TMS-EMG/EEG, NETT, and MVRC as biomarkers in the translational phase from animal models to clinical drug studies. **CHAPTER 3** describes effects of TAK-653 on TEPs, and effects of TAK-653 on MEP amplitude were assessed in the same study and published elsewhere.²⁹ The study showed that comparable plasma concentrations of TAK-653 increased both MEP amplitude in humans, and motor responses to TMS in rats (registered with mechanomyography). These results indicate that MEP amplitude can be considered a useful translational biomarker for AMPA receptor modulation in future drug development programs.²⁹ NETT might also be helpful as a tool to navigate between preclinical studies and early phase clinical studies. NETT protocols have been used to investigate pharmacological effects on nerve excitability properties in vitro, for example using Na_v channel blockers (lidocaine, mexiletine, and tetrodotoxin),^{30,31} propofol,³² and amitriptyline.³³ Effects of K_v7 potassium channel activator flupirtine were even evaluated in vitro, as well as in vivo (a randomized, placebo-controlled trial in healthy subjects), in the same study.³⁴ In addition, measurement of peripheral nerve excitability using NETT in animals is extensively performed. Among this research, several studies investigated effects of Na_v,³⁵ potassium- and HCN³⁶ channel modulators on NETT in animals. Moreover, effects of a novel drug molecule, namely a compound that selectively inhibits Na_v1.8, were successfully tested in a mouse model of Charcot-Marie-Tooth disease.³⁷ The possibility to perform NETT in animal models, and even in vitro, encourages further investigation of its potential as translational biomarker. MVRC measurements have also been performed in animals. Two studies in pigs used MVRC to evaluate muscle membrane properties in faecal peritonitis.^{38,39} Also, a recent publication comparing MVRC in mice and humans, showed differences in muscle

excitability between the species.⁴⁰ So, MVRC could also be considered as a translational biomarker for drug effects, although these differences between species should then of course be taken into account. Future studies should indicate whether pig models are better translatable to humans than mice.

CONCLUSION

This thesis describes a set of excitability measurements – TMS-EMG/EEG, NETT, and MVRC- and the applicability of these tools in early phase clinical drug development. We validated the biomarkers in healthy subjects with registered drugs and showed that the measurements are all repeatable and sensitive to pharmacological effects, even in a small number of subjects. Furthermore, we have evaluated effects of a novel AMPA-PAM with TMS-EMG/EEG, and a first-in-class ClC-1 inhibitor with MVRC, and the findings helped us to confirm proof-of-mechanism of these compounds in healthy subjects. In conclusion, these measurements proved to be valuable pharmacodynamic biomarkers in two drug development programs, encouraging their further use in clinical development of other future drug candidates targeting cortical-, neuronal-, and muscle cell excitability. The use of such clinical pharmacodynamic biomarkers could improve the quality and efficiency of the development process of drugs for e.g. amyotrophic lateral sclerosis, chronic pain, depression, treatment-resistant epilepsy, and neuromuscular diseases.

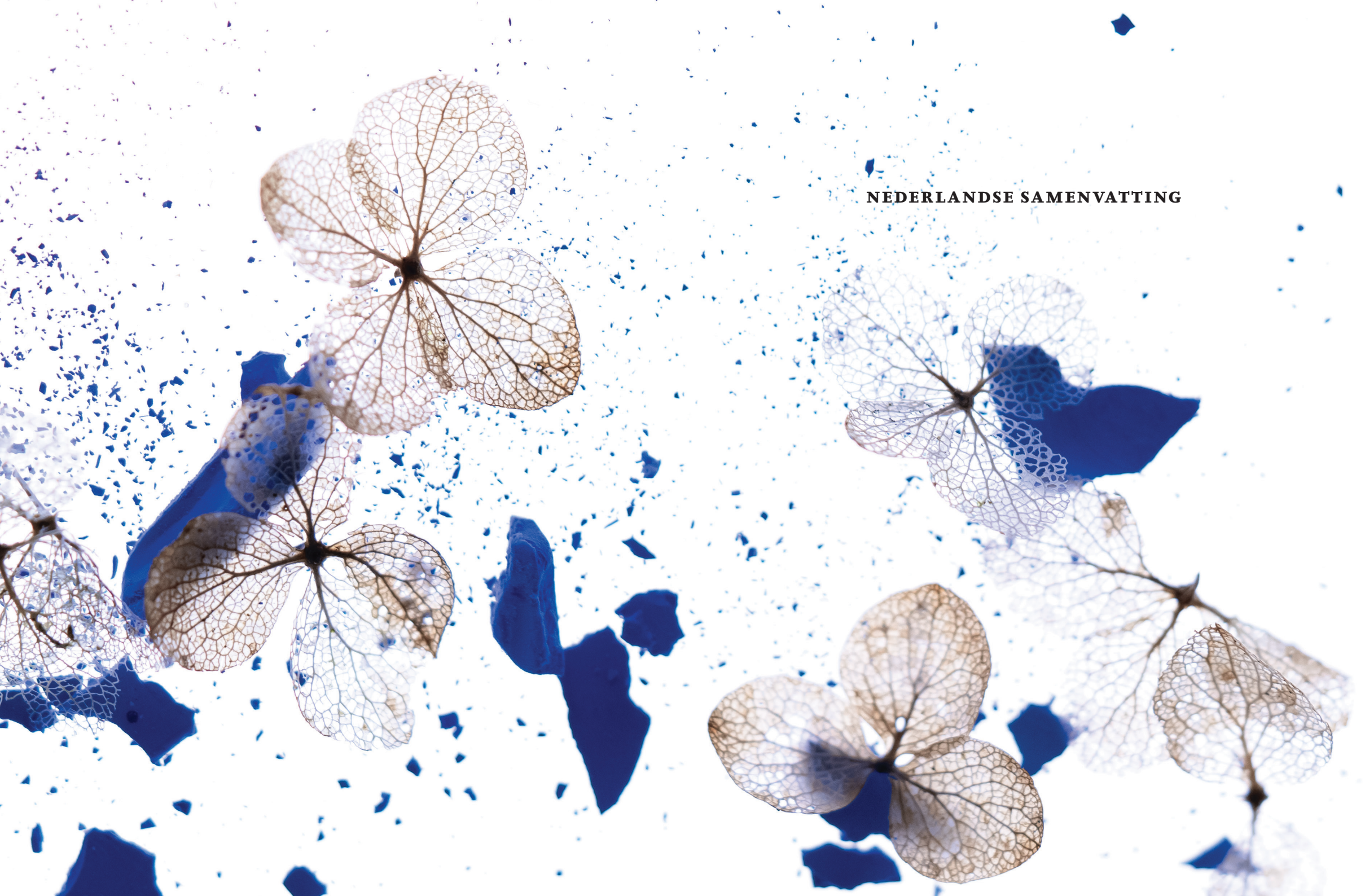
REFERENCES

- de Goede AA, Ter Braack EM, van Putten MJAM. Single and paired pulse transcranial magnetic stimulation in drug naïve epilepsy. *Clin Neurophysiol.* 2016;127(9):3140-3155. doi:10.1016/j.clinph.2016.06.025
- Zanette G, Tamburin S, Manganotti P, Refatti N, Forgiione A, Rizzuto N. Different mechanisms contribute to motor cortex hyperexcitability in amyotrophic lateral sclerosis. *Clin Neurophysiol.* 2002;113(11):1688-1697. doi:10.1016/S1388-2457(02)00288-2
- Menon P, Geevasinga N, van den Bos M, Yiannikas C, Kiernan MC, Vucic S. Cortical hyperexcitability and disease spread in amyotrophic lateral sclerosis. *Eur J Neurol.* 2017;24(6):816-824. doi:10.1111/ene.13295
- Dharmadasa T, Matamala JM, Howells J, Vucic S, Kiernan MC. Early focality and spread of cortical dysfunction in amyotrophic lateral sclerosis: A regional study across the motor cortices. *Clin Neurophysiol.* 2020;131(4):958-966. doi:10.1016/j.clinph.2019.11.057
- Ziemann U, Winter M, Reimers CD, Reimers K, Tergau F, Paulus W. Impaired motor cortex inhibition in patients with amyotrophic lateral sclerosis. Evidence from paired transcranial magnetic stimulation. *Neurology.* 1997;49(5):1292-1298. doi:10.1212/wnl.49.5.1292
- Vucic S, Ziemann U, Eisen A, Hallett M, Kiernan MC. Transcranial magnetic stimulation and amyotrophic lateral sclerosis: pathophysiological insights. *J Neurol Neurosurg Psychiatry.* 2013;84(10):1161-1170. doi:10.1136/jnnp-2012-304019
- Tan SV, Z'Graggen WJ, Boërio D, et al. Chloride channels in myotonia congenita assessed by velocity recovery cycles. *Muscle Nerve.* 2014;49(6):845-857. doi:10.1002/mus.24069
- Camerino DC, Tricarico D, Desaphy JF. Ion channel pharmacology. *Neurotherapeutics.* 2007;4(2):184-198. doi:10.1016/j.nurt.2007.01.013
- Neumann E. Chemical representation of ion flux gating in excitable biomembranes. *Neurochem Int.* 1980;2C:27-43. doi:10.1016/0197-0186(80)90009-1
- Cohen AF, Burggraaf J, van Gerven JMA, Moerland M, Groeneveld GJ. The use of biomarkers in human pharmacology (Phase I) studies. *Annu Rev Pharmacol Toxicol.* 2015;55:55-74. doi:10.1146/annurev-pharmtox-011613-135918
- Ruijs TQ, Heuberger JAAC, de Goede AA, et al. Transcranial magnetic stimulation as biomarker of excitability in drug development: A randomized, double-blind, placebo-controlled, cross-over study. *Br J Clin Pharmacol.* 2022;88(6):2926-2937. doi:https://doi.org/10.1111/bcp.15252
- Abbruzzese G, Trompetto C. Clinical and research methods for evaluating cortical excitability. *J Clin Neurophysiol.* 2002;19(4):307-321. doi:10.1097/00004691-200208000-00005
- Ilmoniemi RJ, Virtanen J, Ruohonen J, et al. Neuronal responses to magnetic stimulation reveal cortical reactivity and connectivity. *Neuroreport.* 1997;8(16):3537-3540. doi:10.1097/00001756-199711000-00024
- Tremblay S, Rogasch NC, Premoli I, et al. Clinical utility and prospective of TMS-EEG. *Clin Neurophysiol.* 2019;130(5):802-844. doi:10.1016/j.clinph.2019.01.001
- Alsalamoun M, Higerd GP, Effraim PR, Waxman SG. Status of peripheral sodium channel blockers for non-addictive pain treatment. *Nat Rev Neurol.* 2020;16(12):689-705. doi:10.1038/s41582-020-00415-2
- Wainger BJ, Kiskinis E, Mellin C, et al. Intrinsic membrane hyperexcitability of amyotrophic lateral sclerosis patient-derived motor neurons. *Cell Rep.* 2014;7(1):1-11. doi:10.1016/j.celrep.2014.03.019
- Kovalchuk MO, Heuberger JAAC, Sleutjes BTHM, et al. Acute Effects of Riluzole and Retigabine on Axonal Excitability in Patients With Amyotrophic Lateral Sclerosis: A Randomized, Double-Blind, Placebo-Controlled, Crossover Trial. *Clin Pharmacol Ther.* 2018;104(6):1136-1145. doi:10.1002/cpt.1096
- Ruijs TQ, Koopmans IW, de Kam ML, et al. Effects of Mexiletine and Lacosamide on Nerve Excitability in Healthy Subjects: A Randomized, Double-Blind, Placebo-Controlled, Crossover Study. *Clin Pharmacol Ther.* 2022;112(5):1008-1019. doi:https://doi.org/10.1002/cpt.2694
- Kiernan MC, Bostock H, Park SB, et al. Measurement of axonal excitability: Consensus guidelines. *Clinical Neurophysiology.* 2020;131(1):308-323. doi:10.1016/j.clinph.2019.07.023
- Sleutjes BTHM, Stikvoort García DJL, Kovalchuk MO, et al. Acute retigabine-induced effects on myelinated motor axons in amyotrophic lateral sclerosis. *Pharmacol Res Perspect.* 2022;10(4):e00983. doi:https://doi.org/10.1002/prp2.983

- 21 Koch MC, Steinmeyer K, Lorenz C, et al. The skeletal muscle chloride channel in dominant and recessive human myotonia. *Science*. 1992;257(5071):797-800. doi:10.1126/science.1379744
- 22 Wang GK, Russell C, Wang SY. Mexiletine block of wild-type and inactivation-deficient human skeletal muscle hNav1.4 Na⁺ channels. *J Physiol*. 2004;554(3):621-633. doi:https://doi.org/10.1113/jphysiol.2003.054973
- 23 Logigian EL, Martens WB, Moxley RT 4th, et al. Mexiletine is an effective antimyotonia treatment in myotonic dystrophy type 1. *Neurology*. 2010;74(18):1441-1448. doi:10.1212/WNL.0b013e3181d1ca3a
- 24 Lehmann-Horn F, Jurkat-Rott K. Voltage-gated ion channels and hereditary disease. *Physiol Rev*. 1999;79(4):1317-1372. doi:10.1152/physrev.1999.79.4.1317
- 25 Ruijs TQ, Koopmans IW, de Kam ML, Tannemaat MR, Groeneveld GJ, Heuberger JAAC. Muscle velocity recovery cycles as pharmacodynamic biomarker: Effects of mexiletine in a randomized double-blind placebo-controlled cross-over study. *Clin Transl Sci*. 2022;15(12):2971-2981. doi:https://doi.org/10.1111/cts.13418
- 26 Gilhus NE, Verschuuren JJ. Myasthenia gravis: subgroup classification and therapeutic strategies. *Lancet Neurol*. 2015;14(10):1023-1036. doi:https://doi.org/10.1016/S1474-4422(15)00145-3
- 27 Misawa S, Sakurai K, Shibuya K, et al. Neuropathic pain is associated with increased nodal persistent Na⁺ currents in human diabetic neuropathy. *Journal of the Peripheral Nervous System*. 2009;14(4):279-284. doi:https://doi.org/10.1111/j.1529-8027.2009.00239.x
- 28 Themistocleous AC, Kristensen AG, Sola R, et al. Axonal Excitability Does Not Differ between Painful and Painless Diabetic or Chemotherapy-Induced Distal Symmetrical Polyneuropathy in a Multicenter Observational Study. *Ann Neurol*. 2022;91(4):506-520. doi:https://doi.org/10.1002/ana.26319
- 29 O'Donnell P, Dijkstra FM, Damar U, et al. Transcranial magnetic stimulation as a translational biomarker for AMPA receptor modulation. *Transl Psychiatry*. 2021;11(1):325. doi:10.1038/s41398-021-01451-2
- 30 Vastani N, Seifert B, Spahn DR, Maurer K. Preconditioning depolarizing ramp currents enhance the effect of sodium channel blockers in primary sensory afferents. *Neuromodulation*. 2013;16(4):336-344. doi:10.1111/ner.12031
- 31 Lang PM, Hilmer VB, Grafe P. Differential contribution of sodium channel subtypes to action potential generation in unmyelinated human C-type nerve fibers. *Anesthesiology*. 2007;107(3):495-501. doi:10.1097/01.anes.0000278862.77981.c8
- 32 Neukom L, Vastani N, Seifert B, Spahn DR, Maurer K. Propofol decreases the axonal excitability in rat primary sensory afferents. *Life Sci*. 2012;90(9-10):343-350. doi:10.1016/j.lfs.2011.12.007
- 33 Freysoldt A, Fleckenstein J, Lang PM, Irnich D, Grafe P, Carr RW. Low concentrations of amitriptyline inhibit nicotinic receptors in unmyelinated axons of human peripheral nerve. *Br J Pharmacol*. 2009;158(3):797-805. doi:https://doi.org/10.1111/j.1476-5381.2009.00347.x
- 34 Fleckenstein J, Sittl R, Averbek B, Lang PM, Irnich D, Carr RW. Activation of axonal Kv7 channels in human peripheral nerve by flupirtine but not placebo-therapeutic potential for peripheral neuropathies: results of a randomised controlled trial. *J Transl Med*. 2013;11:34. doi:10.1186/1479-5876-11-34
- 35 Tuncer S, Tuncer Peker T, Burat İ, Kiziltan E, İlhan B, Dalkılıç N. Axonal excitability and conduction alterations caused by levobupivacaine in rat. *Acta Pharm*. 2017;67(3):293-307. doi:10.1515/acph-2017-0025
- 36 Banzrai C, Nodera H, Okada R, Higashi S, Osaki Y, Kaji R. Modification of multiple ion channel functions in vivo by pharmacological inhibition: observation by threshold tracking and modeling. *J Med Invest*. 2017;64(1.2):30-38. doi:10.2152/jmi.64.30
- 37 Rosberg MR, Alvarez S, Krarup C, Moldovan M. An oral NaV1.8 blocker improves motor function in mice completely deficient of myelin protein Po. *Neurosci Lett*. 2016;632:33-38. doi:10.1016/j.neulet.2016.08.019
- 38 Boërio D, Corrêa TD, Jakob SM, Ackermann KA, Bostock H, Z'Graggen WJ. Muscle membrane properties in a pig sepsis model: Effect of nor-epinephrine. *Muscle Nerve*. 2018;57(5). doi:10.1002/mus.26013
- 39 Ackermann KA, Bostock H, Brander L, et al. Early changes of muscle membrane properties in porcine faecal peritonitis. *Crit Care*. 2014;18(1). doi:10.1186/s13054-014-0484-2
- 40 Suetterlin KJ, Männikkö R, Matthews E, et al. Excitability properties of mouse and human skeletal muscle fibres compared by muscle velocity recovery cycles. *Neuromuscul Disord*. 2022;32(4):347-357. doi:10.1016/j.nmd.2022.02.011

APPENDICES





NEDERLANDSE SAMENVATTING

Sommige cellen in het menselijk lichaam, zoals cellen in de hersenschors, perifere zenuwen, en skeletspieren, zijn ‘prikkelbaar’. Dat betekent dat de cellen in deze weefsels in staat zijn impulsen (elektrische signalen) te transporteren door het lichaam. De eigenschap van deze cellen is cruciaal voor de werking van zenuwen en spieren. In de celmembranen van prikkelbare cellen zitten ion kanalen die de permeabiliteit voor natrium, kalium, calcium en chloor reguleren. Een verandering in permeabiliteit van het celmembranen voor deze ionen zorgt ervoor dat er een elektrisch signaal kan worden doorgegeven. De functie van de prikkelbare cellen is dus grotendeels afhankelijk van de werking van deze kanalen. Afwijkingen in de prikkelbaarheid van zenuwen en spieren kunnen de oorzaak zijn van een verscheidenheid aan neurologische, (neuro)musculaire en psychiatrische aandoeningen. In epilepsie wordt bijvoorbeeld een afwijkende prikkelbaarheid van de hersenschors gezien; in amyotrofe lateraal sclerose (ALS) wordt een afwijkende prikkelbaarheid van de zenuwen en hersenschors gezien; en patiënten met myotonia congenita hebben afwijkende prikkelbaarheid van de skeletspieren. In de zoektocht naar behandelingen voor deze ziektes, is het dus interessant om middelen te ontwikkelen die de ion kanalen—die verantwoordelijk zijn voor de prikkelbaarheid—te beïnvloeden.

In het onderzoek naar nieuwe geneesmiddelen die de prikkelbaarheid zouden beïnvloeden, is het van groot belang om farmacodynamische effecten van deze middelen in de vroege fase van de ontwikkeling te kunnen meten. Conventioneel klinisch geneesmiddelenonderzoek wordt uitgevoerd in vier fases, beginnend bij het onderzoeken van de veiligheid in gezonde proefpersonen. Voor nieuwe onderzoeksmiddelen, met een nieuw werkingsmechanisme, kan deze aanpak ongeschikt zijn. Het beoordelen van de veiligheid is uiteraard cruciaal, maar een meer farmacologische benadering kan het proces van geneesmiddelenontwikkeling verbeteren. Zo kan een middel veilig zijn in een kleine groep gezonde vrijwilligers, maar kan de toegediende dosis niet farmacologisch actief zijn, waardoor negatieve resultaten (geen werkzaamheid) worden gevonden bij de toediening aan patiënten. Een ander mogelijk gevolg zou kunnen zijn dat een geneesmiddel in de vroege fase te hoog gedoseerd wordt, waardoor er bijwerkingen ontstaan die de verdere ontwikkeling in de weg staan, terwijl het farmacologische mechanisme zeer waardevol zou kunnen zijn voor patiënten als het juist gedoseerd wordt. Het kan dus leiden tot risico’s voor deelnemers en hoge kosten als het farmacologische

actiemechanisme niet wordt meegenomen in de vroege fase van het geneesmiddelenonderzoek. Een geschikte farmacodynamische biomarker zou zelfs al in gezonde vrijwilligers kunnen aantonen dat het geneesmiddel zich bindt aan het gewenste doel (zoals een ion kanaal), waardoor het kan dienen als bewijs dat het bedoelde effect wordt bewerkstelligd. Ook kunnen farmacodynamische biomarkers helpen om de farmacologische actieve dosis te bepalen. Ten slotte zou een translationele biomarker kunnen helpen een beter geïnformeerde overgang te bewerkstelligen tussen de preklinische fase en de eerste toediening aan de mens, en de overgang tussen gezonde vrijwilligers en patiënten.

In het geneesmiddelenonderzoek op het gebied van prikkelbaarheid van de zenuwen en spieren is er momenteel geen betrouwbare biomarker voor het aantonen van farmacodynamische effecten. Ontwikkeling van een dergelijke meting zou daarom van groot belang zijn. In dit proefschrift beschrijf ik de validatie en implementatie van drie klinische metingen van prikkelbaarheid, om ze te gebruiken in klinisch geneesmiddelenonderzoek: transcraniële magnetische stimulatie (TMS) gecombineerd met elektromyografie (EMG) en elektro-encefalografie (EEG) voor het meten van prikkelbaarheid van de hersenschors; nerve excitability threshold tracking (NETT) voor het meten van prikkelbaarheid van de perifere zenuw; en muscle velocity recovery cycles (MVRC) voor het meten van prikkelbaarheid van de skeletspier. Eerst hebben we voor elk van deze metingen een concept studie gedaan met geregistreerde geneesmiddelen, waarvan bekend is dat ze de prikkelbaarheid beïnvloeden door beïnvloeding van ion kanalen. In deze onderzoeken wilden we bevestigen of deze metingen gevoelig waren voor het aantonen van geneesmiddelen effecten in gezonde vrijwilligers. Daarnaast beoordeelden we de variabiliteit van de metingen. Nadat we hadden bevestigd dat de metingen gevoelig waren voor farmacodynamische effecten, hebben we de biomarkers ook geïmplementeerd in vroege fase geneesmiddelenonderzoeken, waaronder een eerste toediening aan de mens.

Het vooruitzicht van nieuwe behandelingen gericht op de prikkelbaarheid van de hersenen, heeft ons ertoe aangezet om TMS te implementeren als farmacodynamische biomarker. TMS werkt door hersenstimulatie: een sterke elektrische stroom in de TMS spoel zorgt voor een magnetische impuls, wat vervolgens een actiepotentiaal kan genereren in de hersenschors. Indien de impuls gericht is op de motorische hersenschors, kan het effect van TMS op de elektrische activiteit van een spier in de hand

worden gemeten met EMG. De elektrische activiteit in de hersenen na de impuls kan worden gemeten met EEG. Eerst hebben wij onderzocht of we met TMS-EMG en TMS-EEG farmacodynamische effecten konden aantonen van geregistreerde middelen tegen epilepsie: levetiracetam en valproïnezuur, en een benzodiazepine: lorazepam. Zoals verwacht wordt van deze middelen vonden we een verlaging van de prikkelbaarheid van de hersenschors. We concludeerden dat TMS-metingen algehele veranderingen (door geneesmiddelen) in de prikkelbaarheid van de hersenen kan oppikken, en dat het daarom een zinvolle biomarker zou kunnen zijn in vroege fase geneesmiddelenonderzoek. Vervolgens hebben we TMS gebruikt in een studie met een nieuw onderzoeksmiddel voor de behandeling van therapie-resistente depressie: een positieve allosterische modulator van de α -amino-3-hydroxy-5-methyl-4-isoxazolepropionic acid (AMPA) glutamaat receptor. De effecten van dit middel op TMS-EMG wijzen erop dat het middel de prikkelbaarheid van de hersenen verhoogt (deze resultaten zijn beschreven buiten dit proefschrift). Met TMS-EEG kunnen ook verschillen in de hersengolven worden gevonden als het middel wordt vergeleken met een placebo. Deze resultaten dragen bij aan de verdere ontwikkeling van TMS-EEG als meting van corticale prikkelbaarheid.

We hadden twee redenen om NETT te introduceren als farmacodynamische biomarker voor effecten op de prikkelbaarheid van perifere zenuwen. Ten eerste, omdat er veel interesse is vanuit de farmaceutische industrie om nieuwe pijnstillers te ontwikkelen die veilig en niet verslavend zijn. Een belangrijke klasse middelen voor dat doel zijnde (selectieve) natriumkanalblokkers. Daarnaast zijn er kaliumkanaal activators in ontwikkeling, vergelijkbaar met de werking van retigabine, die de prikkelbaarheid van de zenuwen in ALS zouden moeten te verlagen. Om die reden besloten wij te onderzoeken of NETT effecten van natriumkanalblokkers zou kunnen aantonen in gezonde vrijwilligers. We hebben de effecten van twee natriumkanal blokkers, mexiletine en lacosamide, onderzocht op de prikkelbaarheid van de perifere zenuw. NETT werkt door elektrische stimulatie van de nervus medianus bij de pols, met behulp van een computergestuurd paradigma. De stimulatie wekt een actiepotentiaal op die wordt gemeten in de spier en de sensorische zenuw. NETT variabelen geven informatie over de werking van ion kanalen op de plek van de zenuwstimulatie. Onze resultaten laten zien dat mexiletine en lacosamide de prikkelbaarheid van de perifere

zenuwen verlagen, zoals wordt verwacht van een natriumkanalblokker. Dit betekent dat NETT in staat is subtiele geneesmiddelen effecten op de prikkelbaarheid van de zenuw aan te tonen. We concluderen daarom dat NETT een nuttige meting kan zijn om te gebruiken in ontwikkeling van nieuwe natriumkanalblokkers.

Ten slotte ontstond de noodzaak voor een farmacodynamische biomarker voor geneesmiddelen die effect hebben op de prikkelbaarheid van de spier, toen we van plan waren een fase I studie uit te voeren met een remmer van het chloride kanaal ClC-1. Het nieuwe onderzoeksmiddel in kwestie, NMD670, is de eerste in zijn klasse, en wordt ontwikkeld voor de behandeling van myasthenia gravis. Met MVRC kan de prikkelbaarheid van de spiermembraan worden bepaald door directe elektrische stimulatie van de spiervezels, onafhankelijk van de neuromusculaire overgang. Om de gevoeligheid van MVRC voor geneesmiddelen effecten te onderzoeken, besloten we een studie te doen waarin we effecten van mexiletine onderzochten met MVRC. We vonden een verlaging van de prikkelbaarheid van de spieren na mexiletine. Onze resultaten wijzen erop dat MVRC sensitief is voor farmacodynamische effecten, en we concludeerden dat MVRC nuttig kon zijn voor de geplande studie met ClC-1 remmer NMD670. Vervolgens beschrijven we de eerste toediening van NMD670 aan gezonde vrijwilligers en ook de eerste toediening aan patiënten met myasthenia gravis. We laten zien dat NMD670 significante effecten heeft op MVRC in gezonde vrijwilligers, wat erop wijst dat het middel inderdaad de prikkelbaarheid van de spier verhoogt. Ook in patiënten met myasthenia gravis zien we een effect op MVRC in dezelfde richting. Daarnaast tonen we aan dat NMD670 kleine, maar statistisch significante, verbeteringen geeft in de klinische score (Quantitative myasthenia gravis score). We concluderen dat onze bevindingen het gebruik van MVRC als farmacodynamische biomarker in vroege fase geneesmiddelenonderzoek ondersteunt. MVRC is in staat effecten van verschillende geneesmiddelen op de prikkelbaarheid van de spieren aan te tonen, zowel in gezonde vrijwilligers als patiënten met myasthenia gravis.

Samenvattend hebben wij een drietal metingen – TMS, NETT, en MVRC – gevalideerd, die wij op basis van de resultaten geschikt achten voor het gebruik als farmacodynamische biomarker in vroege fase geneesmiddelenonderzoek. Onze resultaten laten zien dat de metingen gevoelig zijn voor farmacodynamische effecten, zelfs in een kleine groep gezonde

vrijwilligers, zoals gebruikelijk in fase I studies. We zijn van mening dat het van toegevoegde waarde is als deze biomarkers onderdeel vormen van vroege fase geneesmiddelenonderzoek (als het actiemechanisme van het middel daar aanleiding toe geeft). Dit is relevant omdat het gebruik van farmacologische biomarkers in het geneesmiddelenonderzoek de kwaliteit van het onderzoek naar nieuwe middelen voor onder andere epilepsie, pijn, ALS, en myasthenia gravis, kan verbeteren.

CURRICULUM VITAE

Titia Quirine Ruijs, born in 's-Gravenhage, 1990, graduated from secondary school in 2008 (Gymnasium, *Willem de Zwijger College*, Bussum). She studied abroad for one year as an international student (*St. Clare's International College*, Oxford and *Lorenzo de' Medici Institute*, Florence), after which she studied Architecture at *Delft University of Technology* in 2009-2010. In 2010 she started studying Medicine at the *Erasmus University Rotterdam*. As part of her master's degree, Titia did a research elective at the *University of Edinburgh*, where she investigated the use of Optical Coherence Tomography in chronic kidney disease. In 2017 she received her medical degree. The same year, she started as PhD candidate and project leader of early phase drug studies at the *Centre for Human Drug Research*, Leiden. As PhD candidate at *Leiden University*, Titia investigated pharmacodynamic biomarkers for cortical, nerve, and muscle excitability in early phase clinical drug development, under supervision of Prof. Dr. G.J. Groeneveld. Titia lives in Amsterdam with her husband Laurence Moss, and their son Maurits.

LIST OF PUBLICATIONS

Ruijs TQ, Koopmans IW, de Kam ML, Tannemaat MR, Groeneveld GJ, Heuberger JAAC. Muscle velocity recovery cycles as pharmacodynamic biomarker: Effects of mexiletine in a randomized double-blind placebo-controlled cross-over study. *Clin Transl Sci.* 2022;15(12):2971-2981. doi:<https://doi.org/10.1111/cts.13418>

Ruijs TQ, Koopmans IW, de Kam ML, et al. Effects of Mexiletine and Lacosamide on Nerve Excitability in Healthy Subjects: A Randomized, Double-Blind, Placebo-Controlled, Crossover Study. *Clin Pharmacol Ther.* 2022;112(5):1008-1019. doi:<https://doi.org/10.1002/cpt.2694>

Ruijs TQ, Heuberger JAAC, de Goede AA, et al. Transcranial magnetic stimulation as biomarker of excitability in drug development: A randomized, double-blind, placebo-controlled, cross-over study. *Br J Clin Pharmacol.* 2022;88(6):2926-2937. doi:<https://doi.org/10.1111/bcp.15232>

O'Donnell P, Dijkstra FM, Damar U, Quanhong L, de Goede AA, Xu L, Pascual-Leone A, Buhl DL, Zuiker R, **Ruijs TQ**, Heuberger JAAC, MacMullin P, Lubell M, Asgharnejad M, Murthy V, Rotenberg A, Jacobs GE, Rosen L. Transcranial magnetic stimulation as a translational biomarker for AMPA receptor modulation. *Transl Psychiatry.* 2021 May 27;11(1):325. doi: [10.1038/s41398-021-01451-2](https://doi.org/10.1038/s41398-021-01451-2).

Balmforth C, van Bragt JJ, **Ruijs T**, Cameron JR, Kimmitt R, Moorhouse R, Czopek A, Hu MK, Gallacher PJ, Dear JW, Borooah S. Choriorretinal thinning in chronic kidney disease links to inflammation and endothelial dysfunction. *JCI insight.* 2016 Dec 8;1(20).



